COMPREHENSIVE TECHNO-ECONOMIC IMPROVEMENT DIRECTIVES FOR SMART DISTRIBUTION SYSTEM

A Thesis Submitted
In Partial Fulfillment of the Requirements
for the Degree of

DOCTOR OF PHILOSOPHY

by

SHUBHAM GUPTA

(Roll No. 2K19/PHDEE/502)

Under the Supervision of

Prof. Vinod Kumar Yadav and Prof. Madhusudan Singh
Department of Electrical Engineering
Delhi Technological University, Delhi - 110042

Department of Electrical Engineering

DELHI TECHNOLOGICAL UNIVERSITY
(Formerly Delhi College of Engineering)
Shahbad Daulatpur, Main Bawana Road, Delhi - 110042. INDIA

June, 2024

DELHI TECHNOLOGICAL UNIVERSITY

(Formerly Delhi College of Engineering)
Shahbad Daulatpur, Main Bawana Road, Delhi-42

CANDIDATE'S DECLARATION

I hereby certify that the work which is being presented in the thesis entitled **COMPREHENSIVE TECHNO-ECONOMIC IMPROVEMENT DIRECTIVES FOR SMART DISTRIBUTION SYSTEM** in partial fulfillment of the requirements for the award of the Degree of Doctor of Philosophy and submitted in the Department of Electrical Engineering of the Delhi Technological University is an authentic record of my own work carried out during the period from January, 2020 to June, 2024 under the supervision of Dr. Vinod Kumar Yadav, Professor, Department of Electrical Engineering and Prof. Madhusudan Singh, Registrar, Delhi Technological University.

The matter presented in this thesis has not been submitted by me for the award of any other degree of this or any other Institute.

(Shubham Gupta)

This is to certify that the student has incorporated at the corrections suggested by the examiners in the thesis and the statement made by the candidate is correct to the best of our knowledge.

Signature of Supervisors

Signature of External Examiner

DELHI TECHNOLOGICAL UNIVERSITY

(Formerly Delhi College of Engineering)
Shahbad Daulatpur, Main Bawana Road, Delhi-42

CERTIFICATE BY THE SUPERVISORS

Certify that **Shubham Gupta** (2K19/PHDEE/502) has carried out their work presented in this thesis entitled "**COMPREHENSIVE TECHNO-ECONOMIC IMPROVEMENT DIRECTIVES FOR SMART DISTRIBUTION SYSTEM**" for the award of **Doctor of Philosophy** from Department of Electrical Engineering, Delhi Technological University, Delhi, under our supervision. The thesis embodies results of original work, and studies are carried out by the student himself and the content of the thesis do not form the basis for the award of any other degree to the candidate or to anybody else from this or any other University/Institute.

(Vinod Kumar Yadav)
Supervisor

(Madhusudan Singh)
Co-Supervisor

Date:

Abstract

The ongoing transformation of electric power distribution systems involves the gradual adoption of cutting-edge advancements in communication, control, measurement, and metering technologies. This evolution is geared towards realizing the concept of a smart distribution system, characterized by increased flexibility, sustainability, reliability, and efficiency. The future distribution systems are anticipated to engage actively and involve customers while incorporating various distributed energy resources (DERs) like renewable energy sources (RESs), battery energy storage (ESs), and electric vehicles (EVs). This shift is expected to usher in a new era contributing to environmental and economic well-being. However, a comprehensive planning and operational strategy with strategic goals is imperative to reap the benefits of smart distribution systems fully.

This thesis delves into the exploration of methodologies for optimal planning and operation within smart distribution systems, aiming to achieve comprehensive techno-economic advantages. To address existing gaps in current studies, a novel index method, based on Shannon's Entropy (SE-IM), is introduced. This method identifies the optimal location for capacitor bank placement, incorporating multiple criteria such as voltage stability, loss reduction, and system load-ability. Utilizing particle swarm optimization, the thesis determines the optimal size for the capacitor bank placement. The application of this method to three distribution systems—IEEE 12-bus, 34-bus, and a practical 108-bus radial distribution network from an Indian utility—is discussed, demonstrating superior results compared to existing techniques.

Furthermore, the analysis of optimal capacitor bank placement in the presence of distributed generation (DG) and load uncertainty highlights the approach's capacity to enhance network quantities while maintaining security and reliability constraints. Given the increasing significance of planning in smart distribution systems, particularly in analyzing various techno-economic

measures, a method is proposed to assess the weights associated with objectives in a weighted multi-objective optimal DG placement problem. This method employs Shannon's Entropy formula to evaluate the relative importance of each objective function, subsequently determining unbiased weights. The efficacy of this approach is validated through numerical simulations on a 38-bus test system, showcasing its effectiveness across various scenarios.

This work introduces a practical method for optimizing the day-ahead schedule of electric vehicle charging stations (EVCSs) in a smart distribution system. The primary goal is to minimize real power loss payments, accounting for various operational constraints, voltage limits, and the intricate dispatching and storage constraints of EVCSs. The formulation includes sophisticated demand response modeling and addresses uncertainties in electricity prices and load forecasting. The method leverages mixed-integer nonlinear programming, coupled with the strategic use of single-agent and multi-agent control strategies to provide the optimal solution. The real-world applicability and effectiveness of this approach are demonstrated through simulations conducted on a modified 12-bus distribution network, highlighting its tangible benefits.

In addition, this thesis unveils a framework designed to proficiently manage a diverse array of DERs within the smart distribution system. The emphasis is on optimizing the operations of local energy communities and elevating grid services at the utility level. For this, an aggregation modeling of DERs is proposed, assessing cumulative flexibility based on individual preferences, spatial considerations, and temporal behavior. A sophisticated hierarchical control framework is presented to facilitate coordinated dispatch among key entities, namely the electric utility (EU) operator, community aggregators (CAs), and individual DERs. CAs are tasked with minimizing operational costs within their respective energy communities, while the EU operator focuses on enhancing grid services, all within the confines of distribution network constraints. Simulations performed on a modified IEEE-123 bus radial distribution network affirm the efficacy of this proposed approach.

Acknowledgements

First and foremost, my gratitude and appreciation must go to my advisors Professor Vinod Kumar Yadav and Professor Madhusudan Singh, Department of Electrical Engineering, Delhi Technological University, Delhi, for their invaluable support and guidance during the course of my PhD studies. I consider this as the highest degree of privilege to have completed my studies under their supervisions.

I owe my deepest gratitude to my PhD research committee for their valuable comments and input: Professor N.P. Padhy, Director, MNIT Jaipur; Professor Poornima Mittal from the Department of Electronics and Communication Engineering, Delhi Technological University; Professor Rachana Garg from Department of Electrical Engineering, Delhi Technological University.

I would like to express my deepest gratitude towards my family for their love and patience which kept me going on this journey. Their faith and unconditional love towards me are the reason for whatever I have achieved in my life. Without my friends in and out of DTU Delhi, life would have been dull. I am indebted to all of them for their support, valuable input, and constant encouragement.

Finally, I thank God Almighty for giving me strength at all times.

Date: Shubham Gupta

Contents

List of Figures

List of Tables

Chapter 1

Introduction

This chapter offers a concise synopsis of the topics explored in the present thesis. It delineates the research dimensions emanating from the critical review on optimal planning and operations for smart distribution system, subsequently elucidating the contributions made by this thesis.

1.1 Background

Electric power distribution systems serve as the interface between electricity end-users and the power grid. In the past, distribution systems have adhered to a centralized operational model, meaning that only the owner or operator of the distribution system made decisions. In contrast, today's grid undergoes a transformation marked by the rising integration of Distributed Energy Resources (DERs), demand response programs, and initiatives focused on energy efficiency [1]. The growing prevalence of DERs, including energy storage systems (ESs), photovoltaic (PV) plants, wind turbine (WT) farms, and others, enhances dispatch capabilities, enabling them to furnish both energy and vital grid ancillary services, thereby contributing to economic and environmental advantages.

The distribution system is poised to evolve into a network comprising DERs, including smaller microgrids interconnected through the distribution system network. This emerging distribution paradigm is often denoted as an active distribution network (ADN) [2]. Within this innovative operational framework, distribution system management transitions from a passive role of operating and maintaining assets to an active role in dynamically orchestrating networks that

adapt to economically motivated activities. Moreover, a market-driven economic structure becomes imperative to foster healthy competition among DER owners and centralized generation entities on an equitable basis. This approach aims to enhance both economic efficiency and operational security within the distribution system.

Smart distribution systems (SDSs) exhibit several key characteristics, including the deployment of massive installations of DERs, the implementation of system automation, the incorporation of net-metering and bilateral electricity flow, the integration of communication networks for efficient information transfer, and the establishment of free electricity markets with new functionalities and services [3]. These systems are characterized by the presence of micro players, namely electricity end-users or prosumers, who utilize multiple DERs to generate electricity locally. However, the integration of DERs can have significant implications for grid operations, particularly when penetration levels surpass recognized tipping points.

One notable consequence is the alteration of power flows, leading to electricity moving in multiple directions. Additionally, the occurrence of loop flows in distribution circuits emerges as a challenge associated with the integration of DERs into the grid. These changes were not initially foreseen by the current generation of grid controls, confronted with various challenges for distribution network operators (DNOs) in the upcoming years [4]. These challenges include the electrification of both transportation and heating sectors, the proliferation of renewable-based distributed generation systems in low- and medium-voltage networks, and the limited visibility of lower voltage network levels due to inadequate instrumentation and monitoring.

As a result, there is a pressing need for the management and control architecture of distribution systems to undergo a gradual transformation to pragmatically techno-economic feasible accommodation of emerging smart grid technologies, distributed energy resources, and active electricity end-users or prosumers.

1.2 Literature Review

The imperative for a seamless evolution of the distribution system necessitates the formulation of strategic plans serving as roadmaps for the development of novel consumption paradigms. Specifically, the SDS intricately links to the enhancement and modification of existing Distribution Networks (DN), the introduction of innovative distribution concepts, and mechanisms empowered by advanced technologies aligning with anticipated future requirements. Numerous SDS concepts, as reported in the literature, primarily revolve around the modification of DN attributes, DERs, renewable energy sources (RESs), ESs, reliability, Information and Communication Technology (ICT), Power Electronics (PE), and Active Network Management (ANM) techniques.

This thesis provides an extensive review of prior research on SDS planning, focusing on the analysis and categorization of planning models and methods proposed in these scholarly articles. The examination encompasses various perspectives, including objectives, decision variables, constraint conditions, and solving algorithms. Simultaneously, considerable attention is dedicated to elucidating the principal theoretical issues and challenges in planning models and methodologies. These issues are systematically extracted, discussed, and accompanied by applicable suggestions for addressing them.

1.2.1 Optimal Distribution Network Planning with DERs

The integration of RESs into traditional distribution network planning has historically relied on deterministic methods and a "fit and forget" strategy, typically centered around worst-case and low-probability scenarios [5]. Unfortunately, these approaches overlook the inherent uncertainties associated with RESs and diverse operational conditions. The advent of widespread DERs has exacerbated the limitations of deterministic methods, leading to issues such as unnecessary grid reinforcements, increased network losses, and the failure to achieve development and environmental targets. Consequently, these traditional planning methods impede the effective integration of DERs and are deemed inadequate for distribution network planning.

Distribution network planning is a multifaceted and intricate task, requiring the formulation of not only distribution network plans but also the optimal allocation of DERs in terms of economic efficiency, reliability, and safety [6–9]. The planning process is further complicated by high-level uncertainties stemming from DERs, network dynamics, load demands, and other variables, adding complexity to the model and rendering solution-finding more challenging. In contrast to traditional planning methods, distribution network planning tools must conduct comprehensive analyses based on various criteria, such as economic, technical, and environmental considerations, within a multi-objective framework.

The pursuit of optimal distribution network planning has attracted considerable research attention, resulting in the development of numerous models and methodologies with distinctive features and significant references. Several influential reviews have been published on the optimal planning of distribution networks [10–15]. In their comprehensive review [11], the authors examine smart distribution network planning, encompassing intelligent technologies, anticipated functionalities, modern distribution concepts, policies, and plans, while addressing real-world optimization problems with a focus on multi-objective considerations and multi-stakeholder perspectives. Another extensive review [14] delves into the planning of distribution networks, highlighting differences between traditional and active planning models, and proposing a generic multi-dimensional framework for optimal distribution network planning to overcome current research limitations. Similarly, a review in [10] scrutinizes numerous papers from 2007 to 2014, categorizing distribution network planning research based on planning models and solving methods, and outlining future research trends.

Moreover, [15] concentrate on the distribution network planning problem, offering a comprehensive review of multi-objective models and solving algorithms. They underscore potential future directions in modern distribution network planning from a multi-objective perspective. In contrast to these review articles, other scholars [12, 13] focus on reviewing and summarizing the literature related to the allocation of RESs and ESs in distribution networks, respectively.

The transition from conventional distribution networks to ADNs signifies a

paradigm shift where DERs are no longer passive components but are actively controlled and coordinated, aiming to enhance the overall utilization of DERs. Furthermore, as DER penetration continues to rise, the progression from ADNs to SDSs underscores that SDSs transcend their conventional role as mere conduits for delivering electric power to consumers. Instead, they are evolving into comprehensive systems encompassing Distributed Generators (DGs), ESs, dynamically responsive and flexible load demands, active networks, and more.

In SDS planning, the paramount objective is maximizing efficiency while adhering to system constraints. The escalating economic risks associated with investment needs, particularly in restructured networks, have motivated planners to adopt meticulous design approaches. Consequently, the optimal placement of electrical devices in power systems has become a pivotal concern, attracting significant attention from researchers. Over the past decades, diverse solutions and methodologies have been developed for the optimal allocation of shunt capacitors, DGs, ESs, network reconfiguration, and various other electrical resources in both transmission and distribution networks.

This thesis critically examines the existing literature pertaining to the optimal allocation of shunt capacitors and distributed generation. It aims to identify the limitations of current studies, which will be expounded upon in subsequent subsections. The emphasis is on providing a comprehensive review and analysis, shedding light on the drawbacks of existing approaches, and paving the way for advancements in the field.

Optimal Allocation of Capacitor Banks in Distribution Network

Globally, the electrical networks are getting over-stressed due to increasing demand for energy on the one hand and decreasing capacity of the existing networks on the other, because of various factors such as integration of DERs, shortage of reactive power, aging of extant infrastructure, and global warming, etc. This results in incidents of frequent blackouts, and huge monetary loss to society. Installation of shunt capacitor banks (SCBs) is one of the effective methods to de-stress the networks, apart from network expansion, installation of the DGs, voltage regulators (VRs), and FACTS devices [16, 17]. The root cause analysis reports on some of the recent blackout incidents [18, 19] indicate that

deficit reactive power supply in the network was the leading cause behind blackouts.

Fundamentally, The capacitor units are interconnected in parallel-series configurations to constitute a singular-phase SCB, enclosed within a steel housing. The series arrangement mitigates dielectric costs, while the parallel arrangement augments the overall capacitance of the SCB. Adhering to a general guideline, the minimum capacitor units connected in parallel are determined such that the isolation of one capacitor unit within a group does not induce a voltage imbalance exceeding 110% of the rated voltage on the remaining capacitors in the group. Simultaneously, the minimum number of series-connected groups is stipulated to prevent the complete bypass of a group from subjecting the others in operation to a sustained over-voltage exceeding 110% [20]. The reactive power (Q_C) generated by the capacitor is contingent on the applied voltage (V) and capacitive reactance (X_C), as expressed by (1.1) [21].

$$Q_C = \frac{V^2}{X_C} \tag{1.1}$$

Conventionally, the capacitors were installed near the primary substation; however, presently, the trend has changed. Installation of capacitors is now done based on the system requirements such as voltage profile improvement, loss reduction, and increasing the system load-ability by installing the capacitors at optimal locations [22, 23]. SCBs are strategically positioned within a composite of fixed and switched (variable) SCB units. The magnitude of the fixed-type SCB is contingent upon the system's mean reactive power requirements, while the switched-type SCB fulfills the disparity between the current reactive power demand and the available power from the fixed SCB unit. A specialized control mechanism is implemented to regulate the power of the switched SCB unit. The authors [24, 25] have introduced methodologies that yield both continuous and discrete capacitor sizes. In instances of continuous capacitor sizing, it is postulated that the capacitor size will comprise a blend of fixed and switched SCB units. The preliminary adjustment of the capacitor during stable operating conditions will be accomplished through the utilization of the switched SCB unit.

The limitation of computation capacity was the main reason behind earlier capacitor placement methods in the network, which were based on calculus and

defined as an analytical approach. The first work carried out by [26] in 1956 proposed the famous '2/3 rule' for the placement of the fixed capacitor in a uniformly distributed load in a distribution network. In [27] and [28], the methodology is extended by considering the switched capacitors or placement and sizing of capacitors on a uniform distribution network. Following these pioneering works, numerous analytical approaches have been proposed [29–31]. However, the analytical techniques required to make certain assumptions, such as uniformly distributed load, and these techniques also neglect the upfront investment of capacitors.

Later, the capacitor placement and sizing problem was formulated in [22] using dynamic programming, and a class of numerical programming approaches was evolved for capacitor allocation in distribution networks. The mathematical model optimized the objective function while satisfying certain constraints, e.g., voltage limit, capacitor size limit, and limit on the maximum number of capacitors. In [23], the capacitor placement problem was proposed as a mixed-integer programming problem. Integrating the heuristics in analytical or numerical programming approaches reduces the search space and convergence time to the optimal solutions [32]. Heuristic methods for capacitor placement and sizing were also reported by several other researchers [33–35].

Recently, artificial intelligence (AI) techniques have been implemented for capacitor placement and sizing problems, which dramatically reduced the search space and decreased overall computational time. In AI-based techniques, the genetic algorithm [36], particle swarm optimization (PSO) [37], fuzzy [38], flower pollination [32], and ant colony [39] are pretty powerful algorithms in solving complex problems and hence being used extensively. However, these AI methods require high memory space and computational time for solving complex systems. Recently, some authors have also dealt with the capacitor placement problem by combining other network problems like voltage regulators, DGs placement, and load tap changers [40, 41].

The main objectives of the optimal capacitor placement problem are to quantify the location, size, and type of the capacitors to be placed in a power distribution network to enhance the comprehensive techno-economic benefits. For determining the capacitors' optimal location, many index methods have been proposed in the past [39, 42, 43]. These methods identify potential nodes for

capacitor placement based on the identification of nodes having higher power loss, weak voltage magnitude, and other technical quantities. The optimal capacitor placement problems commonly utilize the following set of constraints to identify the size of SCB (1.2) and the position of SCB (1.3).

$$Q_C \leq \sum_{i \in N_b} Q_i \quad \forall\, N_b = \{1, 2, ..., n_b\} \tag{1.2}$$

$$1 \leq Q_C^{Pos} \leq n_{bus} \tag{1.3}$$

In the modern power system, DERs are gaining importance due to major advantages like improving the voltage profile, power loss reduction, and enhancing system security and reliability [44]. Moreover, there are other benefits of the DERs integration as below [45]:

- DERs share the load demands, reducing greenhouse gas and other air pollutants emissions by the central power plants.
- By local generation through DERs, line losses in transmission and distribution are reduced extensively, and less energy production.
- In the case of fossil fuel-based power plants, warm water discharge, land usability, and other factors impact the environment directly or indirectly.

Therefore, multi-dimensional problems become prominent, wherein studies have integrated capacitor placement issues with various other power system considerations. These include DG placement, voltage regulators, and network reconfiguration. In addressing the complexity of the capacitor placement problem, the study in [46] characterizes it as multi-dimensional and extends the scope by incorporating voltage regulator placement to manage volt/var control. Moreover, the investigation in [47] integrates diverse DG types, shunt capacitors, and network reconfiguration into a unified problem. The findings from this study suggest that concurrently addressing these three objectives yields a substantial reduction in power losses, emphasizing the significance of simultaneous optimization in enhancing overall system performance.

Optimum Sizing and Placement of DG in Distribution Network

In contrast to the conventional centralized generation approach, DG represents a paradigm wherein a portion of electric power is generated and distributed to end-users through small-scale generation units situated nearby. This decentralized approach encompasses an array of locally installed power generation units, including both renewable and conventional types. In recent times, the rapid evolution of technology has rendered distributed generators highly advantageous across economic, technical, and environmental domains [48–50].

The integration of DG into power systems manifests a reduction in overall power losses. However, the relationship between DG penetration levels and power losses follows a U-trajectory. Consequently, sub-optimal DG placement may aggravate power losses, compromising the voltage profile below acceptable thresholds [51]. Given the array of technical and non-technical challenges, the imposition of additional issues becomes intolerable for utilities. Therefore, the optimal placement and sizing strategy for DGs is a must to minimize overall system losses and enhance voltage profiles.

Historically perceived solely as an active energy source, DG's role has evolved with the recognition that reactive power control contributes to a superior network voltage profile while concurrently diminishing power losses. Researchers have delved into the impact of DG on the load-ability of distribution networks [52, 53], establishing that the DG augments the load-carrying capacity of the distribution system. The strategic placement of DGs emerges as a critical consideration, as it not only facilitates maximal benefits but also incurs minimal investment costs [54]. Consequently, extensive research efforts have been dedicated to optimal DG planning within distribution systems. These endeavors seek to refine our understanding of the intricate interplay between DG deployment strategies, power system performance, and the overarching goal of achieving maximum benefits with prudent investment costs.

The techniques for the optimal allocation of DGs address challenges associated with the sizing and appropriate placement of DGs. These techniques involve diverse objective functions coupled with numerous compelled technical and operational constraints. Various computational methods are applied,

considering different DG types based on power factor (PF) and varying numbers of units. The problem formulation for loss minimization typically relies on three distinct loss formulae: branch power loss formula, current loss formulae, and exact loss formulae. In a study referenced as [55], the objective based on the power loss formula is formulated according to (1.4). Notably, in 1971, Elgerd [56] introduced a loss formula widely recognized as the exact loss formula, referring to (1.5). Furthermore, (1.6) represents the current loss formula, as demonstrated in [57].

$$P_L = \sum_{i \in N_b} \left(\frac{P_{b,i}^2 + Q_{b,i}^2}{|V_i|^2} \right) R_{b,i} \tag{1.4}$$

$$P_L = \sum_{i \in N_b} \sum_{j \in N_b} \left[\alpha_{ij} \left(P_i P_j + Q_i Q_j \right) + \beta_{ij} \left(Q_i P_j - P_i Q_j \right) \right] \tag{1.5}$$

$$P_L = \sum_{i \in N_b} |I_{b,i}|^2 R_{b,i} \tag{1.6}$$

The minimization of energy loss represents a key objective in the optimal placement of DG units, attracting substantial attention from researchers. Notably, dispatchable DG units exhibit a more pronounced positive impact on energy loss reduction and voltage profile enhancement than their non-dispatchable counterparts. A noteworthy contribution to this discourse is in [58], where an analytical expression (1.7) proposed in [59] was adapted and refined for the optimal allocation of dispatchable and non-dispatchable DG units aimed at the overarching goal of minimizing annual energy losses.

$$E_{\mathrm{L}} = 91.25 \sum_{t=1}^{96} P_{\mathrm{L}}^t \, \Delta t \tag{1.7}$$

An innovative approach in [60] employs a Particle Swarm Optimization (PSO)-based planning model to address the allocation of dispatchable and non-dispatchable DG units within distribution systems, seeking to identify the optimal hourly production profile and DG unit penetration. Nevertheless, their approach assumes a uniform generation load profile over 24 hours throughout the year, with annual energy loss computed using (1.8).

$$E_{\mathrm{L}} = \sum_{t=1}^{T} \left[P_L^{\mathrm{t}}(X) \right]; \qquad X: \text{ variable vector} \tag{1.8}$$

Furthermore, Sultana and Roy [61] employed an opposition-based learning concept in the Krill Herd Optimization algorithm to minimize annual energy loss after the optimal siting and sizing of renewable DG. However, it is imperative to note that their methodology deliberately avoids environmental and geographical constraints considerations.

Researchers have suggested various innovative approaches concerning voltage assessment techniques and problem formulation methods to address voltage security issues. The escalating demand in the future gives rise to a frequent rate of voltage change, particularly at nodes identified as sensitive nodes, leading to the potential occurrence of voltage collapse [62, 63]. Improving load-ability entails the reliable identification of sensitive nodes and the strategic control of voltage at vulnerable buses through optimal placement of DG [62]. Diverse indices for predicting voltage collapse in power systems have been proposed by different researchers using steady-state analytical methods [64–66]. Additionally, literature has explored DG placement techniques based on voltage stability to position DG units on the weakest buses, prone to voltage collapse in the near future [67, 68].

Multi-objective planning (MOP) offers a more pragmatic approach to enhance DG sizing and placement by determining an optimal compromise solution from a range of single objective functions. Within the literature, the amalgamation of various objectives, along with improving voltage profiles, using weighting factors results in a unified objective function termed the Weight Objective Function, as formally articulated in (1.9). In (1.9), α represents the weight coefficient, $F_L(X)$ represents an objective function, for example, the energy loss function, and $F_V(X)$ represents the voltage profile function.

$$\text{Minimize } F(X) = \alpha \frac{F_L(X)}{F_L\left(X^{(base)}\right)} + (1-\alpha) \frac{F_V(X)}{F_V\left(X^{(base)}\right)} \tag{1.9}$$

The stud krill herd optimization technique is used in [69] to solve a weighted-sum MOP for the ideal location and sizing of DGs, where the appropriate weight preferences for the problem objectives have been taken

subjectively. An analytical hierarchical process (AHP) technique is widely utilized for obtaining the weight coefficients in the weighted-sum method of MOP [70–73]. However, the pairwise comparison matrix in the AHP technique is formed based on the decision maker's choice. The weighted normalized decision matrix is constructed based on predetermined weight coefficients in the technique for order preference by similarity to ideal solution (TOPSIS) to find the preferred alternative most near to the positive ideal solution while solving MOP for optimal siting and sizing of DGs in [73, 74]. The selection of appropriate weight factors in weighted-sum MOP is still challenging and poses ambiguity [75].

Various methods have recently been developed based on the Pareto dominance concept to obtain trade-off solutions among the different objectives in a MOP, such as Harris Hawks optimizer [75], non-dominated sorting genetic algorithm (NSGA) [76], and multi-objective differential evolution [77]. However, relatively fewer efforts have been laid into presenting strategies for selecting the best trade-off from a set of non-dominated solutions, which still requires further research. Often, distance-based methods, such as grey relational analysis [75] and fuzzy decision [76–78], are utilized instead of investigating the inherent relationship (*i.e.*, relative influence) among objectives to find the best alternative.

The literature review reveals numerous approaches have addressed the optimal allocation problem of DGs in the distribution network to reduce investment and operational costs, as in [79–84]. Reference [79] proposes a multi-stage planning model and stochastically characterizes the demand and renewable generation uncertainties. Efficient planning strategies are suggested for DG integration in community micro-grids in [80, 81]. A tri-level planning model for DERs amalgamation is presented in [82], and robust optimization has been used to handle different physical and financial uncertainties. Reference [83] suggests a two-stage robust optimization framework for non-dispatchable DG investment planning to facilitate the uncertain charging demand of electric vehicles (EVs). Reference [84] proposes a flexible global strategy for distribution planning in a two-stage optimization process which probabilistically aids the uncertainty modeling. Multi-stage problem formulation in [81–84] solves investment optimization in the prior stage, and then operational objectives are optimized in the later stage subject to security and reliability-related constraints.

A comprehensive model is presented in [85] to optimally select wind power plant technologies and allocate them to distribution networks. A method for combined expansion of the distribution network and generating resources has been proposed in [86] for social welfare maximization. Reference [87] emphasizes distribution network planning methodology to optimize the quality of supply as well as operational costs. A multi-state model for DG optimal allocation has been reported in [88] that accommodates all possible real-world operating conditions of loads and DGs. A non-biased DG allocation strategy has been proposed in [89] to avoid topological biases and incentive self-consumption instead of trading locally or to the grid.

Recently, the optimal planning frameworks for DG allocation have been developed to mitigate the effect of the surge in demand due to the heavy integration of EVs in the distribution systems [83, 90, 91]. A stochastic-based optimization model has been proposed in [90] for optimal sizing and siting of small wind turbines in urban or suburban areas. Reference [91] presents a comprehensive model to co-optimize the size and location of DGs, energy storage units, and EV charging stations. In general, the DG allocation problem is complex, mixed-integer, multi-objective, and stochastic due to the uncertain behavior of renewable energy resources and hard to solve in its present form. Evolutionary algorithms like improved non-dominated sorting genetic algorithm [76] and decomposition-based algorithm [92] effectively solve the optimization problem; however, being trapped into a locally optimal solution raises concern about using such algorithms. An efficient analytical technique has been illustrated in [93] to enhance computational speed and accuracy compared to classical analytical-based methods. A data-driven approach for evaluating the optimal size of renewable distributed generation is suggested in [94], reducing the complexity and computational burden.

The techniques and methods employed for the sizing and siting of DG can be broadly categorized into analytical, classical optimization, meta-heuristic, and other techniques. Analytical techniques involve mathematical modeling and direct numerical solutions, suitable for small and simple systems. However, for large and complex systems, they may face challenges in computational efficiency. Examples include Eigen-Value based Analysis [95], Index method [96], Sensitivity-Based Method [97], and Point Estimation Method [98].

Classical optimization techniques aim to optimize formulated problems under given conditions and constraints. This category includes Linear Programming [95], Mixed Non-linear Programming [99], Dynamic Programming [100], Sequential Quadratic Programming [99], Ordinal Optimization [101], Optimal Power Flow [102], and continuous power flow [103]. These methods cater to linear and nonlinear objective functions and constraints, handling optimization efficiently. Meta-heuristic techniques, such as Fuzzy Logic [104], Genetic Algorithm [105], Ant Colony Search Algorithm [98], Artificial Bee Colony [101] and others, offer efficient, accurate, and optimal solutions for complex problems. These methods are up-and-coming for addressing challenges in diverse areas.

Other techniques encompass various approaches like Clustering-based [106], Tabu-Search Algorithm [107], Bat Algorithm [108], Big Bang Big Crunch Optimization [109], Brute Force algorithm [110], Backtracking Search Optimization [111], and Modified Teaching-Learning Based Optimization [112]. Each technique serves specific purposes, ranging from clustering patterns to adaptive memory-based optimization.

These methods collectively present a comprehensive toolkit for addressing challenges related to DG sizing and siting in power distribution systems, offering a range of options suited to different system complexities and optimization objectives [104, 113].

1.2.2 Optimal Distribution Network Operations with DERs

The design of utility distribution systems is aimed at efficiently delivering reliable electric power to consumers at their point of use. However, in the past decade, the electric power grid has undergone unprecedented transformations, necessitating a substantial shift in the design, operation, and control of traditional power systems. Factors such as the increased penetration of DERs, the integration of EVs, bi-directional power flow, and the implementation of smart metering are reshaping the power grid. The inherent variability of renewable generation and the susceptibility of traditional power systems to demand and generation fluctuations pose potential challenges at the system level. Nevertheless, these emerging technologies can offer essential grid services

to enhance efficiency, reliability, and resilience if strategically deployed and controlled.

Traditionally, distribution system operations have been predominantly passive, relying on rule-based methods to control a few legacy voltage control devices like capacitor banks and voltage regulators along the feeder. These controls operated based on pre-designed rules and local measurements, suitable for predictable loads and systems lacking local generation resources. However, integrating DERs introduced variability and uncertainty, rendering rule-based and local-control-only algorithms inadequate. Studies have indicated that incorporating active grid-edge resources, such as PVs, WTs, ESs, or new load types like EVs, may lead to various system-level challenges, including voltage limit violations, increased voltage variability, three-phase voltage unbalance, and thermal limit violations [114, 115].

Additionally, it has been observed that relying solely on local control may result in unnecessary tap changes and capacitor bank operations, which, being mechanical devices, are prone to failure with an increased number of operations [116]. Addressing these system-level operational challenges necessitates a coordinated operation of controllable devices within the system, including the integration of new resources. Recognizing the potential of these grid-edge resources to provide additional grid services, such as capacity, flexibility, ramping, and voltage support, has spurred the development of new methods and advanced applications for actively managing these resources in power distribution systems [117].

This thesis conducts a thorough analysis of the current literature related to the optimization of EV Fleet Operations in smart distribution systems, and DERs within distribution systems, focusing on their modeling and optimization aspects. The primary focus is on delivering a comprehensive review and analysis, spotlighting the limitations of existing methodologies, and laying the groundwork for progress in the domain, that will be elaborated upon in the following subsections.

Optimizing EV Fleet Operations in Smart Distribution System

Worldwide, there is a global shift towards converting vehicles to electric power as a strategic response to address climate change and mitigate pollution. To sustain and facilitate this transition, it is imperative to expand the infrastructure of electric vehicle charging stations (EVCS) to cater to the growing demand among the general population. However, the simultaneous and uncoordinated proliferation of EV and the corresponding expansion of EVCS may have far-reaching consequences on the distribution network, environmental conditions, EV users, and the charging stations themselves. These repercussions pose substantial challenges of a technical, economic, and environmental nature [118]. Effectively the charging and discharging coordination and scheduling activities of EVs at EVCSs becomes crucial to preemptively address these challenges [119]. Furthermore, recognizing EVs as potential sources of energy storage opens avenues for leveraging their capabilities to enhance network performance and efficiency through adept control mechanism [120].

The electrification of vehicles constitutes a key aspect in realizing a zero-emission transportation system [121]. EVs serve as a primary alternative in this paradigm shift [122]. However, challenges such as the high cost of EVs and the scarcity of EVCS significantly influence public preference during the transition to EVs [123, 124]. The uncoordinated EVCS in the distribution system poses challenges for power network management, operation, and control, thereby jeopardizing system reliability [122, 125]. Over the past decade, research has intensified concerning the optimal placement of EVCSs and the impact of EV dispatching on the distribution network [126, 127].

As the EV count on the road increases, regulating their charging/discharging becomes more complex, akin to the challenges posed by the "egg or chicken" theory [124]. Establishing a charging infrastructure necessitates a visible presence of EVs, creating a cycle where investors await more EVs on the road while potential users delay EV purchases until more EVCSs are available. Lopes et al. [26] highlight four key considerations associated with the widespread integration of EVs. The outlined investigations encompass:

1. an assessment of the effects of battery charging on power system operations;

2. the delineation of appropriate operational management and control methodologies concerning the charging intervals of EV batteries;
3. the identification of optimal strategies for prioritizing the utilization of RES in charging EVs and
4. an evaluation of the potential for EVs to contribute to power system services, encompassing provisions for reserves and power delivery.

Extensive research has been conducted to elucidate the advantages of EVs and mitigate the associated challenges. The literature reveals that adapting the dispatch of EVs can lower the adverse effects of their integration into the grid, thereby contributing substantially to enhancing overall system efficiency [128–130]. Furthermore, the systematic deployment of EVs through aggregators exhibits the potential to mitigate grid load fluctuations and provide diverse ancillary services. It has the consequential effect of optimizing the operational aspects of the grid, encompassing economic efficiency, security, and stability [131].

Primarily, the literature has classified three distinct control strategies to pursue the techno-economic objectives. These strategies are centralized control, and decentralized framework involving transactive and price control. Centralized control entails direct scheduling and control of EVs. In contrast, decentralized control typically relies on pricing signals, where individual EVs optimize their charging based on electricity price information provided by EV aggregators or DSOs. The primary distinction between transactive and price control lies in the information exchange requirements; transactive control necessitates explicit responses from individual EVs, while price control does not require such responses. It is generally acknowledged that centralized control yields system-level decisions, ensuring superior results such as power system security [132, 133]. However, the drawback is the high cost of communication infrastructure for centralized charging. A notable advantage of decentralized control is the potential to minimize communication infrastructure costs [134]. Nonetheless, the optimality of the dispatch solution depends on information sharing and the methods employed for scheduling.

The authors [135, 136] conducted a comparative analysis of centralized and decentralized control methods against devising optimal plans for energy

delivery to EVs while mitigating grid congestion. Their study primarily focused on the communication aspects of both strategies, delineating their respective advantages and disadvantages. However, a more thorough investigation is required to assess how the control strategy and the optimization technique influence the performance and requirements at the physical and information layers of the system.

The author [137] employed linear approximation to characterize the battery state of charge, formulating the charging process of an EV fleet as a Linear Programming (LP) optimization problem aimed at minimizing charging costs. The lower computational time and simple linear order problem formulation make the LP technique widely utilized in prevailing studies [138]. The author in [139] formulated a Sequential Quadratic Optimization problem for the power losses stemming from significant EV penetration into the grid. The approach presented in [140] introduced a classical dynamic programming formulation to minimize charging costs through participation in the regulation market. Results from [139] indicate that the disparity in charging profiles between Quadratic Programming (QP) and Dynamic Programming (DP) techniques is negligible. However, due to the heavier storage requirements of DP compared to QP, the computational time for DP is longer.

In [141], Mixed-Integer Linear Programming was utilized to assess the impact of EVs in power systems characterized by high wind generation and demand response programs. The application of Mixed-Integer Non-Linear Programming was explored in EV scheduling, particularly when considering other distributed resources with non-linear operational characteristics. It is crucial when introducing network technical constraints such as line thermal limits and bus voltage operation boundaries [142]. Recently, as observed in studies [137, 140], assumes deterministic knowledge of load profiles, the initial state of charge, driving patterns, grid conditions, and electricity prices. However, this assumption does not align with realistic scenarios. Therefore, there is a compelling need to adopt a stochastic approach [143–145] and robust optimization techniques [146, 147] to mitigate risks associated with uncertainties in the mentioned aspects.

An exploration into the potential of EVs to contribute to load recovery, enhance network stability, and improve power system metrics emerges as a

critical avenue. This investigation necessitates a delicate approach that integrates economic objectives and accounts for the preferences of key stakeholders such as the system operator, EV aggregator, and EV owner. Determining the most effective strategy for EV dispatching requires a delicate balance, acknowledging the varied interests and priorities of each party involved [127]. As society witnesses a proliferation of diverse EV models in the coming years, the necessity arises for a charging infrastructure that is not only readily accessible but also equipped with unique charging tactics tailored to individual EV specifications. Recognizing the evolving significance of EVs as valuable assets, the impending transition from the existing centralized grid to a decentralized structure and an upgraded communication network is poised to facilitate their widespread integration. Smart charging methods, coupled with the increased utilization of Vehicle-to-Grid (V2G) and connected mobility technologies, will underscore the multifaceted benefits of EVs [148, 149]. To effectively coordinate the diverse objectives in the smart charging of EVs, recent trends emphasize the integration of interests encompassing EV owners, ancillary services required by the transmission system operator, and the distribution system operator. These integrative approaches acknowledge potential conflicts, particularly concerning EV flexibility, necessitating real-time EV fleet management for optimal functionality [150, 151].

DERs on Distribution Network: Modelling and Optimization

In recent years, there has been a notable surge in the interest enfolding DERs, primarily attributed to their fast deployment in power capacity installations and their presence in distribution systems. DERs largely implicate DGs and ESs, with some definitions extending to include EVs, demand response (DR) strategies, and intelligent electronic devices (IEDs) utilized for grid coupling. The integration of DERs introduces challenges to the overall operating system due to the diverse nature of energy generation from RESs, the probabilistic aspects of EV charging, and the exponential integration of IEDs by end-users. This section organized a literature review on DERs, including aspects such as modeling, control techniques, energy flexibility, objective functions, and the impacts of DERs on distribution network operation.

The literature review primarily focuses on the definitions and fundamental characteristics of DERs, including the modeling of RESs, especially WTs and PVs, ESs, DR, and EVs. The produced energy estimation of a WT relies on historical wind data from the specified location and the turbine's power curve. Commonly employed probabilistic load flow models utilize Weibull or Rayleigh density functions for representing wind behavior [152]. Power curves, integral to the modeling process, can be supplied by manufacturers [153] or calculated using mathematical formulations, as exemplified by (1.10) [154] and (1.11) [155]. These equations involve variables such as wind speed (v), power generated from the wind turbine (P_w), a constant (F) accounting for turbine efficiency and air density, initial and final cutting speeds (v_{ci}andv_{co}), and wind turbine nominal power (P_N).

$$P_w = \begin{cases} 0, & v < v_{ci} o v > v_{co} \\ Fv^3, & v_{ci} \leq v \leq \sqrt[3]{P_N/F} \\ P_N, & \sqrt[3]{P_N/F} < v \leq v_{co} \end{cases} \tag{1.10}$$

$$P_w = \begin{cases} 0 & v < v_{ci} o v > v_{co} \\ P_N \frac{v^3 - v_{ci}^3}{v_N^3 - v_{ci}^3} & v_{ci} \leq v \leq v_N \\ P_N & v_N < v \leq v_{co} \end{cases} \tag{1.11}$$

In PV systems, the output power can be characterized through mathematical modeling or empirical measurements [154, 156, 157], catering to deterministic and probabilistic methods. (1.12) and (1.13) provide a means to calculate the power of a PV panel (P_{PV}), incorporating parameters such as panel area (A_{pv}), global horizontal irradiance (G_{inc}), temperature coefficient (β_{ref}), nominal efficiency (η_{ref}), operating temperature (T_{op}), and reference temperature (T_{ref}). To determine the (T_{op}), standard test conditions must be considered like ambient temperature (T_a), PV cell temperature under normal conditions ($NOCT$), T_{ref}, and solar irradiance of reference ($1000\ W/m^2$).

$$P_{PV} = A_{pv} \cdot G_{\text{inc}} \cdot \eta_{\text{ref}} \left[1 + \beta_{\text{ref}} \left(T_{\text{op}} - T_{\text{ref}}\right)\right] \tag{1.12}$$

$$T_{\text{op}} = T_{\text{a}} + \frac{NOCT - 20}{800} \cdot G_{\text{inc}} \tag{1.13}$$

Furthermore, (1.14) and (1.15) elucidate models for ESs, facilitating the computation of both charging and discharging the battery's energy over time. These models factor in instant energy, charge or discharge power, and battery and inverter efficiencies [158].

$$E_{bat,ch(t+\Delta t)} = E^{\min}_{bat(t0)} + \Delta t^* {P_{bat,ch(t)}}^* \eta_{bat,inv} \tag{1.14}$$

$$E_{bat,dis(t+\Delta t)} = E_{bat(t)} + \Delta t^* \frac{P_{bat,dis(t)}}{\eta_{bat,inv}} \tag{1.15}$$

The modeling of EVCS involves time step-based approaches [156, 159] using models such as constant power, constant impedance, and constant current (ZIP models) [160] or probabilistic representations, such as probability density functions, describing the stochastic aspects of EV trajectories, arrival and departure times, and daily journey counts [161, 162]. Additionally, the literature outlines EVCS modeling in either the time domain [163, 164] or frequency domain [163], providing insights into the non-linearity of these EVCSs concerning the power grid. The preceding subsection has already conducted a thorough literature review on EVs and EVCSs.

Finally, electrical loads are modeled as linear components subject to hourly variations [165], incorporating probability functions [166]. These loads may exhibit changes in behavior influenced by incentive programs, such as demand response [167]. DR involves altering electricity consumption patterns in response to energy price fluctuations. The Department of Energy in the United States defines DR as an incentive framework to curtail electricity consumption during high energy price periods in the wholesale market or compromise power system reliability. The International Energy Agency (IEA) broadens this definition to encompass intentional modifications to end-users electricity consumption patterns involving shifts in time, power, or energy consumption [168].

The literature review reveals a growing utilization of DERs in electric power systems, necessitating extensive research for a smooth transition into the existing distribution infrastructure. Reference [169] emphasizes the importance of DER integration to meet future electricity demands in industrialized countries. Reference [170] conducts a steady-state and dynamic analysis of a microgrid, showing that the insertion of DER significantly improves voltage profiles and

reduces power flows and losses. Reference [171] defines microgrids as aggregations of electrical loads and RESs, emphasizing the role of Energy Management Systems (EMS). Reference [172] employs the DER Customer Adoption Model to study small-scale onsite generators. References [173, 174] stress the benefits of integrating various DERs via microgrids, with [174] proposing an agent-based control framework.

The literature further discusses challenges and solutions in DER integration [175, 176], benchmarks for modeling DER integration [177], and methods for hierarchically integrating DERs into existing power distribution systems [178, 179]. Reference [180] stresses the importance of integrating RESs, while [181] discusses challenges and solutions in smart power distribution networks. Reference [182] proposes a two-layer simulation-based optimization method for optimal DER allocation. Reference [183] presents a MILP model for DER system design, and [184] delineates a method for determining the optimal size of an ES for primary frequency control. Reference [185] reviews modeling, planning, and energy management of DERs integrated microgrids, emphasizing their potential to solve energy-related problems.

Effectively managing a large fleet of DER devices poses significant challenges in system-wide operation and control, primarily due to computational intricacy [186–188]. Power aggregation has emerged as a promising solution to address this challenge, garnering considerable attention for harnessing flexibility from the distribution side. Each DER device's power generation or consumption can be encapsulated within a feasible region defined by its operational constraints and dynamics. Power aggregation involves modeling and characterizing the aggregate flexibility at the substation, representing the achievable net power injection into the distribution feeder. By succinctly presenting this feasible region, the distribution grid can actively engage in transmission system operation and control, effectively functioning as a virtual power plant [189].

Essentially, power aggregation can be viewed as a projection of high-dimensional operational constraints onto the feasible region of the net substation load. However, computational intensity and impracticality arise when dealing with tens of thousands of electric devices and multiple time steps. Therefore, much research focuses on constructing inner or outer approximations of the exact feasible region. Reference [190] employs time-moving ellipsoids to

model the aggregate P-Q feasible domain over time, employing a data-driven system identification procedure for obtaining model parameters. In [191, 192], the individual flexibility of each DER is described as a polytopic feasible set, with aggregate flexibility calculated as the Minkowski sum of individual polytopes. Reference [193] applies polytopic projection to derive aggregate flexibility and formulates an approximated optimization problem for a tractable solution. Robust optimization models for estimating and optimally scheduling aggregate reserve capacities, considering uncertainties in regulation signals and forecast errors, are developed in [[194, 195].

Following these developments, various control strategies have been proposed for utilizing DER flexibility for grid services. Strategies in [196–198] incentivize DER owners for grid services, considering the DER aggregator's revenue maximization and/or DER owners' cost minimization, with decoupled energy exchange and regulation periods. In [199], a multilayered decentralized DER coordination approach is presented for tracking a given profile while maximizing aggregator revenues. In [200], real-time controllers are developed for following the trajectory of a regulation service signal without considering cost objectives. Notably, these studies do not account for interactions between DERs and the distribution feeder; DERs merely track predetermined profiles.

Studies [201–203] consider the distribution feeder's network topology and develop algorithms for DER coordination. In [201], DERs generate their schedules via self-optimization, and subsequently rescheduled for distribution feeder operation cost minimization without considering their self-optimization preferences. MPC-based strategies for EV charging stations with EVs as DERs are developed in [202, 203]. In [202], the cost of power generation and EV charging is minimized, with EVs having only grid-to-vehicle capability. In [203], the cost of generators in the distribution feeder is minimized while fulfilling only EV charging constraints.

DERs present an exciting challenge for the current engineering sector, particularly in the energy field. Every advance and effort made by the public or private sector to develop and deploy reliable, affordable, and accessible DERs is crucial for integration. Notably, much research on DERs often focuses on studying one or two technologies simultaneously, with the analysis of three technologies in a row occurring infrequently. Furthermore, the typical

distribution network topology considers the radial configuration for DER integration, emphasizing that DERs contribute to reducing expenditures in power grid reinforcement. Achieving this goal requires combining DER technologies with optimization algorithms for allocation, dispatch, and operative control.

1.3 Research Gap

Some of the gaps identified in the literature are as follows:

1. The previous studies mainly focus on a single criterion, *e.g.*, either of loss reduction, voltage stability, or system load ability and neglect some of the equally critical quantities while proving the solution for determining the capacitors' optimal location.

2. The past studies postulate the multi-objective problem formulation for obtaining the optimal solution of DG placement; however, no adequate technique is proposed to quantify the relative weight coefficient in multi-objective optimization.

3. Economic consideration has become an inevitable factor in the present electricity paradigm. Therefore, electric vehicle charging schedule optimization to reduce operation costs from the perspective of the distribution system operator.

4. Control techniques for dispatching DERs lack a few important considerations, like eliminating discrete decision variables in problem formulation, flexibility evaluation without considering network constraints, and self-optimization preferences.

1.4 Research Objectives

Based on the research gaps identified in Section 1.3. The main objective of the thesis is to provide comprehensive techno-economic improvement directives for

a smart distribution system. For this, the following research studies need to be conducted:

1. **Optimal allocation for shunt capacitors in the smart distribution system.**

   To develop a suitable method for optimal allocation of capacitors, including multiple criteria (e.g., voltage stability, loss reduction, and system load-ability) for obtaining a pragmatically feasible techno-commercial solution.

2. **Optimal solutions for distributed energy resource placement in the smart distribution system.**

   To formulate a multi-objective problem that incorporates different technical and economic impact indices (i.e., real power loss, reactive power loss, voltage deviation, and DER installation cost) based on their degree of importance in distribution network planning.

3. **Effective cost analysis of electric vehicle.**

   Optimizing the system operation cost by capturing charging/ discharging modes provides a nearly optimal solution to the smart distribution system's global EV charging scheduling problem.

4. **Day-ahead scheduling optimization of DERs and EV based on dynamic pricing signal for a smart distribution system.**

   To minimize the operation costs by optimal day-ahead scheduling of DERs and EVs in a smart distribution system. The proposed approach will reduce the computational burden by eliminating the discrete decision variables in the problem formulation.

1.5 Structure of the Thesis

The remainder of the thesis is organized as follows: Chapter 2 introduces a novel index method for identifying the optimal node to deploy a capacitor bank in the smart distribution system. The optimization of the capacitor bank size is conducted using a particle swarm optimization technique. The chapter

illustrates the efficacy of this innovative approach by applying it to three distinct RDN topologies, namely the IEEE 12-bus, 34-bus, and a practical 108-bus RDN from an Indian utility.

In Chapter 3, a method is outlined for establishing the weights assigned to objectives in a multi-objective optimization problem related to the optimal placement of DG. The chapter emphasizes the importance of impartially assessing these weights during the planning stages of DG placement in a smart distribution system. The effectiveness of this approach is validated through numerical simulations conducted on a 38-bus test system, considering various cases to showcase its efficacy.

In Chapter 4, a cost-effective analysis of EVs is presented through the optimization of charging and discharging schedules within the smart distribution system. This optimization integrates demand response, robust optimization, and single or multi-agent control strategies. Through case studies, the chapter provides a comprehensive analysis of different aspects involved in solving the global EV charging scheduling problem.

Chapter 5 presents a comprehensive framework that initially proposes an aggregation model for a sizable EV fleet and deferrable residential loads. Subsequently, it introduces a hierarchical control strategy to establish dispatch coordination among the utility operator, community aggregator, and DERs. The chapter conducts numerical simulations on the IEEE 123-bus system to demonstrate the applicability of the method on a large distribution network.

In Chapter 6, the primary focus is on presenting the key conclusions and contributions derived from the research. Additionally, the chapter outlines potential directions for future work, providing insights into areas that warrant further exploration and development.

Chapter 2

Optimal Allocation of Capacitor in Smart Distribution System

2.1 Preamble

This chapter focuses on enhancing power quality and reliability in electrical networks through strategically positioned shunt capacitor banks (SCB). The primary objective is to develop a method for the optimal allocation of capacitors, allowing for the consideration of multiple objective functions or criteria. The proposed approach begins with a load flow study to determine network quantities in an uncompensated state. Subsequently, optimal capacitor bank locations are identified using a novel indexing method based on Shannon's Entropy. The sizes of the optimal capacitor banks are then determined by applying the particle swarm optimization algorithm. The cost function is formulated as the minimization of the sum of active power loss cost and capacitors' annual costs while adhering to various operational constraints. The proposed approach is compared with previously published methods on radial distribution networks (RDN) of varying sizes (IEEE-12 bus, 34-bus, and 108-bus) to assess its effectiveness, revealing its superior performance.

The remainder of the chapter is organized as follows: In Section 2.2, the nomenclature for the parameters, indices, and variables employed in the problem formulation of optimal allocation for shunt capacitors in smart distribution systems is outlined. Section 2.3 describes the problem formulation and the approach for load flow analysis. Section 2.4 delineates Shannon's Entropy approach applied for raking the potential solutions of optimal allocation

and presents the proposed SE-IM approach for indexing the potential buses for optimal siting of the capacitors. Section 2.5 presents the simulated results carried out on three standard RDN, *i.e.*, IEEE-12 bus, 34 bus, and 108 bus, followed by the summary of the chapter in Section 2.6.

2.2 Nomenclature

Sets

U_b	Set of buses in the network
Γ	Set of lateral branches in the network
U_{cap}	Set of optimal location for capacitor placement

Variables

$I_{line}(I_{bus})$	Branch (bus) current
$I_{line}^{real}\left(I_{line}^{imag}\right)$	Real (imaginary) component of line current
V_{bus}/V_{Li}	i^{th} bus voltage in l^{th} lateral
$V_s\,(V_r)$	Voltage at sending (receiving) end of the node
$P_{Li}(Q_{Li})$	Real (reactive) power at i^{th} sending end bus in l^{th} lateral
$P_e^{eff}\left(Q_r^{eff}\right)$	Effective real (reactive) power at receiving end node
P^{loss}	Total active power loss
$\bar{I}_{kl}$	Normalized index score of k^{th} entity for l^{th} model

Parameters

λ_p	Active power loss cost per kW per annum
λ_{cap}	Capacitor installation cost per kVAr per annum
Q^T	Total demanded reactive power load
R	Line resistance in Ω
X	Line Reactance in Ω
Ω^{cap}	Capacitor size in kVAr
Q_t^{load}	Total demanded load

2.3 Optimal Capacitor Allocation Problem Formulation

The optimal allocation of capacitors is one of the most effective methods of minimizing power losses, and improving the voltage profile as they are significant in the distribution network [204]. The objectives comprise the optimal capacitor allocation problem are: defining of location, size, type, and control methods associated so that the technical and economic benefits could be maximized against the installation and annual running cost of the SCB. In this section, the primary focus is on conducting a load flow analysis using a direct approach to assess the network parameters both before and after the integration of capacitors in a distribution network. Following that introduces the problem formulation, which aims to minimize the annual energy loss cost.

2.3.1 Direct Approach for Load Flow Analysis

The direct approach-based load flow analysis is more suitable for radial networks than the classical load flow analysis techniques and also requires less computational time to converge [205]. It evaluates two matrices using topological network attributes, which are bus injection to branch current (BIBC)

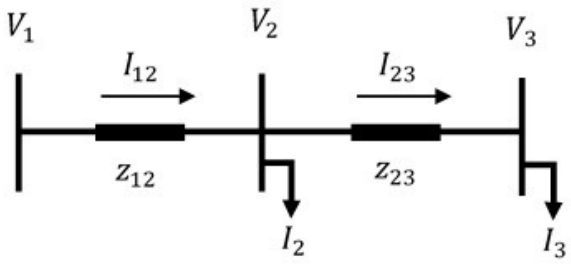

FIGURE 2.1: 3-bus network depicting bus and line parameters.

and branch current to bus voltage (BCBV) matrices. These matrices relate bus current to the bus voltage through branch current in the network. For a 3-bus RDN (see Figure 2.1), the relationship between the bus current, branch current, and bus voltage may be expressed by (2.1) and (2.2):

$$\begin{bmatrix} I_{12} \\ I_{23} \end{bmatrix}_{2\times1} = \begin{bmatrix} 1 & 1 \\ 0 & 1 \end{bmatrix}_{2\times2} \begin{bmatrix} I_2 \\ I_3 \end{bmatrix}_{2\times1} \tag{2.1}$$

$$\begin{bmatrix} V_1 \\ V_1 \end{bmatrix}_{2\times1} - \begin{bmatrix} V_2 \\ V_3 \end{bmatrix}_{2\times1} = \begin{bmatrix} z_{12} & 0 \\ z_{12} & z_{23} \end{bmatrix}_{2\times2} \begin{bmatrix} I_{12} \\ I_{23} \end{bmatrix}_{2\times1} \tag{2.2}$$

The bus voltage (V_1) is a slack bus in (2.2) and its magnitude is equal to 1. The voltages at bus 2 and 3 in (2.2) can be quantified using the branch currents I_{12} and I_{23}, which are determined by (2.1) using the bus currents I_2 and I_3. In general, for a main feeder radial distribution network having $\{1, 2, \ldots, n\} \in U_b \backslash N^0$ buses; the formulation of the BIBC and BCBV matrices may be represented by (2.3) and (2.4), respectively.

$$\left(I^k_{line}\right)_{(n-1)\times1} = [BIBC]_{(n-1)\times(n-1)} \left(I^k_{bus}\right)_{(n-1)\times1} \tag{2.3}$$

In (2.3), BIBC is a $((n-1)\times(n-1))$ matrix that dictates the relationship between bus and branch currents at k^{th} iteration. Similarly, the BCBV is a $((n-1)\times(n-1))$ matrix that portrays the relationship between the branch currents and bus voltages in the RDN.

$$\left(V_1 - V^k_{bus}\right)_{(n-1)\times1} = [BCBV]_{(n-1)\times(n-1)} \left(I^k_{line}\right)_{(n-1)\times1} \tag{2.4}$$

From (2.3) and (2.4), the distribution load flow matrix can be formed as:

$$\left(V_1 - V_{bus}^k\right)_{(n-1)\times 1} = [BIBC]_{(n-1)\times(n-1)}[BCBV]_{(n-1)\times(n-1)}\left(I_{bus}^k\right)_{(n-1)\times 1} \tag{2.5}$$

where

$$[BIBC]_{(n-1)\times(n-1)}[BCBV]_{(n-1)\times(n-1)} = [DLF]_{(n-1)\times(n-1)} \tag{2.6}$$

Several load flow studies have utilized this approach to carry out the load flow analysis, e.g., [206], [207], and found to be superior as the method saves computational time by avoiding LU factorization and backward-forward swapping of the Y admittance matrix or Jacobian matrix. Instead, it exploits the topological characteristics of RDN to solve load flow problems directly [205].

2.3.2 Minimization of Cost of Annual Energy Loss

The proposed approach focuses on the minimization of cost of annual energy loss (AEC) in \$/year, which is constituted by the annual active power loss cost (\$/kW) and the capital investment cost (\$/kVAr) of siting the capacitors at potential locations.

Mathematically, the AEC (in \$) function $S(\mathrm{P}^{loss}, \Omega^{cap})$ can be presented as:

$$S(\mathrm{P}^{loss}, \Omega^{cap}) = \left[\lambda_p \sum_{L\in\Gamma}\sum_{i\in U_b\setminus\{n\}} R_{Li+1}\frac{P_{Li}^2 + Q_{Li}^2}{V_{Li}^2}\right] + \left[\lambda_{cap}\sum_{j\in U_{cap}}\Omega_j^{cap}\right] \tag{2.7}$$

where λ_p and λ_{cap} are the cost parameters for active power loss cost (\$/kW/year) and capacitor installation cost (\$/kVAr/year), respectively. The expected life considered for a capacitor bank is ten years. The capacitor allocation problem can be formulated as a minimum of AEC function subjected to line flow and variable bound constraints, given by (2.8)-(2.12):

$$\min_{[P,Q,V,\Omega]} . \; S(\mathrm{P}^{loss}, \Omega^{cap}) \tag{2.8}$$

$$\text{subject to:} \quad (V_1 - V_{bus}) + [DLF]\,(I_{bus}) = 0 \tag{2.9}$$

$$U_{cap} - U_{cap}^{\max} \leq 0 \tag{2.10}$$

$$\Omega_t^{cap} - \alpha.Q_t^{load} \leq 0 \tag{2.11}$$

$$\Pi(V_{bus}, \Omega^{cap}) \leq 0 \tag{2.12}$$

where (2.8) represents the annual energy cost ($/year) as an objective function, (2.9) dictate the load flow analysis explained earlier, (2.10) represents the limit on capacitors number $U_{cap}^{\max}$ that can be installed, (2.11) represents the bound on total maximum capacitor size $\alpha.Q_t^{load}$ that can be installed and (2.12) represents the bounds on voltage and individual capacitor size. The value of α in (2.11) is selected so that the power factor will remain lagging or unity. However, due to intermittent capacitor sizes in a fixed-type capacitor scheme, it may be possible that the power factor becomes marginally leading. The minimum and maximum capacitor sizes (range) based on the two type schemes (switched or fixed) considered in this article are:

$$\Omega^{cap} = \begin{cases} (0 - 1200)\ kVAr; & \text{switched type capacitor} \\ \begin{bmatrix} 150,\ 300,\ 450, \\ 600,\ 750,\ 900, \\ 1050,\ 1200 \end{bmatrix}\ kVAr; & \text{fixed type capacitor} \end{cases}$$

To determine the optimal size of the capacitors in the considered RDN, classic Particle Swarm Optimization (PSO) is applied in the present work [208], as this algorithm requires lesser computational resources and time, and is also easy to implement compared to other meta-heuristic algorithms. To obtain the optimal sitting of the capacitors, the novel approach based on Shannon's Entropy (SE) is evaluated in the following Section.

2.4 Solution Methodology

The prevailing index methods for optimal allocation of capacitors are mainly focused on a single criterion, which is either of reduction of losses in the line or improvement of voltage at buses or increase in the load ability of the network. This work presents a novel methodology that enables the distribution network operator to include as many criteria as desired at a time for optimal capacitor allocation. In this approach, the optimal capacitor allocation problem is solved in

two stages. First, a load flow study is conducted for given busloads and line data, termed as the base case (un-compensated), to get the active power flow in each line and voltage profiles at the buses. In the second stage, the optimal site to place the capacitor is determined using the SE; and the optimal size is computed through classic PSO and given in Appendix A. The following sub-section briefly describes the concept of Shannon's Entropy.

2.4.1 Modeling of Shannon's Entropy

The concept of SE was proposed to quantify the degree of randomness in a variable in information theory by C.E. Shannon in 1948 [209]. This work utilizes the principle to acquire the degree of importance of an indexing model to obtain a cumulative index score. The SE formula e_l can be represented as:

$$e_l = -e_0 \sum_{k=1}^{s} \bar{\mathrm{I}}_{kl} . \ln \bar{\mathrm{I}}_{kl} \tag{2.13}$$

where e_0 denotes the entropy constant and is equal to $(\ln s)^{-1}$, $\bar{\mathrm{I}}_{kl}$ represents the normalized index scores of k^{th} entity (*i.e.*, bus in this case) for all considered indexing models (l) in the formulation. Furthermore, the degree of diversification can be obtained as: $\delta_l = 1 - e_l$; by normalizing $\mu_l = \delta_l / \sum_{l=1}^{r} \delta_l$, where μ_l is the degree of importance of an index model. The cumulative index score of any k^{th} entity is evaluated as:

$$\eta_k = \sum_{k=1}^{s} \mu_l I_{kl} \tag{2.14}$$

2.4.2 Proposed Shannon's Entropy-based Index Method

After the formulation of load flow study for an un-compensated network, Shannon's Entropy-based Index Method (SE-IM) prioritizes the buses based on their index score, which is computed by combining three existing indices, which are loss sensitivity index (LSI) [39], power loss index (PLI) [42], and voltage sensitivity index (VSI) [43]; a parametric study is summarized in Table 2.1. This approach allows the distribution network operator (DNO) to incorporate many criteria at a time to emulate the real-world scenario. The central aid of using SE is

to define the degree of importance for each index method (or criteria). The steps involved in solving the optimal capacitor problem using the novel SE-IM approach are described in the flow chart of the algorithm shown in Figure 2.2.

1. Data mining: load the bus data and line data of the network under study.
2. Identify or define the criteria required for improvement in RDN.
3. Optimal capacitor placement stage k = 1.
4. Do the load flow analysis as given in Section 2.3 for the base case (*i.e.*, uncompensated RDN).
5. Solve different existing index methods that improve the criteria mentioned in STEP 2.
6. Combine the index scores using the SE described in Section 2.4.
7. Sort the SE-IM score and their respective bus in descending order. The buses with high scores get priority for siting of capacitors.
8. Initialize an empty set G and set the candidate node count n = 1.
9. Apply the classic PSO algorithm to evaluate the optimal capacitor size Ω^{cap}, and repeat load flow analysis after capacitor placement.
10. Check whether the criteria obtained in STEP 9 are improved than those obtained in STEP 4. If yes, store the candidate node and capacitor size in G. Increment the count n by 1.
11. If $n > \max(N)$: go to STEP 12; else, go to STEP 9.
12. If G is an empty set: go to STEP 14; else, go to STEP 13. Empty G set signifies that no further significant improvement can be gained with further addition of capacitor, so algorithm stops.
13. If the next capacitor placement stage is to be carried, then increment k by one and check $k < \max(K)$; if yes, go to STEP 4.
14. Stop and print the obtained results.

TABLE 2.1: Existing index methods for optimal capacitor placement

Method	Index	Formulae	Feature/Comment
Method 1	LSI_1	$\frac{2\times Q_r^{eff}\times R_{line}}{\lvert V_r\rvert^2}$	- Obtained through the first derivative of P_{loss} with respect to the Q_r.
Method 2	LSI_2	$-2\times R_{line}\left[\frac{\left(P_r^{eff}\right)^2+\left(Q_r^{eff}\right)^2}{\lvert V_r\rvert^3}\right]$	- Obtained through the first derivative of P_{loss} with respect to the V_r.
Method 3	PLI	$\frac{1}{\lvert V_r\rvert^2}+\frac{I_{line}^{imag}}{I_{line}^{real}}+\frac{Q_r^{eff}}{Q^T}$	- Both capacitor location and size can be evaluated analytically.
Method 4	VSI	$\lvert V_s\rvert^4-4\times(P_rX_{line}-Q_rR_{line})^2$ $-4\times(P_rR_{line}+Q_rX_{line})\times\lvert V_s\rvert^2$	- Identify node which most sensitive to voltage collapse.

TABLE 2.2: Load flow analysis for uncompensated networks (before capacitor placement)

Test system	P-Loss (MW)	V_{max}/V_{min} (p.u.)	Weakest voltage bus	Computational time (sec.)	Load demand (MW)	AEC ($)
12-Bus	0.0207	1 / 0.9434	12	0.022	0.435	3479.28
34-Bus	0.2217	1 / 0.9417	27	0.025	4.637	37248.94
108-Bus	0.6450	1 / 0.8944	105	0.041	12.132	108363.14

2.5 Results and Discussion

The simulations study are carried out on radial distribution networks for IEEE 12 bus, 34 bus and 108-bus practical RDN of Indian utility to demonstrate the efficacy of the proposed approach. The comparison of the proposed approaches has been made with four prevailing index methods, which are loss sensitivity index methods 1 and 2 (LSI_1&2), vector-index method (PLI), and voltage sensitivity index method (VSI). The cost parameters $(\lambda_p$ and $\lambda_{cap})$ are considered as 168 \$/kW/annum and 5 \$/kVAr, respectively. The base quantities are considered for load flow studies are: $S_{base} = 100MVA$ and $kV_{base} = 11kV$. Table 2.2 reports the load flow solutions for base (before capacitor placement) RDNs at one p.u. load level. In Table 2.2, the computational time (including the time elapsed in solving the load flow problem, data/results calculations, and display of results) to converge the load flow solutions is stated. It is noteworthy that, as the network size increases, the considered load flow method becomes more time-efficient.

For the compensation of network, two cases based on the capacitor type have been considered; switched and fixed capacitor type schemes; the ranges or available sizes for capacitors are mentioned in Section 2.3. After determining the optimal siting, the optimal capacitor size is evaluated using the classic PSO algorithm. The result of the above approach is delineated in subsequent paragraphs.

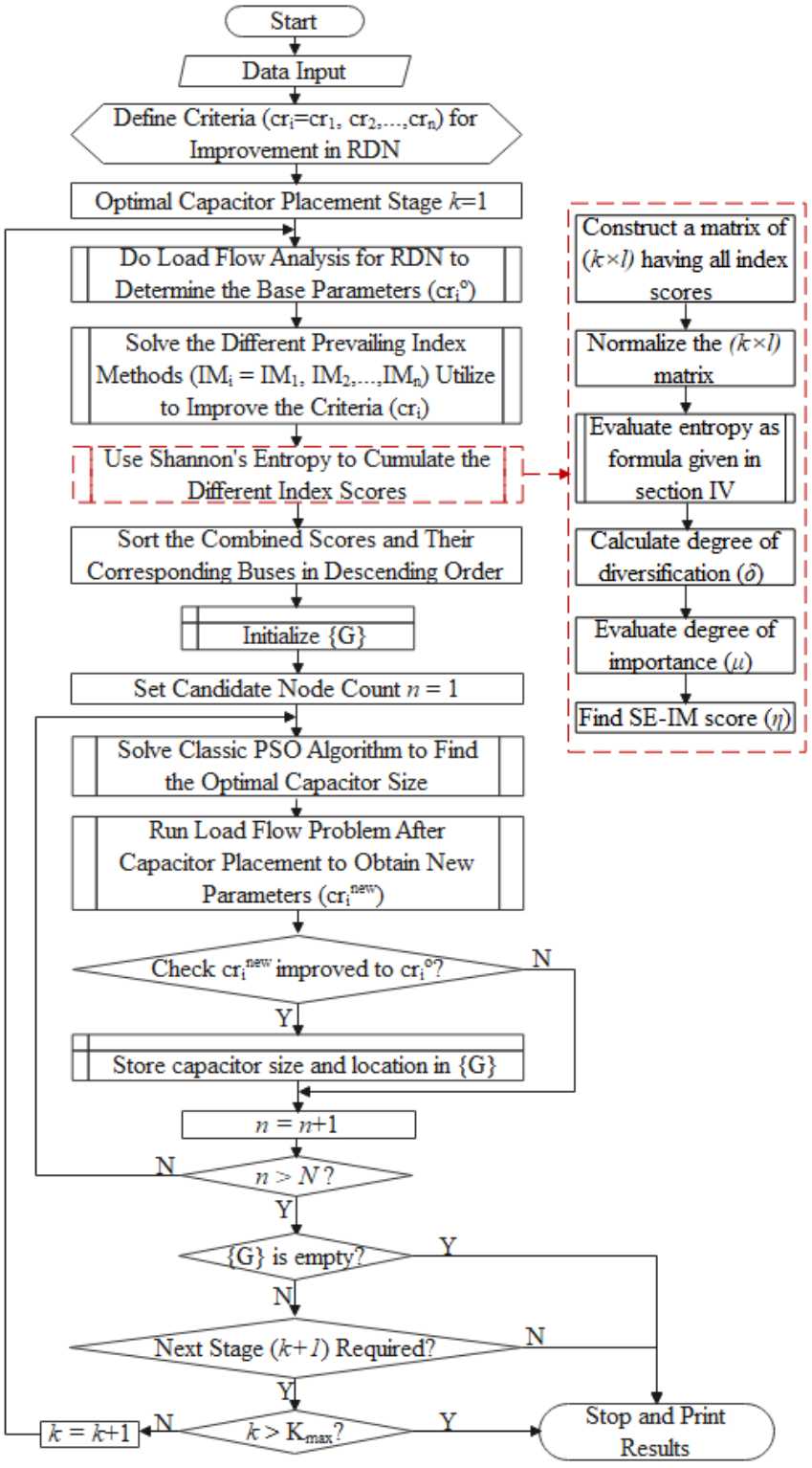

FIGURE 2.2: The workflow of the proposed SE-IM approach.

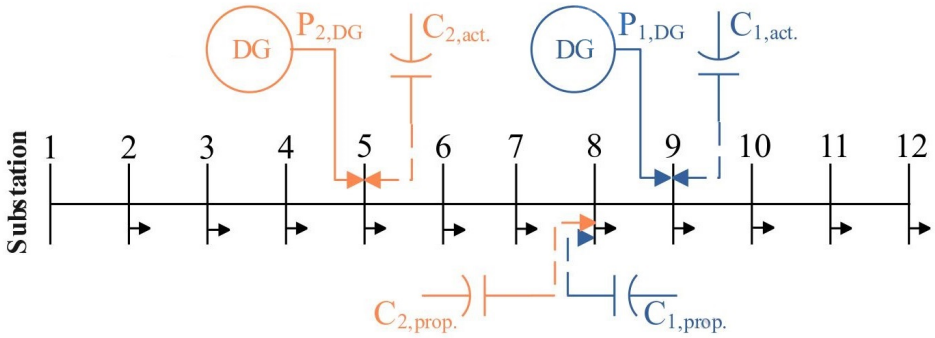

FIGURE 2.3: Single line diagram of IEEE-12 bus RDN including a distributed generator in case-1 (blue) and case-2 (orange).

2.5.1 Results of IEEE-12 Bus Radial Distribution Network

The IEEE-12 bus RDN is structurally simple and small network consisting of 11 lines connecting 12 buses radially as shown in Figure2.3. The total active and reactive powers supplied from the substation are 0.456 MW and 0.413 MVAr, respectively. The total active power loss that occurred in the RDN is 0.0207 MW as shown in Table 2.2. The SE-IM index score is quantified for all the nodes at one p.u. load level and presented in Figure 2.4. A comparative analysis between the prevailing index approaches and the proposed approach for the optimal allocation and sizing of the capacitor is performed and results are given in Table 2.3. For simulations of these approaches, it was considered that the upper and lower voltage limits are bounded to be 0.95 and 1.05 p.u., respectively. The maximum number of locations $\left(U_{cap}^{\max}\right)$ where the capacitor can be placed is restricted to one in each case. In Table 2.3, Case-1 and Case-2 represent the fixed capacitor type and switched capacitor type scheme, respectively. Followings are the main findings of the simulation study.

1. After the capacitor placement, there are significant improvements in techno-economical quantities that can be seen in comparison to the base case. The major technical quantities considered in the present analysis are the power loss reduction, voltage profile improvements, and reduction in the network's current (or power) flows. In addition, the analysis of economic quantity is the annual cost incurred due to the active power loss.

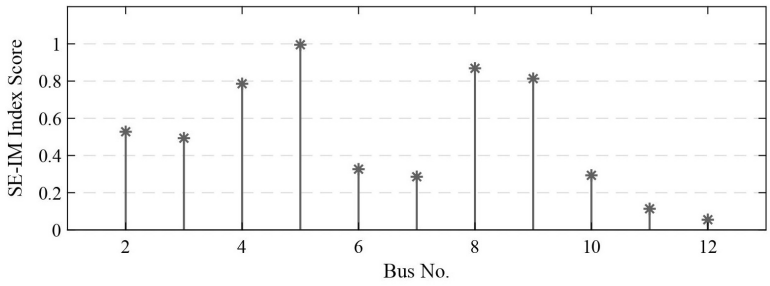

FIGURE 2.4: SE-IM index score for 12 bus RDN at 1 p.u. load level.

TABLE 2.3: Comparison among different existing index methods and proposed approach for IEEE-12 bus RDN

Method	Capacitor Position / Size (MVAr)	P-Loss (MW)	V_{max}/V_{min} (p.u.)	AEC ($)	Net Saving (%)
Method 1: Loss Sensitivity Index (1)					
Case-1	8 / 0.300	0.0129	1 / 0.9574	2169.52	33.33
Case-2	9 / 0.1284	0.0138	1 / 0.9515	2317.68	31.54
Method 2: Loss Sensitivity Index (2)					
Case-1	5 / 0.300	0.0141	1 / 0.9518	2365.37	27.70
Case-2	5 / 0.2333	0.0145	1 / 0.95	2437.85	26.58
Method 3: Vector Index (PLI)					
Case-1	4 / 0.450	0.0163	1 / 0.9506	2735.33	14.92
Case-2	4 / 0.4107	0.0161	1 / 0.95	2698.72	16.53
Method 4: Voltage Sensitivity Index (VSI)					
Case-1	12 / 0.150	0.0136	1 / 0.9545	2283.71	32.21
Case-2	12 / 0.1110	0.0144	1 / 0.9518	2417.59	28.92
Method 5: Shannon's Entropy based Index Method (Proposed)					
Case-1	8 / 0.300	0.0129	1 / 0.9574	2169.52	33.33
Case-2	9 / 0.1284	0.0138	1 / 0.9515	2317.68	31.54

2. The loss sensitivity index (Method 1) and the proposed approach prioritized the same buses for optimal capacitor placement, *i.e.*, 8^{th} bus for fixed capacitor and 9^{th} bus for switched capacitor type schemes.

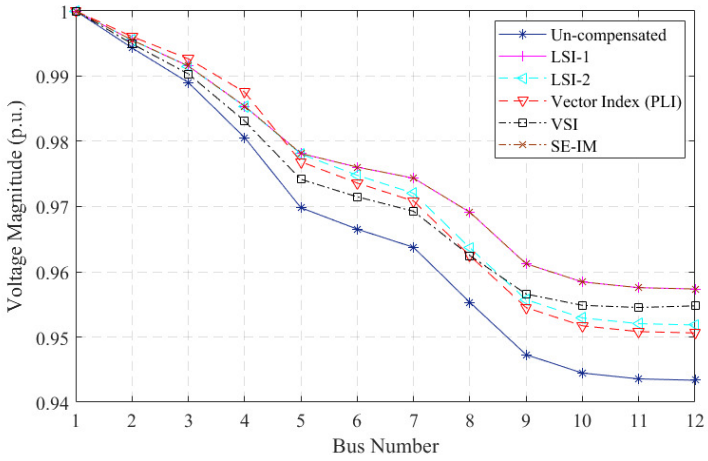

FIGURE 2.5: Voltage profiles for IEEE-12 bus RDN in case-1 (fixed capacitors).

3. The SE-IM approach mainly improves all the techno-economic quantities as compared to other method, except the node voltages in Case 2, which is significantly improved by the VSI (Method 4). The voltage profiles are delineated in Figures 2.5-2.6.

4. The results show that node 8 is best suited for a fixed capacitor placement scheme while node 9 is appropriate for a switched capacitor placement scheme. Finally, the PLI (Method 3) shows node 4 for optimal capacitor placement and generating the least preferable results in all manner.

Discussion on the capacitor size is omitted as this work mainly focuses on determining the optimal location for capacitor placement. However, the capacitor size is determined to enable the techno-economical comparison between the prevailing methods and the proposed method.

Optimal Capacitor Placement in the Presence of Distributed Generation

An analysis is carried out to understand the effectiveness of the proposed approach in the presence of distributed generation (DG). The computed results only consider the fixed type capacitor placement for the sake of simplicity and presented in Table 2.4. It is assumed that DG is of Type-1 (supply only real power P_{DG}), and two cases based on the location of DG are considered as follow (see Figure 2.3):

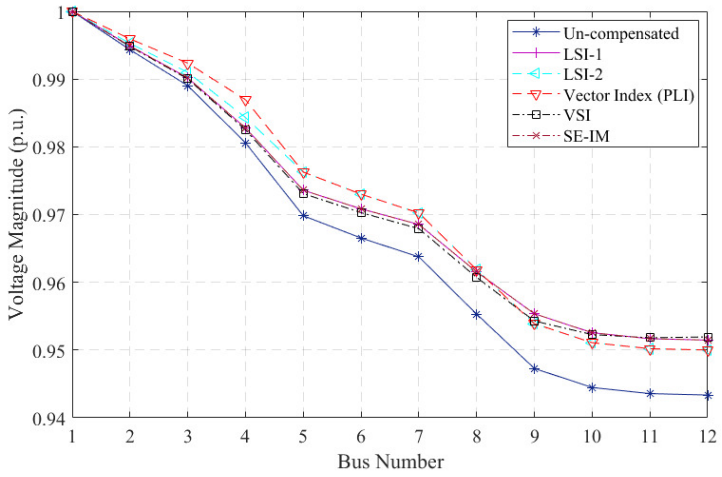

FIGURE 2.6: Voltage profiles for IEEE-12 bus RDN in case-2 (switched capacitors).

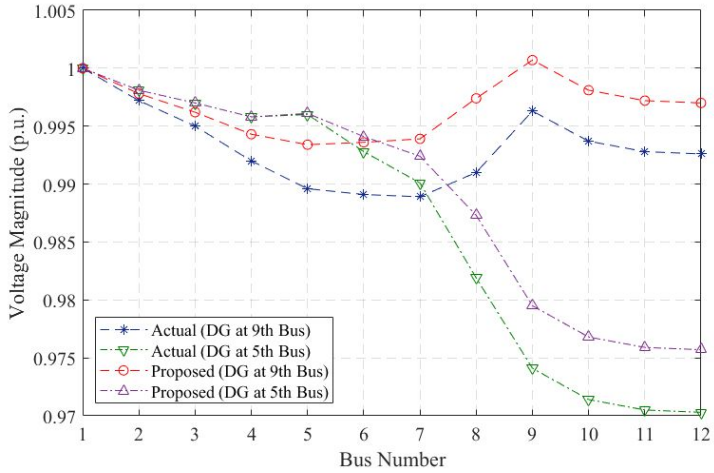

FIGURE 2.7: Voltage profile for IEEE-12 bus RDN after capacitor placement in the presence of single DG.

Case-1. When DG of 0.235 MW is placed at the 9^{th} bus.

Case-2. When DG of 0.280 MW is placed at the 5^{th} bus.

It is observed that the total real power loss reduction is more using the SE-IM approach for both cases (i.e., 83.09% and 73.43%, respectively) in comparison to the actual scenario (DG and capacitor are placed at the same node). The voltage profile improvement and real power flow curves are shown in Figure 2.7 and Figure 2.8, respectively.

TABLE 2.4: Comparison between two methods for adding single capacitor in the presence of DG

Method	DG Location / Size (MW)	Capacitor Position / Size (MVAr)	P-Loss (MW)	V_{max}/V_{min} (p.u.)	Net P-loss Reduction (%)
Actual*					
Case-1	9 / 0.235 [35]	9 / 0.150	0.0038	1 / 0.9889	81.64
Case-2	5 / 0.280 [35]	5 / 0.300	0.0066	1 / 0.9703	68.12
Proposed Approach					
Case-1	9 / 0.235	8 / 0.300	0.0035	1.0007 / 0.9934	83.09
Case-2	5 / 0.280	8 / 0.300	0.0055	1 / 0.9757	73.43

* It is assumed to place DG and capacitor at the same location.

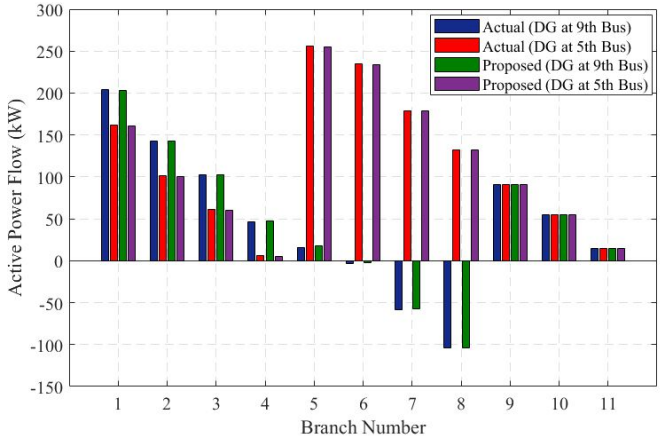

FIGURE 2.8: Active power flow in IEEE-12 bus RDN after capacitor placement in the presence of single DG.

2.5.2 Result of 34 Bus Radial Distribution Network

The proposed approach synergizes four prevailing methodologies through Shannon's entropy. The comparison of the result of the proposed approach vis-à-vis that of the prevailing index methods is presented in Table 2.5. The load flow results for the base network are given in Table 2.2, where total active loss was 221.72 kW and total annual loss cost incurred was USD 37248.94. For

simulations study using these approaches, it was considered that the maximum number of locations $U_{cap}^{\max}$ where the capacitors can be placed is limited to four in each case, and the minimum and maximum voltages limits on the buses are considered to be 0.95 p.u. and 1.05 p.u., respectively. In (2.11), the value of α is assumed to be 1.1, *i.e.*, the total kVAr capacity that can be injected into the network is limited to 1.1 times the total demand (*i.e.*, 2873.5 kVAr). In Table 2.5, Case-1 represents the fixed capacitor placement, and Case-2 represents the switched capacitor placement in RDN. Some of the important findings of this analysis are discussed below.

1. It is observed that there is a reduction in active power loss, and annual saving in \$/year and optimum for the proposed approach compared to the existing index methods. Though in Case-1, the active power loss reduced more by VSI method and voltage profile is better for vector-index (PLI) method; however, the combined active power loss and voltages profile is significantly improved for the SE-IM approach. The minimum and maximum voltage magnitudes are tabulated in Table 2.5 as well.

2. The annual energy loss cost (AEC) is minimum for the proposed approach in Case-2 (switched capacitor scheme), *i.e.*, USD 28252.64.

3. Figures 2.9 and 2.10 show the voltage profiles before and after compensation in Case-1 and Case-2, respectively. Figure 2.11 depicts the potential locations for capacitors allocation in 34 bus RDN, red color represents the switched capacitors, and green color represents the fixed capacitors.

4. The optimal locations and capacitors' sizes computed for the proposed approach is presented in Table 2.6.

2.5.3 Result of 108 bus RDN of an Indian utility

The comparative results for 108-bus practical RDN of an Indian utility are reported in Table 2.7. The maximum number of locations where the capacitors can be placed is limited to 15 in each case. The minimum and maximum voltages on the buses are considered as 0.90 p.u. and 1.10 p.u., respectively. In (2.11), the

TABLE 2.5: Comparison among different existing index methods and proposed approach for 34-bus RDN

Method	Total Capacitor Size (MVAr)	P-Loss (MW)	V_{max}/V_{min} (p.u.)	AEC ($)	Net Saving (%)
Method 1: Loss Sensitivity Index (1)					
Case-1	3.000	0.1624	1 / 0.9505	27285.32	22.72
Case-2	1.7773	0.1688	1 / 0.95	28350.90	21.50
Method 2: Loss Sensitivity Index (2)					
Case-1	2.850	0.1613	1 / 0.9504	27095.32	23.43
Case-2	1.7620	0.1688	1 / 0.95	28356.70	21.51
Method 3: Vector Index (PLI)					
Case-1	3.000	0.1610	1 / 0.9509	27040.14	23.38
Case-2	1.6261	0.1716	1 / 0.95	28820.98	20.44
Method 4: Voltage Sensitivity Index (VSI)					
Case-1	2.400	0.160	1 / 0.9505	26874.67	24.63
Case-2	1.7221	0.1684	1 / 0.95	28295.59	21.72
Method 5: Shannon's Entropy based Index Method (Proposed)					
Case-1	2.550	0.1609	1 / 0.9506	27037.32	23.99
Case-2	1.7472	0.1682	1 / 0.95	28252.64	21.81

TABLE 2.6: Optimum location and size in MVAr obtained using proposed approach

Case	Optimal Location and Size in MVAr
Case-1	19 (0.600); 7 (1.050); 23 (0.450); 25 (0.450)
Case-2	20 (0.2176); 23 (0.4592); 9 (0.2261); 25 (0.8444)

value of α is assumed to 1, which implies that the maximum total kVAr capacity that can be injected into the network is considered to be equal to the total demanded load (*i.e.*, 9.099 MVAr). Table 2.7 shows that active power loss reduced significantly for the proposed approach compared to that of the

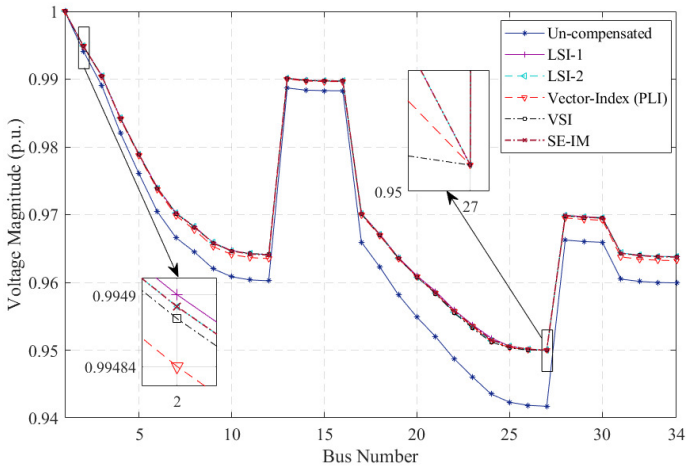

FIGURE 2.9: Voltage profiles for 34 bus RDN in Case-1 (fixed capacitors).

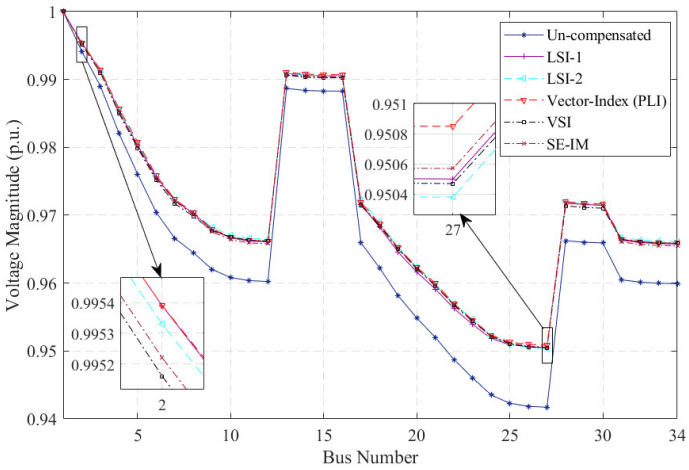

FIGURE 2.10: Voltage profiles for 34 bus RDN in Case-2 (switched capacitors).

prevailing methods; as a result, the AEC noticeably reduced. In Table 2.7, Case-1 and Case-2 represent the fixed and switched capacitor placement type schemes in RDN.

The SE-IM approach gives flexibility to the network operators for selecting the various criterion based on requirements. The inclusion of as many criteria into the formulation will make the optimal capacitor allocation problem more realistic. Figure 2.12 and Figure 2.13 present the voltage profiles calculated through the prevailing and the proposed methods.

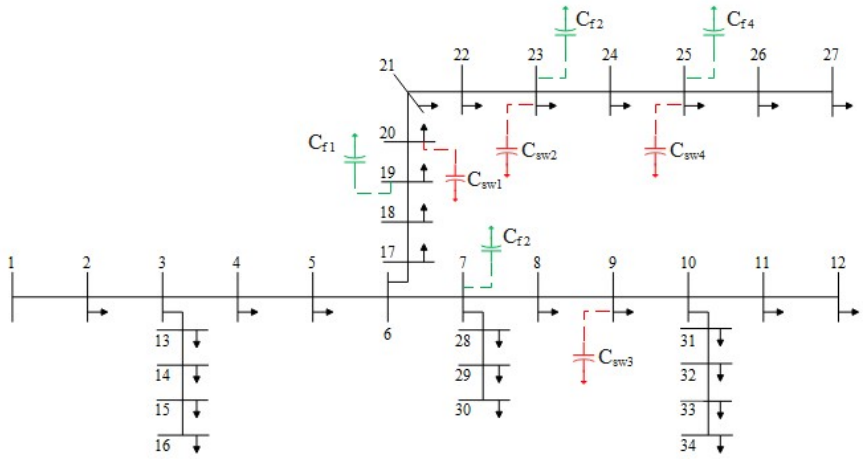

FIGURE 2.11: 34 bus RDN depicting potential locations for switched capacitors (red) or fixed capacitors (green) using SE-IM approach.

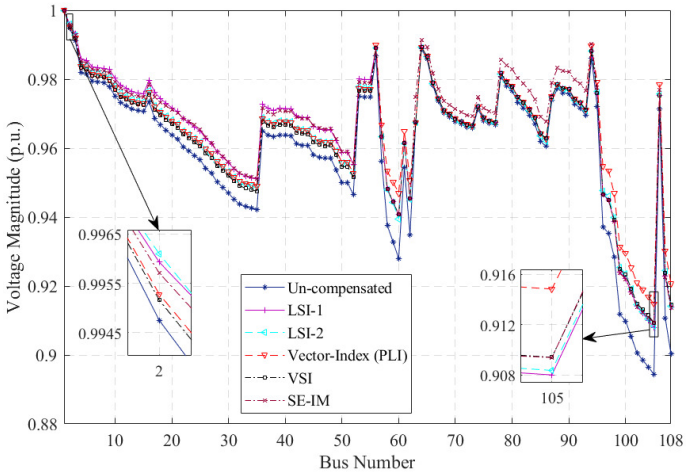

FIGURE 2.12: Voltage profiles for practical 108 bus Indian RDN in Case-1.

Optimal Capacitor Placement in the Presence of Load Uncertainty

To examine the effectiveness of the proposed SE-IM approach in the presence of load uncertainty, three load levels are considered, *i.e.*, light, nominal, and peak, and their respective load multiplying factors are 0.5, 1.0, and 1.6. The results are obtained for fixed capacitor type scheme, reported in Table 2.8. Figures 2.14 and 2.15 show the voltage profiles and active power flow profiles before and after the compensation during light, nominal and peak load conditions, respectively. Followings are the main findings from the above study.

TABLE 2.7: Comparison among different existing index methods and proposed approach for 108-bus RDN

Method	Total Capacitor Size (MVAr)	P-Loss (MW)	V_{max}/V_{min} (p.u.)	AEC ($)	Net Saving (%)
Method 1: Loss Sensitivity Index (1)					
Case-1	8.850	0.4363	1 / 0.9164	73302.56	28.27
Case-2	3.1958	0.4954	1 / 0.9080	83218.08	21.73
Method 2: Loss Sensitivity Index (2)					
Case-1	8.700	0.4485	1 / 0.9152	75353.64	26.45
Case-2	3.4878	0.5108	1 / 0.9084	85805.31	19.21
Method 3: Vector Index (PLI)					
Case-1	7.800	0.4356	1 / 0.9132	73186.85	28.86
Case-2	3.4793	0.4935	1 / 0.9148	82903.68	21.89
Method 4: Voltage Sensitivity Index (VSI)					
Case-1	6.750	0.4630	1 / 0.9173	77777.22	25.11
Case-2	2.2140	0.5082	1 / 0.9094	85383.18	20.18
Method 5: Shannon's Entropy based Index Method (Proposed)					
Case-1	9.000	0.4227	1 / 0.9175	71012.79	30.32
Case-2	6.0445	0.4699	1 / 0.9094	78942.33	24.36

1. At light load condition, the net real power loss is reduced by 31.55%, while the AEC saving is 22.71% after the placement of capacitors of total capacity 4.50 MVAr.

2. At nominal load condition, the power loss reduction and AEC saving are optimum than light and peak load condition.

3. AEC savings are less in peak load conditions. It is because of the limitation on the total number of places where capacitors could be placed, same as the nominal or light load condition.

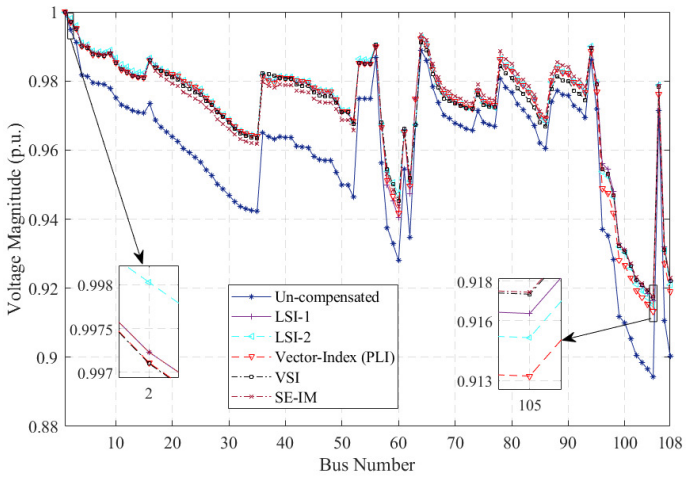

FIGURE 2.13: Voltage profiles for practical 108 bus Indian RDN in Case-2.

TABLE 2.8: Results of optimal capacitor placement problem for practical 108 bus Indian RDN in the presence of load uncertainty

Load Level	Before Compensation		After Compensation			Net AEC Saving (%)
	P-Loss (MW)	V_{max}/V_{min} (p.u.)	Total Capacitor Size (MVAr)	P-Loss (MW)	V_{max}/V_{min} (p.u.)	
Case-1: Fixed Capacitor Type Scheme						
Light	0.1515	1 / 0.9499	4.500	0.1037	1 / 0.9571	22.71
Nominal	0.6450	1 / 0.8944	9.000	0.4227	1 / 0.9175	30.32
Peak	1.8028	1 / 0.8177	16.650	1.6073	1 / 0.9001	8.10

2.6 Summary

The main focus of this work is to present an approach that allows the network operators to select multiple criteria in the formulation at a time for optimal capacitor siting. The efficacy of the proposed approach is evaluated by implementing it on an IEEE-12 bus, 34 standard bus, and a 108-bus practical RDN of an Indian utility, and the result is compared with that of the prevailing four methods and the proposed method is found to be superior. The significant contributions of the work are summarized below.

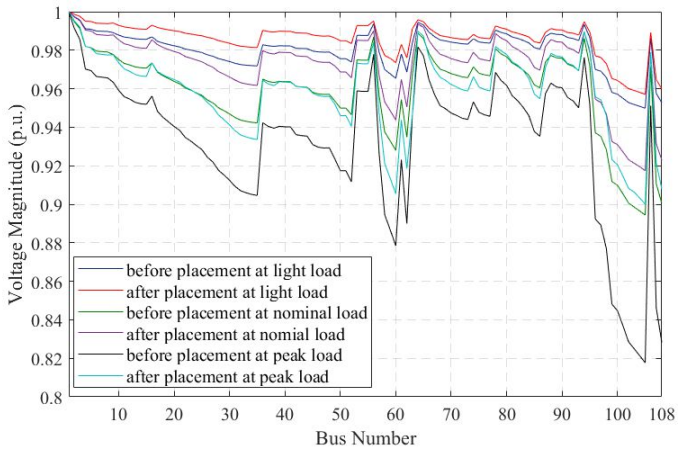

FIGURE 2.14: Voltage profiles for practical 108 bus Indian RDN in the presence of load uncertainty.

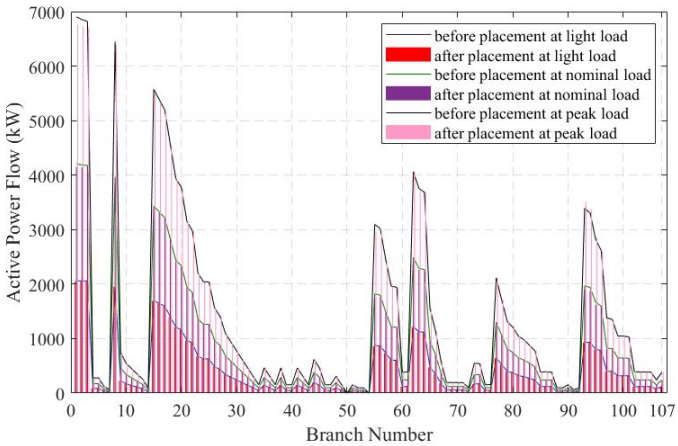

FIGURE 2.15: Active power flows in practical 108 bus Indian RDN in the presence of load uncertainty.

1. In this work, two cases of analysis have been considered based on the capacitor types, which are switched and fixed types.

2. The proposed approach comprehensively improved the techno-economic quantities, which fulfilled the objectives of the optimum siting problem effectively.

3. An impact on optimal capacitor placement problem is analyzed in the presence of DG and load uncertainty in the RDN. It is noted that; the

proposed approach improved the network's quantities while satisfying all the considered security and reliability constraints.

4. The proposed SE-IM approach offers flexibility in selecting multiple criteria, and also enables combining the index scores obtained from the methods considered based on their degree of importance and thereby improves the network quantities.

Chapter 3

Optimal Solutions for DG Placement in Smart Distribution System

3.1 Preamble

Distributed generation (DG) has become essential to ensure the quality, reliability, and security of distribution network (DN) operations. Consequently, the integration of DGs into power DNs is experiencing a significant surge. However, with the increased penetration of DGs, the responsibilities of the distribution network planner (DNP) are also on the rise. It is crucial to conduct impact analyses of DGs in the power network to prevent degradation of reliability and power availability. Unplanned and arbitrary DG placement may lead to adverse effects on DN parameters, such as power loss increase, system voltage drops, and reduced loading capability. This chapter focuses on devising a technique to strategically place DG units in DNs. The approach involves assigning weights calculated according to the relative influence of various techno-economic objective functions considered in a multi-objective problem, utilizing Shannon's Entropy. The proposed approach has been applied to a lossy 38-node test system to illustrate its efficacy. The results indicate that the suggested method enhances system response compared to prevailing methods addressing the multi-objective DG placement problem.

The remainder of the chapter is organized as follows: In section 3.2, the nomenclature for the parameters, indices, and variables employed in the problem formulation of optimal placement of DG in the smart distribution system is outlined. Section 3.3 discusses how the influence of an objective

function is changed with the alteration in the network's physical properties. Section 3.4 discusses the modeling of voltage-dependent loads and different techno-economic objective functions considered in problem formulation. Section 3.5 delineates the proposed approach for quantifying the weights associated with the objectives in a multi-objective DG placement problem and presents the solution approach to optimal placement of DG. Simulated results and discussions are reported in Section 3.6, followed by the summary of the chapter in Section 3.7.

3.2 Nomenclature

Sets and Indices

U_ρ, U_σ, U_τ	Set of industrial, residential, and commercial type of load buses, respectively
U_t	Set of time intervals in 24 hours
U_d	Set of number of days intervals in a year
U_{dg}	Set of DGs to be placed in distribution system
U_b, U_l	Set of buses (except substation bus) and lines in the network, respectively

Variables

$\mathrm{P}_{Loss}(\mathrm{Q}_{Loss})$	Real (reactive) power loss
V_b^t	Bus voltage magnitude during t^{th} time
$\overline{S}_l$	MVA flow in the l^{th} line
P^{dg}	Real power generated by DG
O_{kl}	Index score of k^{th} entity for l^{th} criteria

λ_l	Weight value for l^{th} criteria (objective)
η_k	Comprehensive score of k^{th} entity (*i.e.*, bus)

Parameters

P_L^{cp} (Q_L^{cp})	Constant power real (reactive) load demand
$P_{L,i}$ $(Q_{L,i})$	Real (reactive) load demand at i^{th} bus
$V_{spec.}^t$	Voltage at root node at t^{th} time interval
T	Total number of time intervals
$S_l^{\max}$	MVA capacity of l^{th} line
UIC^{dg}	Unit installation cost of DG ($/MW)
UOC^{dg}	Unit O&M cost of DG ($/MW)
UC_{sub}	Unit cost of electricity purchased from grid ($/MW)

3.3 Impact Assessment of Power Loss Index in DG Placement Problem

It is known that the integration of DG significantly influences both technical and economic quantities within a DN. This section demonstrates that variations in DN configurations result in differing relative impacts on these quantities. Consequently, their significance as an objective function in a multi-objective assessment must be adjusted based on their varying impacts in the context of the DG placement problem. To demonstrate this, the mathematical formula for the power loss index is derived in equations (3.1)-(3.5) and subsequently, applied to evaluate two distinct configurations of a 7-bus distribution system, as depicted in Figure 3.1.

$$P_{loss} = \sum_{n \in U_l} \left[r_{n,n+1} . (I_{n,n+1})^2 \right] \tag{3.1}$$

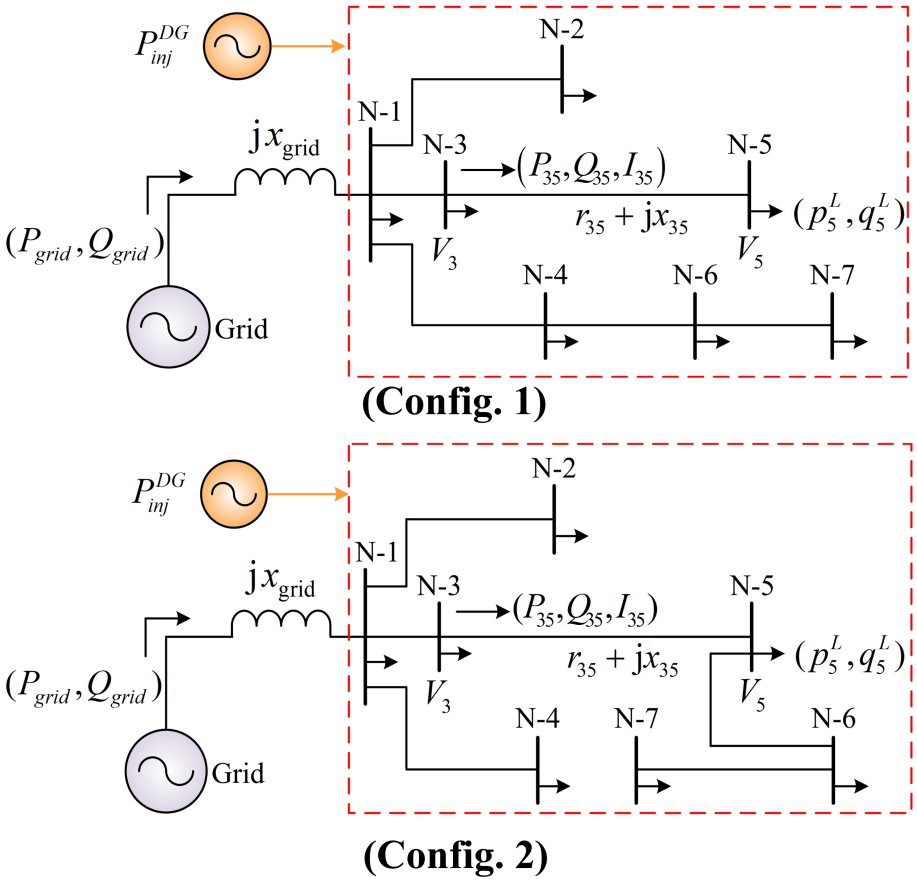

FIGURE 3.1: 7-bus distribution system depicting 0.10 MW of DG integration at each potential node in (a) config. 1, (b) config. 2.

$$P_{loss} = \sum_{n \in U_l} \left[r_{n,n+1}. \left((P_{n,n+1})^2 + (Q_{n,n+1})^2 \right) \right] \tag{3.2}$$

$$\begin{aligned} P_{loss}^{dg} = & \sum_{m \in U_l} \left[r_{m,m+1}. \left((P_{m,m+1} - P^{dg})^2 + (Q_{m,m+1})^2 \right) \right] \\ & + \sum_{i=(n-m) \in U_l} \left[r_{i,i+1}. \left((P_{i,i+1})^2 + (Q_{i,i+1})^2 \right) \right] \end{aligned} \tag{3.3}$$

$$P_{loss}^{dg} = P_{loss} - \sum_{m \in U_l} \left[r_{m,m+1}. \left(2.P_{m,m+1}.P^{dg} - \left(P^{dg} \right)^2 \right) \right] \tag{3.4}$$

$$\%P_{loss}^{\Delta} = \left| \frac{P_{loss}^{dg}}{P_{loss}} - 1 \right| = \frac{\sum_{m \in U_l} \left[r_{m,m+1}. \left(2.P_{m,m+1}.P^{dg} - \left(P^{dg} \right)^2 \right) \right]}{\sum_{n \in U_l} \left[r_{n,n+1}. \left((P_{n,n+1})^2 + (Q_{n,n+1})^2 \right) \right]} \tag{3.5}$$

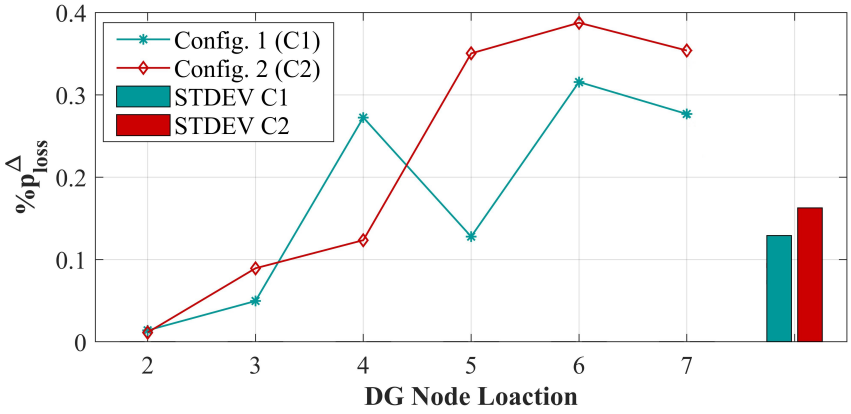

FIGURE 3.2: Evaluated power loss index at each bus after placing 0.10 MW of DG in config. 1 and 2.

In equations (3.2)-(3.5), it is assumed that the voltage is 1 p.u. at all nodes in the network, allowing it to be neglected in the illustration. The power loss index, depicted in Fig. 3.2, illustrates the computed impact of successively placing 100 kW of DG at each potential node in two distinct configurations. Concurrently, the standard deviation is calculated for each configuration. The analysis reveals that the DG in configuration two has a more significant effect on power loss compared to configuration one. Consequently, it is advisable to additionally prioritize the power loss objective function in formulating a multi-objective problem for configuration two.

3.4 Modelling of Load Demands and Problem Formulation

This section articulates the formulation of the multi-objective DG placement problem, considering diverse technical and economic objective functions. The multi-objective function is subjected to equality and inequality constraints, including active and reactive power flows, voltage limits, and bounds on DG size and location. Additionally, a subsection is dedicated to the load modeling based on their dependence on voltage, aiming to scrutinize the influence of different load models on the optimal DG placement problem.

3.4.1 Mathematical Modeling of Load Demand

The primary objective of the DNP is to conduct a mathematical assessment of the techno-economic implications of DG on the DN before its integration, accounting for the dynamic characteristics of various loads. This analysis incorporates voltage-dependent load modeling and classifies loads into industrial, commercial, and domestic categories, departing from the conventional constant power load demands represented as (P_L^{cp} and Q_L^{cp}). The mathematical formulation expresses the active ($P_{L,i}$) and reactive ($Q_{L,i}$) loads for the i^{th} bus as detailed in [165].

$$P_{L,i} = P_{L,i}^{cp} . V^{\alpha} \tag{3.6}$$

$$Q_{L,i} = Q_{L,i}^{cp} . V^{\beta} \tag{3.7}$$

In equations (3.6) and (3.7), the parameters α and β represent the exponential factors associated with distinct load categories. Specifically, the respective values for α are 0.18, 0.92, and 1.51, while the corresponding values for β are 6.0, 4.04, and 3.40, corresponding to industrial, residential, and commercial loads. The overall expressions for the active and reactive power requirements of a DN are articulated in equations (3.8) and (3.9), respectively.

$$P_{TL} = \sum_{b \in U_\rho} P_{L,b}^{cp} . V_b^{0.18} + \sum_{b \in U_\sigma} P_{L,b}^{cp} . V_b^{0.92} + \sum_{b \in U_\tau} P_{L,b}^{cp} . V_b^{1.51} \tag{3.8}$$

$$Q_{TL} = \sum_{b \in U_\rho} Q_{L,b}^{cp} . V_b^{6.0} + \sum_{b \in U_\sigma} Q_{L,b}^{cp} . V_b^{4.04} + \sum_{b \in U_\tau} Q_{L,b}^{cp} . V_b^{3.40} \tag{3.9}$$

The anticipation is that the introduction of a capacitor into the network enhances the voltage profile, leading to a reduction in losses and subsequently a decrease in demand from the substation. However, contrary to expectations, empirical evidence indicates that as the voltage profile improves, there is an observed increase in demand from the substation [210]. Consequently, this work explores the impact of voltage-dependent load modeling, as defined in equations (3.8) and (3.9), on the planning of DG placement.

3.4.2 Multi-objective DG Placement Problem Formulation

In generic, a weighted-sum multi-objective optimization problem for DG placement in DN can be written as follows:

$$minimize \sum_{\phi=1}^{N} \lambda_{\phi}.f_{\phi}(x,u) \tag{3.10}$$

$$s.t. \quad h(x,u) = 0 \tag{3.11}$$

$$g(x,u) \geq 0 \tag{3.12}$$

In (3.10), the variable N denotes the total number of objectives considered in the multi-objective problem for DG placement. The symbol λ_{ϕ} signifies the relative weight assigned to the ϕ^{th} objective function (OF). In equations (3.11)-(3.12), the equality and inequality constraints encompass factors such as power flow balance, node voltage limitations, boundaries on active and reactive power, as well as other operational and security constraints. The proposed study incorporates both technical and economic OFs to facilitate a techno-economic performance analysis while adhering to constraints related to power flow and limits on variable quantities.

Technical Objective Functions

It is widely acknowledged that the integration of DG has a substantial impact on several technical parameters within a DN, including changes in real and reactive power losses, adjustments to node voltage profiles, and the regulation of line capacities. Therefore, evaluating the extent of these changes in network parameters during the analysis of DG placement is essential for practical applications, considering the numerous OFs involved. In this investigation, four specific technical OFs are utilized to scrutinize the influence of DG integration within the network. These OFs are expressed mathematically as:

$$\text{Active power loss:} \quad L_P = \sum_{t \in U_t} \sum_{n \in U_l} \left[r_{n,n+1}.\left(I^t_{n,n+1}\right)^2 \right] \tag{3.13}$$

$$\text{Reactive power loss:} \quad L_Q = \sum_{t \in U_t} \sum_{n \in U_l} \left[x_{n,n+1}.\left(I^t_{n,n+1}\right)^2 \right] \tag{3.14}$$

$$\text{Voltage deviation:} \quad V_D = \sum_{t\in U_t}\sum_{b\in U_b}\left(\frac{V_b^t - V_{spec.}^t}{V_{\max}^t - V_{\min}^t}\right)^2 \tag{3.15}$$

$$\text{Line capacity limit:} \quad I_C = \frac{1}{T}\sum_{t\in U_t}\max\left(\left|\overline{S}_l^{k,t}\right|\right)^{l\in U_l} \tag{3.16}$$

The primary objective of these OFs is to identify suitable nodes for the placement of DG. Consequently, the optimization of DN parameters can be achieved post-DG placement, resulting in an augmented level of reliability. In the context of this study, the impact analysis of DG is quantified on a singular phase within a three-phase system, with the assumption of a balanced DN system. To maintain a streamlined analysis without compromising the integrity and scholarly contribution of the work, the inherent uncertainty associated with the time-varying nature of the load is deliberately excluded from consideration.

Economic Objective Function

Essentially, the economic aspect of the DG placement problem holds comparable significance to the incorporation of various technical OFs. As a result, a cost index, denoted as E_{Cost}, has been formulated and integrated into the proposed methodology. This index is articulated as:

$$E_{cost} = C_{ins}^{dg} + \sum_{t\in U_t}\left[C_{o\&m}^{dg,t} + C_{sub}^t\right] \tag{3.17}$$

$$\text{where} \quad C_{ins}^{dg} = \sum_{i\in U_{dg}}\left[\left(P_i^{dg}.UIC_i^{dg}.CRF\right)\Big/365\right] \tag{3.18}$$

$$\text{and} \quad C_{o\&m}^{dg} = \sum_{i\in U_{dg}}\left(P_i^{dg}.UOC_i^{dg}\right) \tag{3.19}$$

$$\text{and} \quad C_{sub} = UC_{sub}.\left[eq.(4) + \left(P_{TL} - P_T^{dg}\right)\right] \tag{3.20}$$

$$\text{and} \quad CRF = \frac{\zeta(1+\zeta)^\gamma}{(1+\zeta)^\gamma - 1} \tag{3.21}$$

The capital recovery factor (CRF) mentioned in (3.21) represents the complete installation cost disbursed in γ uniform payments at an interest rate of ζ%. Notably, several existing studies tend to overlook the economic dimension in the

formulation of the DG placement problem. Nevertheless, the financial operation of the system aligns with the current dynamics of the competitive electricity market. Hence, it is imperative to incorporate an economic aspect into the DG placement problem, alongside the consideration of other technical OFs.

Constraints

Every optimization problem operates within a defined set of constraints. Consequently, this work employs both equality and inequality conditions to restrict variables and refine feasible solutions, as outlined below:

$$P_{br}^{fr} = P_{br}^{to} + \left(P_L^{to} - P^{dg,to}\right) + \left[r^{fr}\left(I_{br}^{fr}\right)^2\right] \tag{3.22}$$

$$Q_{br}^{fr} = Q_{br}^{to} + \left(Q_L^{to} - Q^{dg,to}\right) + \left[x^{fr}\left(I_{br}^{fr}\right)^2\right] \tag{3.23}$$

$$V_b^{to} = V_b^{fr} - \left[\left(r^{fr} + jx^{fr}\right).\left(I_{br}^{fr}\right)^*\right] \tag{3.24}$$

$$V_b^{i,min} \leq V_b^i \leq V_b^{i,max} \tag{3.25}$$

$$P_{i,min}^{dg} \leq P_i^{dg} \leq P_{i,max}^{dg} \tag{3.26}$$

$$\sum_{i \in U_{dg}} P_i^{dg} \leq P_{max}^{dg} \tag{3.27}$$

Equations (3.22)-(3.24) signify the power flow constraints for real and reactive power. Equation (3.25) outlines restrictions on voltage, specifying upper and lower limits. Additionally, (3.26)-(3.27) establish constraints on both individual and overall installed capacity of DG.

3.5 Solution Methodology

Recently, several approaches have been put forth for optimal DG placement, with an emphasis on multi-objective optimization. However, these methods often lack a well-defined strategy for determining weight factors assigned to each objective, a crucial aspect in achieving optimal decision-making. As a result, there exists a potential risk of obtaining sub-optimal solutions for the DG

placement problem. The subsequent subsection introduces an approach that leverages Shannon's Entropy to quantify the pertinent weight factors for the objectives. This is done based on their respective degrees of influence in the multi-objective optimal DG placement problem.

3.5.1 Shannon's Entropy for Weight Evaluation Incorporating DNP Priority Information

The entropy formula is applied in information theory to quantitatively assess the spread of a variable in multi-criteria decision-making. The fundamental concept behind entropy is that a higher dispersion in the measured variable indicates greater disparity among criteria, leading to the extraction of more information. Additionally, greater weight (signifying importance) should be assigned to a criterion with higher dispersion, and conversely [211]. Mathematically, the empirical weights are determined through the following steps.

1. Reconstruct techno-economic OFs to impact indices for unitless measurement.
$$O_{kl} = 1 - \left(f_l^k \Big/ f_l^{base} \right) \tag{3.28}$$

2. Normalize the measured values (*i.e.*, index)
$$\overline{O}_{kl} = \frac{O_{kl}}{\sum\limits_{k=1 \to E} O_{kl}} \tag{3.29}$$

3. Evaluate Shannon's Entropy value e_l for l^{th} index, and is defined as
$$e_l = -e_0 \sum_{k=1}^{s} \overline{O}_{kl} \times \ln \overline{O}_{kl} \tag{3.30}$$
here, e_0 is termed as entropy constant and is equal to $(\ln s)^{-1}$. Furthermore, the degree of diversification is obtained by $\delta_l = 1 - e_l$.

4. Compute the degree of importance (*i.e.*, relative weight)
$$\lambda_l = (1 - e_l) \Big/ \sum_{l=1}^{\mathrm{N}} (1 - e_l) \tag{3.31}$$

In this work, λ_l represents the relative weights in the multi-objective DG placement problem. In some given conditions, the DNP strategically sets a preference for an objective; thus, relative weights must be changed accordingly. This priority information (PI) can be incorporated by modifying the λ_l in (3.31) for indices with PI as in (3.32) and indices without PI as in (3.33).

$$\lambda_{n\in \mathrm{N}} = \frac{(1-e_n) + \left(\zeta_n * \sum_{l=1}^{\mathrm{N}} (1-e_l)\right)}{\sum_{l=1}^{\mathrm{N}} (1-e_l)} \tag{3.32}$$

$$\lambda_{m\in\{\mathrm{N}\setminus n\}} = \frac{(1-e_m)}{\sum_{l=1}^{\mathrm{N}} (1-e_l)} - \frac{\sum_{n\in \mathrm{N}} \zeta_n * (1-e_m)}{\sum_{l=1}^{\mathrm{N}} (1-e_l) - \sum_{n\in \mathrm{N}} (1-e_n)} \tag{3.33}$$

where n and m represent a set of indices with PI and without PI, respectively.

3.5.2 Proposed Approach for Optimal DG Planning

The weighted sum of various technical and economic OFs is used to create a weighted multi-objective function, determining the optimal placement of DG in the distribution system. This weighted multi-objective problem, denoted as (MO_w^k), is expressed as:

$$MO_w^k = \left\{\lambda_1 L_P^k + \lambda_2 L_Q^k + \lambda_3 V_D^k + \lambda_4 I_C^k + \lambda_5 E_{cost}^k\right\} \tag{3.34}$$

$$s.t. \quad (3.8) - (3.9) \text{ and } (3.22) - (3.33) \tag{3.35}$$

$$\sum_{\phi=1}^{\mathrm{N}} \lambda_\phi = 1 \ \wedge \ \lambda_\phi \in [0,1] \tag{3.36}$$

In equation (3.34), L_P^k denotes the active power loss, L_Q^k refers to reactive power loss, V_D^k represents the maximum voltage deviation, I_C^k signifies the line capacity limit and E_{cost}^k stands for the total cost associated with the k^{th} distribution network configuration during the t^{th} time interval or peak hour of the d^{th} day. The relative weights generally determine the extent of influence of technical and economic objectives in the DG placement problem. To quantify these empirical weight values, this study adopts the concept of Shannon's Entropy, as elucidated in the preceding subsection.

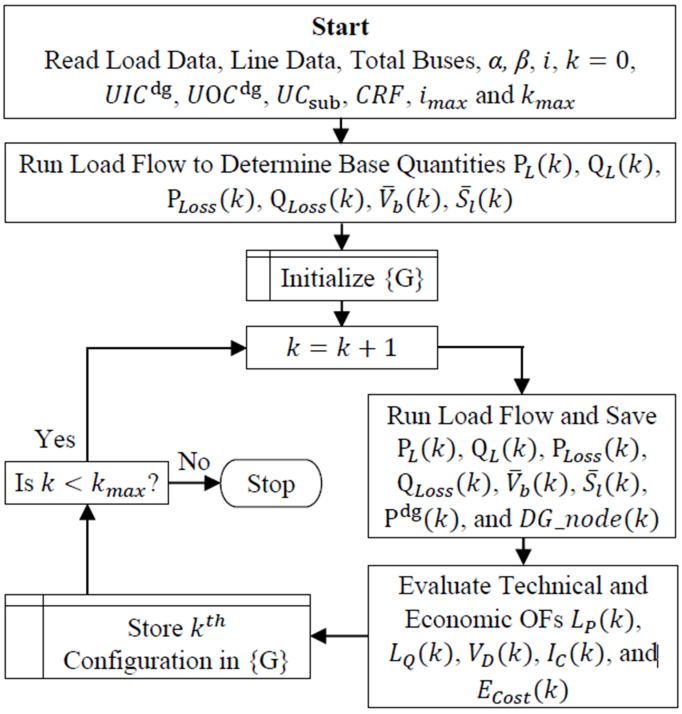

FIGURE 3.3: Workflow to evaluate different techno-economic OFs.

The process for assessing various techno-economic OFs is depicted in Figure 3.3. A detailed outline of the proposed solution methodology is presented in the flowchart featured in Figure 3.4. The effectiveness of this approach is scrutinized using a 38-node test system within the MATLAB environment. The ensuing section presents and discusses the simulated results.

3.6 Results and Discussion

The 38-node test system consists of the combined active and reactive power demand, totaling 3501.6 kW and 1870.2 kVAr, respectively. Various load types, including industrial, commercial, and residential, are integrated into the system configuration (see Figure 3.5). The simulation utilizes base quantities S_{base} and kV_{base} for analysis, with values set at 100 MVA and 12.66 kV, respectively. The specific numerical values for cost parameters used in calculating the total cost are provided in Table 3.1. In the context of mixed loads, the base case real and reactive power losses are documented as 152.8 kW and 101.5 kVAr, respectively.

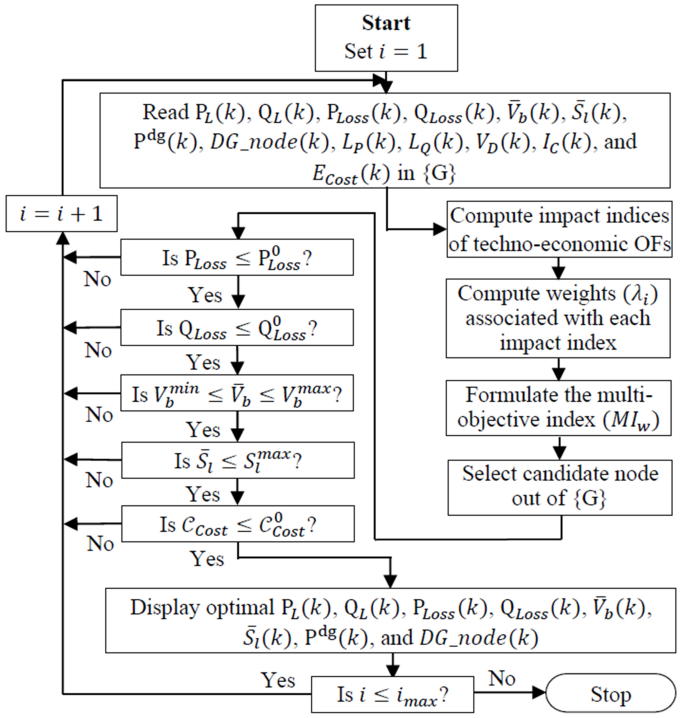

FIGURE 3.4: Workflow for the proposed approach based on Shannon's Entropy formula.

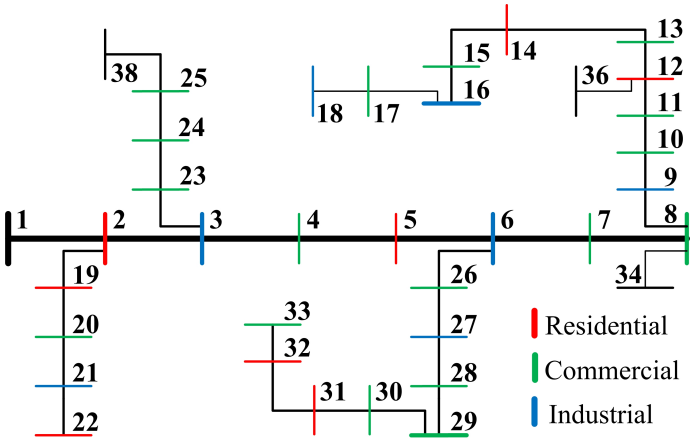

FIGURE 3.5: Single line diagram of 38-node test system depicting residential, commercial, and industrial loads.

This work assesses relative weights by considering the extent of influence each objective has in the DG placement problem. Four distinct cases are outlined in the following subsections to demonstrate the effectiveness of the proposed approach, emphasizing variations in the physical properties of the network.

TABLE 3.1: Numerical values for cost parameters to evaluate overall cost

Parameters	Numerical Values
C_{ins}^{dg}	750 \$/kVA
$C_{o\&m}^{dg}$	0.04 \$/kWh
C_{sub}	0.0656 \$/kWh
ζ	10%
γ	18 years

TABLE 3.2: Evaluated optimal weights considering a change in DG location and size in 38-node test system

	Weight factors				
DG size (kW)	λ_1	λ_2	λ_3	λ_4	λ_5
150	0.25	0.27	0.38	0.09	0.01
300	0.22	0.24	0.33	0.20	0.01
600	0.17	0.19	0.24	0.40	0.00

Finally, a comparison between the proposed method and the weight allocation approach, previously examined in past studies, is presented.

3.6.1 Case 1: Effect on Weights for Change in DG Location and Size

In this case, each node is viewed as a potential site for placing DG. Subsequently, DG units of three different sizes (150 kW, 300 kW, and 600 kW) are successively installed at every candidate node. The optimal weights (λ_ϕ) determined through evaluation are documented in Table 3.2. The resulting weighted multi-index (MIW) scores for each configuration of the k^{th} distribution network are illustrated in Figure 3.6. The key outcomes of the simulation study are outlined below.

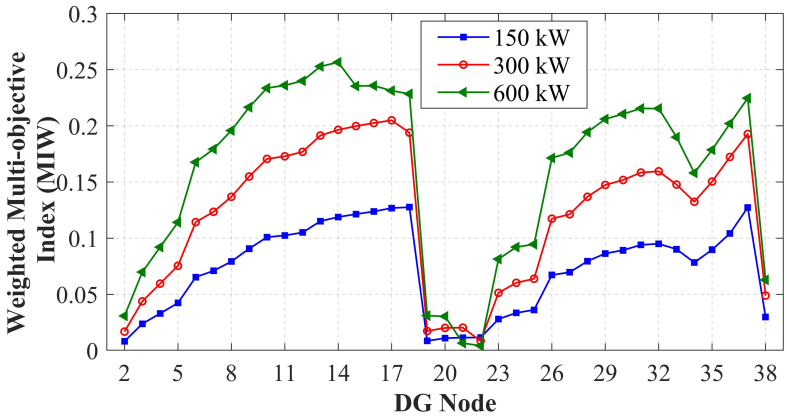

FIGURE 3.6: Multi-objective score for the 38-node test system, considering diverse sizes of DG positioned at each node within the circuit.

1. ***With the placement of 150 kW DG:*** Bus 18 has been identified as the optimal site for placing DG, as illustrated in Figure 3.6. Figure 3.7 reveals a more pronounced dispersion for the voltage deviation index (VDI) compared to other indices. Consequently, the impact is substantial, and the assigned weight value for VDI, namely 0.38, is the highest among all indices. In contrast, the economic index (EIC) has a negligible influence in this scenario, with a quantified weight of 0.01, as depicted in Figure 3.7, where the dispersal is minimal.

2. ***With the placement of 300 kW DG:*** Bus 17 has been determined as the optimal site for placing DG, as indicated in Figure 3.6. The weight value for the voltage deviation index (VDI) is higher compared to other impact indices, specifically 0.33.

3. ***With the placement of 600 kW DG:*** The ideal node identified for placing the DG is bus 14, as illustrated in Figure 3.6. In 12 configurations for this DG size, the line capacity limit constraint is breached, as depicted in Figure 3.8. Consequently, it can be concluded that the line capacity index (ICC) has a more pronounced impact compared to other indices. The computed weight value for ICC using SE, specifically 0.40, is the highest among all the indexes.

It is noteworthy that the ICC index carries a weight of 0.09 when incorporating a 150 kW DG into the RDN. However, as the DG size increases,

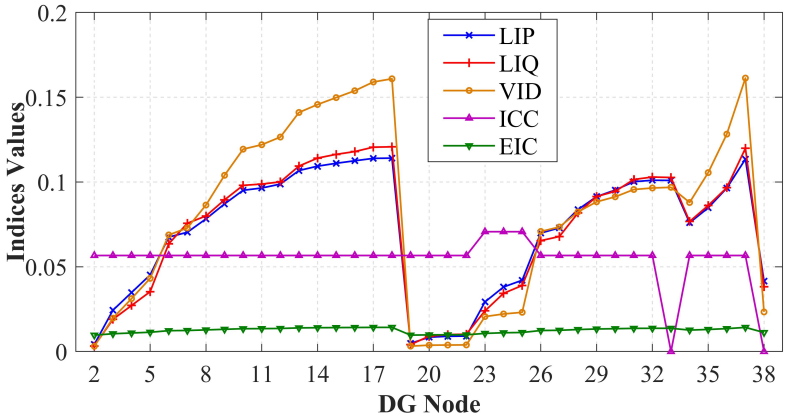

FIGURE 3.7: Techno-economic index scores for 38-node test system with DG of 150 kW sited at each circuit node.

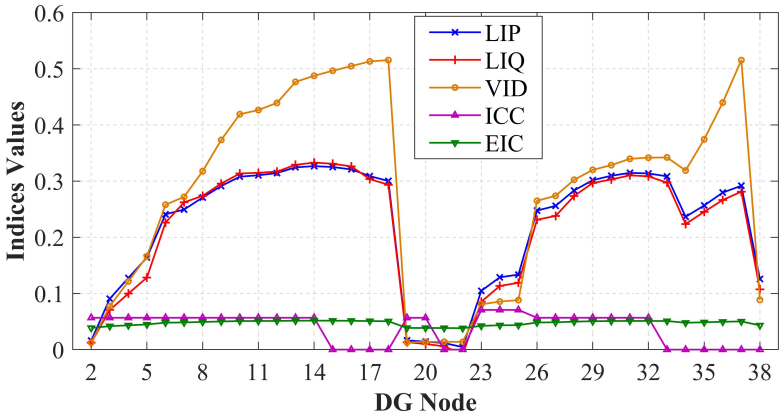

FIGURE 3.8: Techno-economic index scores for 38-node test system with DG of 600 kW sited at each circuit node.

resulting in more instances of line capacity limit violation, the influence of the ICC index rises, reaching 0.20 and 0.40 for DG installations of 300 kW and 600 kW in the RDN, respectively. Following the optimal DG placement, improvements in various network parameters such as power loss, voltage magnitude, and annual cost expenditure (including DG installment cost, O&M cost, and power purchase from the grid) are detailed in Appendix B {refer to Table B.1}.

TABLE 3.3: Evaluated optimal weights when varying DG size at 6^{th} bus in 38-node test system

	Weight factors				
Bus location	λ_1	λ_2	λ_3	λ_4	λ_5
6	0.19	0.20	0.25	0.00	0.36

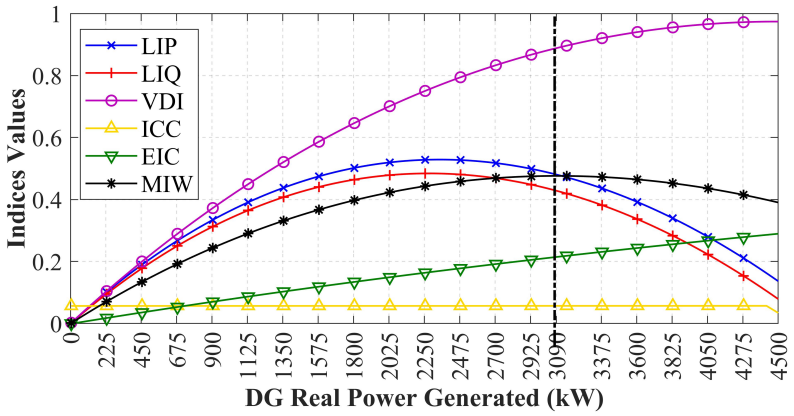

FIGURE 3.9: Techno-economic index scores and multi-index score for 38-node test system with varying DG placed at 6^{th} bus.

3.6.2 Case 2: Effect on Weights for Varying the DG Size at a Bus

The candidate bus location is consistently set at the 6^{th} bus for DG siting, and the problem is defined by varying the DG size from 0 to 4500 kW in increments of 5 kW. The computed weight scores for various techno-economic indices are presented in Table 3.3. In Figure 3.9, it can be observed that the dispersion measure is more pronounced for EIC (specifically, $\lambda_{l=5} = 0.025$). As the DG size changes, the impact correspondingly increases. Consequently, the weight assigned to EIC, amounting to 0.36, is the highest among all indices. The influence of ICC is minimal, as no deviation is detected (*i.e.*, $\lambda_{l=4} \approx 0$) during the increment in DG size.

In contrast to Case 1, where the weight attributed to EIC had minimal impact on determining the optimal DG configuration, in this scenario, EIC plays a crucial role in selecting the optimal DG. This shift is because the increase in DG size leads to a rise in installation costs. The quantified network parameters before and after

TABLE 3.4: Evaluated optimal weights considering the change in DG location and power factor (pf) in 38-node test system

	Weight factors				
Power factor (pf)	λ_1	λ_2	λ_3	λ_4	λ_5
0.80	0.17	0.20	0.25	0.31	0.07
0.90	0.18	0.21	0.26	0.33	0.02
1.0	0.18	0.21	0.26	0.35	0.00

the placement of DG are detailed in Appendix B (refer to Table B.1).

3.6.3 Case 3: Effect on Weights with Different Power Factor

In this scenario, an analysis of the weight formulation for various indices is performed for distinct power factors. To achieve this, each node in the RDN is considered a potential location for 500 kW of DG placement, and simulations are conducted for three different power factors: 0.80, 0.90, and unity. The resulting optimal weights (λ_ϕ) are presented in Table 3.4. Across all power factor conditions, the influence of ICC stands out as more substantial than that of other indices, and the associated weight values for ICC are nearly identical. The key findings of the simulation study are outlined below.

1. For all examined power factor conditions, Bus 15 is identified as the prospective node for the placement of 500 kW of DG. The quantified weight measures for each index under all power factor conditions remain nearly constant.

2. In addition to ICC, VDI has a greater impact on the DG placement problem compared to LIP and LIQ. The influence of EIC is the least significant in determining the optimal DG placement.

3. The calculated network parameters following the optimal placement of DG are documented in Appendix B (refer to Table B.1). The conclusion drawn from the results suggests that operating the system under a power factor condition of 0.9 is advisable for achieving optimum performance.

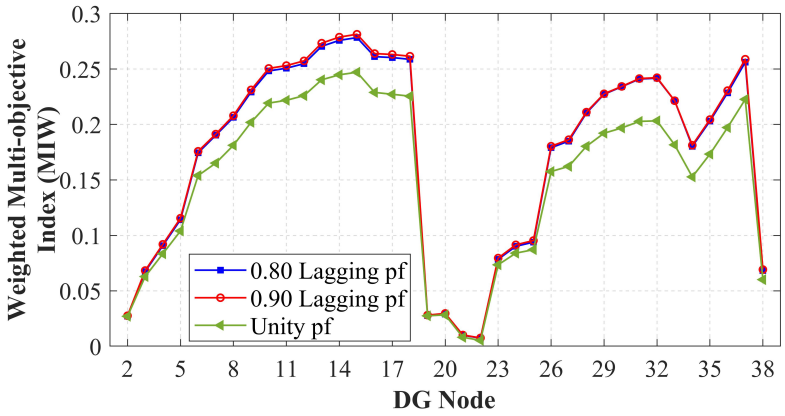

FIGURE 3.10: Multi-index scores for each node considering different power factors in the 38-node test system (DG of 500 kW).

Figure 3.10 illustrates the MIW scores obtained when 500 kW of DG is placed at each potential node under distinct power factor conditions.

3.6.4 Case 4: Effect on Weights for Change in Bus Load Type

The alteration of load bus types within a network affects the problem of DG placement. Hence, the suggested method is simulated under varying load bus types, as outlined in Section 3.4.1. Each node within the RDN represents a prospective location for the optimal placement of 300 kW DG units. Weight scores quantified across different load types, are presented in Table 3.5. The ensuing paragraphs detail the primary outcomes of the simulation study.

1. In scenarios with constant power loads, ICC exerts the greatest influence on the DG placement problem. Conversely, across all voltage-dependent load models, VDI demonstrates a more pronounced impact compared to other indices.

2. After systematically placing a 300 kW DG within the network to pinpoint the optimal node, only 12 configurations are found where line capacities adhere to the specified limit.

3. The influence of each index remains consistent across all voltage-dependent load models, as depicted in Figure 3.11. Consequently, the quantified weight measures for each index also exhibit minimal variation.

TABLE 3.5: Evaluated optimal weights considering the change in the type of load buses in 38-node test system

	Weight factors				
Load type	λ_1	λ_2	λ_3	λ_4	λ_5
Constant power	0.08	0.09	0.13	0.70	0.00
Industrial load	0.21	0.24	0.32	0.22	0.01
Residential load	0.22	0.24	0.33	0.20	0.01
Commercial load	0.22	0.24	0.33	0.20	0.01
Mix-type load	0.22	0.24	0.33	0.20	0.01

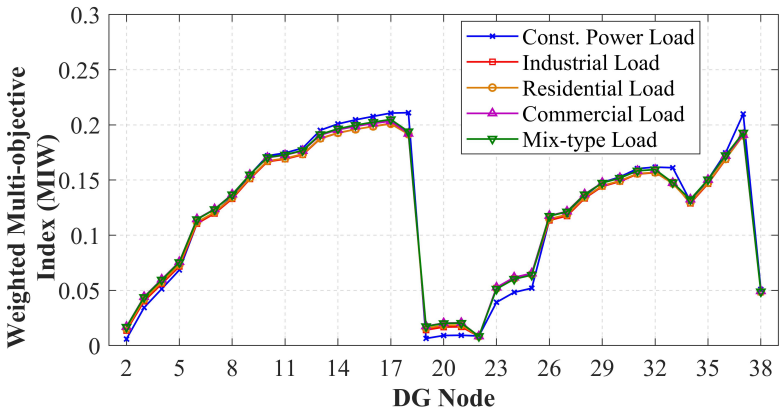

FIGURE 3.11: The multi-index scores considering the change in the type of load buses in the 38-node test system (DG of 300 kW).

4. With the identical DG capacity, bus 18 emerges as the optimal node in scenarios involving constant power loads. Conversely, when considering voltage-dependent load buses, bus 17 is identified as the preferable location.

Figure 3.11 illustrates the multi-index scores obtained when a 300 kW DG unit is positioned at each potential node, accounting for various load models. The computed network parameters after the optimal DG placement are detailed in Appendix B (refer to Table B.2).

TABLE 3.6: Evaluated optimal weights considering the DNP priority information and optimal solution for DG planning

Cases	Weight factors						PI Information	Optimal
	λ_1	λ_2	λ_3	λ_4	λ_5	λ_6	(ζ_i)	Solution
Case-1	0.24	0.27	0.10	0.39	-	-	-	6^{th} bus/2523 kW
Case-2	0.34	0.23	0.09	0.34	-	-	$\zeta_1 = 10\%$	6^{th} bus/2480 kW
Case-3	0.29	-	-	-	0.34	0.37	$\zeta_1 = 10\%$	6^{th} bus/2834 kW

3.6.5 Case 5: Effect of Incorporating DNP Priority Information

The three cases are simulated and compared for the DG placement problem to illustrate the effect of incorporating DNP priority information while evaluating the relative weights. This evaluation includes an additional objective function, annual energy not supplied (AENS), that accounts for system reliability, in addition to the technical and economic objectives outlined in section 3.4.2. In mathematical terms, the AENS is formulated as follows:

$$R_{AENS} = \sum_{q=1}^{L} P_q^k \times U_q \tag{3.37}$$

1. Solve DG placement problem, considering technical objective functions (OFs).

2. Solve DG placement problem, considering technical OFs and DNP priority information.

3. Solve DG placement problem, considering one technical, economic, and reliability OFs and DNP priority information.

The evaluation of weight factors while incorporating priority information, alongside the determination of optimal solutions for DG planning, is pivotal in enhancing the performance and reliability of distribution networks. In Table 3.6, three distinct cases (Case-1, Case-2, Case-3) are meticulously examined, each presenting unique weight factors (λ_i) allocated to various parameters influencing DG planning decisions. The inclusion of priority information (ζ_i) further refines

TABLE 3.7: Distribution network (DN) quantities for all three considered cases

Cases	DN Quantities				
	APL (kW)	RPL (kVAr)	$V_{min}(p.u.)$	AEC (M$)	AENS
Base	152.80	101.50	18 / 0.9252	-	1.6732
Case-1	72.23	52.74	18 / 0.9616	1.718	1.6236
Case-2	72.06	52.58	18 / 0.9611	1.724	1.6227
Case-3	75.04	54.92	18 / 0.9660	1.678	1.6165

the optimization process, guiding the placement and capacity determination of DG units. The optimal solutions derived from these analyses delineate specific locations and capacities for DG integration, exemplifying Case-1 where the optimal placement is identified at the 6^{th} bus with a capacity of 2523 kW. Moreover, Table 3.7 provides a comprehensive assessment of DN quantities across all considered cases, facilitating a comparative analysis against base values. These quantified metrics, encompassing parameters such as Average Power Loss (APL), Reactive Power Loss (RPL), and Annual Energy Cost (AEC), offer insights into the efficacy of DG integration strategies in mitigating losses and enhancing network performance. Such meticulous evaluations underscore the importance of informed decision-making in optimizing distribution network operations.

3.6.6 Case 6: Comparison of the proposed approach to prevailing studies

This thesis juxtaposes the proposed methodology against previously published approaches, namely analytical hierarchical analysis (AHP), grey relational analysis (GRA), and fuzzy decision method (FDM), to ascertain its effectiveness. The comparative outcomes are documented in Table 3.8. The evaluation of the optimal size and placement of DG takes into account objective functions such as

TABLE 3.8: Comparison among different existing methods and proposed approach

Methods		AHP	GRA*	FDM*	Proposed Approach
Weight factors	λ_1	0.54	-	-	0.19
	λ_5	0.16	-	-	0.39
	λ_6	0.30	-	-	0.42
Optimal Solution		6^{th} bus / 2492 kW	6^{th} bus / 1995 kW	6^{th} bus / 1995 kW	6^{th} bus / 3180 kW
APL (kW)		72.11	73.52	73.52	81.09
RPL (kW)		52.63	52.95	52.95	59.22
$V_{\mathbf{min}}$ (p.u.)		18 / 0.9613	18 / 0.9543	18 / 0.9543	18 / 0.9707
AEC (M$)		1.722	1.788	1.788	1.636
AENS		1.6234	1.6332	1.6332	1.6096

* GRA and FDM strategies determine the best-compromised solution from a set of non-dominated solutions of Pareto-front.

active power loss (L_P), economic factor (E_{cost}), and AENS as a measure of reliability.

Table 3.8 indicates a significant enhancement in network quantities compared to the base network configuration (*i.e.*, without DG), for the approaches under comparison. The prevailing technique shows further improvements in technical quantities. However, when DG is placed according to the proposed approach reduces annual expenditure by a total of 1.636 M$, while ensuring system operation within standard limits and reducing annual energy not supplied.

3.7 Summary

This thesis explores a new method for evaluating weights based on the relative impact of indices in a weighted multi-objective problem concerning optimal DG

placement in RDN. The effectiveness of this approach is assessed by applying it to a 38-node test system and analyzing various scenarios based on alterations in network physical properties. A comparative analysis is performed, revealing that the proposed approach outperforms existing methods. The primary contributions of this study include:

1. To achieve a practical and economically viable solution, the problem formulation takes into account a range of technical and economic impact indices.

2. DN buses are classified as voltage-dependent loads to assess how different load models affect DG placement.

3. The proposed method calculates weights associated with indices by considering their relative influence in the multi-objective problem of optimal DG allocation, thus removing the subjectivity associated with selecting weight measures.

4. The primary benefits of the proposed method include its integration of the priority information for the indices provided by DNP in unavoidable circumstances, its straightforward execution, and its compatibility with other similar multi-objective optimization problems.

5. The choice of indices relies on the perspectives of the DNP regarding both technical and commercial aspects of DG placement.

Chapter 4

Cost Effective Analysis of Electric Vehicle in Smart Distribution System

4.1 Preamble

In this chapter, we delve into a novel method to address the efficient day-ahead (DA) scheduling of electric vehicle charging stations (EVCSs) within a smart distribution system. The primary objective is the minimization of real power loss payments while adhering to a spectrum of operational constraints encompassing real and reactive power flow, bus voltage limits, and the nuanced dispatching and storage constraints characteristic of EVCSs. A key facet of our approach lies in the integration of sophisticated demand response modeling and uncertainties inherent in electricity prices and load forecasting. The solution is derived through mixed-integer nonlinear programming, with the distribution network operator (DNO) assuming a pivotal role in orchestrating secure and efficient daily operations. The work explores both single-agent and multi-agent system control strategies, underpinned by the secure exchange of data between the DNO and EVCSs to facilitate effective dispatching. The efficacy of the proposed methodology is rigorously examined through simulations conducted on a modified 12-bus radial distribution network, ultimately showcasing substantial optimization gains vis-à-vis conventional techniques.

The remainder of the chapter is organized as follows: In Section 4.2, the nomenclature for the sets, indices, variables, and parameters employed in the problem formulation of optimal DA scheduling of EVCS within the smart distribution system. Section 4.3 provides a succinct overview of the smart

distribution system architecture. Section 4.4 outlines the formulation of the DA scheduling problem incorporating the demand response model. Section 4.5 then elaborates on the problem formulation, considering uncertainty modeling in the DA scheduling process. Section 4.6 presents and analyzes the numerical results obtained from our approach. Finally, Section 4.7 offers a summary of the chapter to encapsulate our findings and contributions.

4.2 Nomenclature

The notation used in this article to represent the sets, indices variables, and parameters are stated as follows:

Sets and Indices

$i/j/k$	Indices for network buses
T	Set of 24 hours of a day
t	Index for the time horizon
Φ	Set of buses participating in DR

Variables

$p^t_{g,j}/q^t_{g,j}$	Active/reactive power generation of RERs at the j^{th} bus during the t^{th} hour
$p^t_{d,j}/q^t_{d,j}$	Active/reactive load demand at the j^{th} bus during the t^{th} hour
P^t_{ij}/Q^t_{ij}	Active/reactive branch power flow between the i^{th} and j^{th} buses during the t^{th} hour
l^t_{ij}	Squared current magnitude flow between the i^{th} and j^{th} buses during the t^{th} hour
v^t_i	Squared voltage magnitude at the i^{th} bus during the t^{th} hour

$E^{t}_{RC,i}/E^{t-1}_{RC,i}$	Available SoC of a RCS at the i^{th} bus during the $t^{th}/\ (t-1)^{th}$ hour
$P^{t}_{RC,i}$	Active power injected from a RCS at the i^{th} bus during the t^{th} hour
$\Omega^{t}_{i}/\mho^{t}_{i}$	Binary decisions for charging/discharging a RCS at the i^{th} bus during the t^{th} hour
$P^{dch,t}_{RC,i}/P^{ch,t}_{RC,i}$	Discharging/charging power of a RCS at the i^{th} bus during the t^{th} hour
$E^{arr/dep,t}_{REV,i}$	SoC of REVs upon arrival/departure to/from a RCS at the i^{th} bus during the t^{th} hour
$E^{t}_{CC,i}/E^{t-1}_{CC,i}$	Available SoC of a CCS at the i^{th} bus during the $t^{th}/\ (t-1)^{th}$ hour
$P^{ch,t}_{CC,i}$	Charging power of a CCS at the i^{th} bus during the t^{th} hour
$E^{dep,t}_{CEV,i}$	SoC of CEVs upon departure from a CCS at the i^{th} bus during the t^{th} hour
μ^{t}_{i}	DR decision variable for altering demand pattern
Θ_i	Binary decisions, whether the i^{th} bus participate in DR or not
$\delta^{\psi/d}_{t}$	Prediction error in price/loads during the t^{th} hour, respectively

Parameters

r_{ij}/x_{ij}	Resistance/reactance of a line connecting the i^{th} and j^{th} buses
$\underline{p}^{t}_{g,i}/\overline{p}^{t}_{g,i}$	The minimum/maximum limits of $p^{t}_{g,i}$
Δ_t	Time interval, i.e., one
η_{dch}/η_{ch}	Discharging/charging efficiency coefficients of RCSs and CCSs

$\underline{E}^t_{RC,i}/\overline{E}^t_{RC,i}$	The minimum/maximum limits of $E^t_{RC,i}$
$\overline{P}^{dch,t}_{RC,i}/\overline{P}^{ch,t}_{RC,i}$	The maximum limits of $P^{dch,t}_{RC,i}/P^{ch,t}_{RC,i}$
$\underline{E}^t_{CC,i}/\overline{E}^t_{CC,i}$	The minimum/maximum limits of $E^t_{CC,i}$
$\overline{P}^t_{CC,i}$	The maximum limit of $P^t_{CC,i}$
$\left(p^t_{d,i}\right)^0/\left(q^t_{d,i}\right)^0$	Original active/reactive load demand at the i^{th} bus during the t^{th} hour
Y_i	Demand flexibility at the i^{th} bus
$\overline{\Theta}_i$	The maximum limit of Θ_i
ψ_t	Energy price during the t^{th} hour
$\hat{\alpha}_t$	Maximum perturbation during the t^{th} hour
Γ	Level of robustness

4.3 Smart Distribution System Architecture

A Smart Distribution System integrates advanced information and communication technologies, interactive software, and robust methodologies. It boasts high-level automation and intelligent electronic components, rendering it bi-directional and interactive. This enables self-healing capabilities, enhanced power quality, dependable power provision, and efficient utilization of DERs. The architecture of a typical SDS, as depicted in Figure 4.1, illustrates centralized information flow, where DER entities directly interface with the DNO without intermediary interactions.

This discussion revolves around a distribution network featuring Renewable Energy Sources (RESs) in the form of solar photovoltaic plants and wind farms, EVCSs catering to both residential and commercial sectors, and load aggregators. The Distribution Network Operator (DNO) assumes responsibility for managing the operational schedules of RESs. Residential Charging Stations (RCSs) are simulated to capture the extensive adoption of Electric Vehicles (EVs) for personal use (REVs), either through Vehicle-to-Grid (V2G) or Grid-to-Vehicle

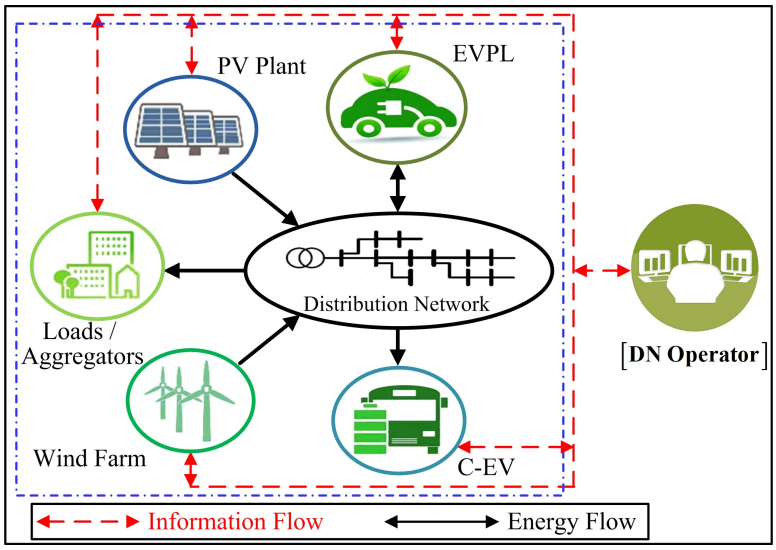

FIGURE 4.1: Architecture of a generic smart distribution system.

(G2V) modes. Commercial EVs (such as electric buses and trucks), exhibiting distinct behavior from REVs, are treated as a separate entity and integrated into the network via Commercial Charging Stations (CCSs) in G2V mode exclusively.

End-user consumers actively participate in Demand Response (DR) scheduling. The DNO manages loads at specific nodes involved in the DR program through a mutual agreement for sharing benefits between the DNO and proactive consumers. Load aggregators represent consumers' interests by submitting controllable load demands to the DNO. Assuming a non-profit stance, the DNO operates as a price-taker from the independent system operator or forecasts electricity prices when engaging in the wholesale market paradigm. Subsequently, it establishes generation and consumption profiles for DERs based on dynamic pricing signals, optimizing system utilization and DER deployment.

4.4 Day-Ahead Scheduling Problem Formulation

Traditionally, RESs transmit their power output to the grid whenever it's available, leading to potential mismatches between supply and demand. This study introduces a novel approach where EVCSs and DR modeling are leveraged to mitigate the intermittent nature of RESs' power output. Specifically, an optimal DA schedule for EVCSs is devised to minimize real loss payments

within the SDS. The DA scheduling problem for EVCSs is dissected into two parts: one addressing DR modeling and the other handling uncertainties in electricity prices and load demands. It is assumed that the DNO has the authority to validate the DA schedules for EVCSs based on dynamic pricing signals. This research aims to minimize payments associated with real power losses in the network while adhering to various constraints such as real and reactive power flow equations, bus voltage limits, EVCS dispatching and storage constraints, and DR constraints.

4.4.1 Objective Function and Constraints

From a mathematical perspective, the objective function for minimizing real power loss payments can be formulated as follows:

$$\min \sum_{t \in T} \psi_t . \left(\sum_{i,j \in \mathcal{E}} \left(r_{ij} . l_{ij}^t \right) \right) \tag{4.1}$$

In equation (4.1), ψ_t represents the energy price at the t^{th} time interval, while equation (4.1) denotes the total real power loss payment over the 24 hours. The objective function (4.1) is constrained by the following conditions.

$$-\left(p_{g,j}^t - p_{d,j}^t \right) = P_{ij}^t - r_{ij} . l_{ij}^t - \sum_{k:j \to k} P_{jk}^t - P_{CC,j}^{ch,t} + \left[\left(\Omega_i^t . P_{RC,i}^{dch,t} \right) - \left(\mho_i^t . P_{RC,i}^{ch,t} \right) \right] \tag{4.2}$$

$$-\left(q_{g,j}^t - q_{d,j}^t \right) = Q_{ij}^t - x_{ij} . l_{ij}^t - \sum_{k:j \to k} Q_{jk}^t \tag{4.3}$$

$$v_j^t = v_i^t - 2. \left(r_{ij} . P_{ij}^t + x_{ij} . Q_{ij}^t \right) + \left(r_{ij}^2 + x_{ij}^2 \right) . l_{ij}^t \tag{4.4}$$

$$v_i^t . l_{ij}^t \geq \left(P_{ij}^t \right)^2 + \left(Q_{ij}^t \right)^2 \tag{4.5}$$

$$v_i := |V_i|^2 \in \{ \underline{V}_i, \overline{V}_i \} \text{ and } l_{ij} := \left| I_{ij} \right|^2 \tag{4.6}$$

Equations (4.2)-(4.5) are commonly referred to as the *DistFlow* equations within the relaxed branch flow model [212], employed for power flow analysis during the t^{th} time interval. Initially, these equations were defined utilizing variables (S, l, v, s_0), which were subsequently transformed into variables

$\left(P_{ij},\ Q_{ij},\ l_{ij}, (i,j) \in \mathcal{E},\ v_i,\ i \in \mathcal{N}, (p_g - p_l)_0, (q_g - q_l)_0\right)$ commonly utilized in the formulation.

Solar photovoltaic panels and wind turbines are supplying real power $p_{g,i}^{SPV/WT}$ to the i^{th} bus during the t^{th} time interval, constrained by upper and lower limits as specified in equations (4.7)-(4.8):

$$\left(\underline{p}_{g,i}^{SPV}\right)^t \leq \left(p_{g,i}^{SPV}\right)^t \leq \left(\overline{p}_{g,i}^{SPV}\right)^t \tag{4.7}$$

$$\left(\underline{p}_{g,i}^{WT}\right)^t \leq \left(p_{g,i}^{WT}\right)^t \leq \left(\overline{p}_{g,i}^{WT}\right)^t \tag{4.8}$$

The operational behavior of an RCS is illustrated by the REV's behavioral tendencies, such as stored energy, time of arrival/departure, and driving demand.

$$\mathrm{E}_{RC,i}^t = \mathrm{E}_{RC,i}^{t-1} + \left[\mathrm{E}_{REV,i}^{arr,t-1} - \mathrm{E}_{REV,i}^{dep,t-1}\right] - \left[\left(\Omega_i^t.P_{RC,i}^{dch,t}/\eta_{dch} - \mho_i^t.P_{RC,i}^{ch,t}.\eta_{ch}\right).\Delta_t\right] \tag{4.9}$$

$$P_{RC,i}^t = \left[\left(\Omega_i^t.P_{RC,i}^{dch,t}\right) - \left(\mho_i^t.P_{RC,i}^{ch,t}\right)\right] \tag{4.10}$$

$$\Omega_i^t + \mho_i^t \leq 1 \tag{4.11}$$

$$\underline{\mathrm{E}}_{RC,i}^t \leq \mathrm{E}_{RC,i}^t \leq \overline{\mathrm{E}}_{RC,i}^t \tag{4.12}$$

$$0 \leq P_{RC,i}^{dch,t} \leq \overline{P}_{RC,i}^{dch,t} \tag{4.13}$$

$$0 \leq P_{RC,i}^{ch,t} \leq \overline{P}_{RC,i}^{ch,t} \tag{4.14}$$

In the above, equation (4.9) signifies the state of charge (SoC) $\left(\mathrm{E}_{RC,i}^t\right)$ of an RCS connected to the i^{th} bus for scheduling. Equation (4.10) represents the total injected power $(P_{RC,i}^t)$ into the network. The constraint in Equation (4.11) prevents simultaneous charging/discharging $\left(P_{RC,i}^{ch,t}/P_{RC,i}^{dch,t}\right)$. Equations (4.12)-(4.14) set the upper and lower bounds on $\mathrm{E}_{RC,i}^t$, $P_{RC,i}^{ch,t}$, and $P_{RC,i}^{dch,t}$ power for an RCS, respectively, at the t^{th} time interval.

CCS equipped with high-power transfer capacity chargers are exclusively modeled for Grid-to-Vehicle (G2V) operation mode. Commercial Electric Vehicles (CEVs), utilized for commercial purposes, have limited integration time with the grid, making it challenging to allocate sufficient time solely for

charging. Additionally, upon arrival, their State of Charge (SoC) tends to be close to the lower limit.

$$\mathrm{E}^{t}_{CC,i} = \mathrm{E}^{t-1}_{CC,i} + \left[\left(P^{ch,t}_{CC,i}.\eta_{ch}\right).\Delta_t\right] + \mathrm{E}^{dep,t-1}_{CEV,i} \tag{4.15}$$

$$\underline{\mathrm{E}}^{t}_{CC,i} \leq \mathrm{E}^{t}_{CC,i} \leq \overline{\mathrm{E}}^{t}_{CC,i} \tag{4.16}$$

$$0 \leq P^{t}_{CC,i} \leq \overline{P}^{t}_{CC,i} \tag{4.17}$$

In the above, equation (4.15) represents the SoC $\left(\mathrm{E}^{t}_{CC,i}\right)$ of a CCS at t^{th} time interval. The constraints for the upper and lower limits on CCS variables are outlined in equations (4.16)-(4.17).

The DR model is defined by the following constraints.

$$p^{t}_{d,i} = \left(p^{t}_{d,i}\right)^{0} \times \mu^{t}_{i} \tag{4.18}$$

$$q^{t}_{d,i} = \left(q^{t}_{d,i}\right)^{0} \times \mu^{t}_{i} \tag{4.19}$$

$$(1 - \Theta_i.\mathrm{Y}_i) \leq \mu^{t}_{i} \leq (1 + \Theta_i.\mathrm{Y}_i) \tag{4.20}$$

$$\sum_{t\in T}\left(p^{t}_{d,i}.\Delta_t\right) = \sum_{t\in T}\left(p^{t}_{d,i}\right)^{0}.\Delta_t \tag{4.21}$$

$$\sum_{t\in T}\left(q^{t}_{d,i}.\Delta_t\right) = \sum_{t\in T}\left(q^{t}_{d,i}\right)^{0}.\Delta_t \tag{4.22}$$

$$\sum_{i\in\Phi}\Theta_i \leq \bar{\Theta} \tag{4.23}$$

In the equations provided, (4.18)-(4.19) denote the adjusted real $(p^{t}_{d,i})$ and reactive $(q^{t}_{d,i})$ power demands, respectively. Equation (4.20) defines the feasible range within which the demand can be modified. Θ_i represents a binary variable indicating whether the i^{th} bus is participating in the DR program. Constraints (4.21)-(4.22) ensure that the total demand over 24 hours remains constant, *i.e.*, matching the original demand. Equation (4.23) limits the total number of buses permitted to participate in the DR program.

4.4.2 Optimization Model

The formulation of the DA scheduling problem presented here is an MINLP problem, which stands as a quintessential instance of an NP-complete

optimization problem. In its inherent structure, an MINLP model can be articulated as:

$$\min_{x} \; f(x) \tag{4.24}$$

$$\text{subject to :} \quad c\,(x) \leq 0, \tag{4.25}$$

$$x \in X, \;\; x_i \in \mathbb{Z}, \;\; \forall\, i \in \{0,1\} \tag{4.26}$$

$$\begin{aligned} \text{where,} \;\; x = \Big\{ & \psi_t, (\Omega/\mho)_i^t, \mu_i^t, \Theta_i, (P/Q)_{ij}^t, V_i^t, I_{ij}^t, (p/q)_{g,i}^t, P_{RC,i}^{dch,t}, P_{RC,i}^{ch,t}, \\ & P_{CC,i}^{ch,t}, \mathrm{E}_{RC,i}^t, \mathrm{E}_{REV,i}^{arr,t-1}, \mathrm{E}_{REV,i}^{dep,t-1}, \mathrm{E}_{CC,i}^t, \mathrm{E}_{CEV,i}^{dept,t} \Big\} \end{aligned} \tag{4.27}$$

4.4.3 Control Strategies for RCSs Dispatch

This work employs both single-agent system (SAS) and multi-agent system (MAS) control strategies to track the optimal DA scheduling solution, contingent upon the level of data-sharing consensus between the DNO and RCSs.

Single-Agent System (SAS)

In this study, the formulated problem is addressed within a SAS framework when RCSs reach a consensus to share their data with the DNO and authorize the control of operational schedules for RCSs. The objective function within the SAS framework is expressed as follows:

$$\min \; f\,(x) = \sum_{t \in T} \psi_t . \left(\sum_{i,j \in \varepsilon} \left(r_{ij} . l_{ij}^t \right) \right) \tag{4.28}$$

Multi-Agent System (MAS)

MAS framework can be employed to address the provided optimization model by decomposing the problem into sub-problems, thereby separating the independent variables and constraints. In this study, the MAS approach is utilized when RCSs are unwilling to share their data with the DNO due to concerns regarding security breaches or other issues. Instead, they provide their scheduling preferences while seeking to maximize their benefits. The objective function within the MAS framework is reformulated as follows:

$$\min\ f(x) = \sum_{t\in T} \psi_t.\left(\sum_{i,j\in\varepsilon}\left(r_{ij}.l_{ij}^{t}\right)\right) + \left\{\max \sum_{t\in T} \psi_t.\left(\left(\Omega_i^t.P_{RC,i}^{dch,t} - \mho_i^t.P_{RC,i}^{ch,t}\right)\right)\right\} \tag{4.29}$$

Equation (4.29) introduces the *min-max* problem, aiming to minimize payment losses while maximizing the benefits for RCSs when dispatching their available SoC in an optimized schedule. The MAS strategy demands less computational time compared to the SAS approach, albeit with a higher likelihood of obtaining a sub-optimal solution. This study explores the disparity between SAS and MAS control strategies through simulations. In this study, the branch and bound (BnB) technique [213] is employed to search for the optimal solution within a bounded search space, systematically exploring all subsets of potential solutions organized in a rooted tree structure. Appendix C presents **Algorithm 1**, which outlines the BnB algorithm employed for addressing the Mixed Integer Programming (MIP) problem associated with optimizing the scheduling of RCSs.

4.5 Day-Ahead Scheduling Problem Formulation Incorporating Uncertainties

The electricity price can fluctuate due to various factors, including competition among generator companies in the unbundled electricity market, variations in energy demands from different distribution companies, and contingencies at the transmission level. To tackle the uncertainty in load demand, it's modeled to reflect real-world behavior. Consequently, DNO are consistently vigilant in mitigating the impact of unforeseen events on the DA schedule, where both electricity prices and load demands may deviate from forecasted values.

Within this section, we convert the formulated problem into a robust optimization challenge aimed at addressing the worst-case scenario while incorporating a predetermined level of conservatism (denoted by Γ). Generally, an uncertainty set (U_α) is established, defining the realized value (α_t^r) of an uncertain variable (α_t) as follows [214]:

$$U_\alpha = \left\{(\alpha_t^r = \alpha_t + \delta_t.\hat{\alpha}_t)\middle|\ \sum_{t\in T}\delta_t = \Gamma,\ \forall\,\delta_t \in [0,1]\right\} \tag{4.30}$$

$$\text{where} \quad \hat{\alpha}_t = \begin{cases} \left(\alpha_t^U - \alpha_t\right), & \text{if } \alpha_t^r \geq \alpha_t \\ \left(\alpha_t^L - \alpha_t\right), & \text{otherwise} \end{cases} \tag{4.31}$$

In equation (4.30), δ_t denotes the prediction error, while α_t^L and α_t^U represent the lower and upper limits of the nominal value α_t during the t^{th} time interval in equation (4.31). The parameter Γ can be adjusted from 0 to 24 to control the level of robustness in the formulated problem, and its value is determined based on the desired degree of conservatism that the DNO wishes to maintain. Consequently, the uncertainty sets for electricity price (U_ψ) and load demand (U_{p_d}) are described as follows:

$$U_\psi = \left\{ \left(\psi_t^r = \psi_t + \delta_t^\psi.\hat{\psi}_t\right) \mid \sum_{t\in T} \delta_t^\psi = \Gamma^\psi, \forall\, \delta_t^\psi \in [0,1] \right\} \tag{4.32}$$

$$U_{p_d} = \left\{ \left((p_{d,j}^t)^r = p_{d,j}^t + \delta_t^d.\hat{p}_{d,j}^t\right) \mid \sum_{t\in T} \delta_t^d = \Gamma^d, \forall\, \delta_t^d \in [0,1] \right\} \tag{4.33}$$

Therefore, the robust version of the problem introduced in Section 4.4 has been developed, and the objective function is now expressed as follows.

$$\min \sum_{t\in T} \psi_t.\left(\sum_{i,j\in\varepsilon}\left(r_{ij}.I_{ij}^t\right)\right) + \left[\max \sum_{t\in T} \delta_t^\psi.\hat{\psi}_t\left(\sum_{i,j\in\varepsilon}\left(r_{ij}.I_{ij}^t\right)\right)\right] \tag{4.34}$$

The objective function in equation (4.34) poses a *min-max* problem, necessitating a bi-level optimization approach. The inner layer maximizes the effect of uncertainties to address the worst-case scenario, while the outer layer minimizes deviations from the forecasted value. However, this paper has reconfigured the bi-level problem into a single-level optimization task to alleviate computational complexity. This was achieved by redefining equation (4.34) and subjecting it to the following constraints:

$$\min \left[\sum_{t\in T} \psi_t.\left(\sum_{i,j\in\varepsilon}\left(r_{ij}.I_{ij}^t\right)\right) - \sum_{t\in T} \delta_t^\psi.\hat{\psi}_t\left(\sum_{i,j\in\varepsilon}\left(r_{ij}.I_{ij}^t\right)\right)\right] \tag{4.35}$$

$$\text{subject to}: \ (4) - (23) \ \text{and} \tag{4.36}$$

$$\delta_t^{\psi/d} \in [0,1]\,; \ \textstyle\sum_{t\in T} \delta_t^{\psi/d} = \Gamma^{\psi/d} \tag{4.37}$$

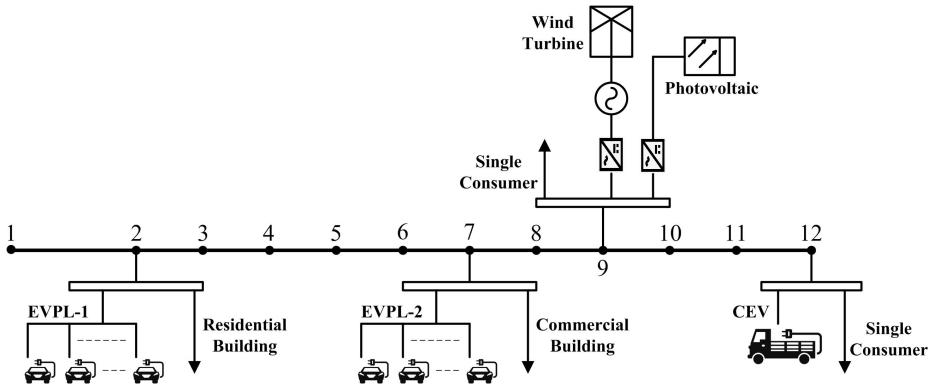

FIGURE 4.2: Modified IEEE-12 bus radial distribution system.

$$\left(p^t_{d,j} + \delta^d_t . \hat{p}^t_{d,j}\right) - p^t_{g,j} = P^t_{ij} - r_{ij}.l^t_{ij} - \sum_{k:j\to k} P^t_{jk} - P^{ch,t}_{CC,j} + \left[\left(\Omega^t_i . P^{dch,t}_{RC,i}\right) - \left(\upsilon^t_i . P^{ch,t}_{RC,i}\right)\right] \tag{4.38}$$

$$\left(q^t_{d,j} + \delta^d_t . \hat{q}^t_{d,j}\right) - q^t_{g,j} = Q^t_{ij} - x_{ij}.l^t_{ij} - \sum_{k:j\to k} Q^t_{jk} \tag{4.39}$$

In the problem formulation outlined in equations (4.35)-(4.39), it is presumed that the sequences of intervals for deviations in load demand from the forecasted value adhere to a descending order of electricity price intervals. This assumption is rooted in the objective of the problem, which aims to enhance robustness against undesired events.

4.6 Results and Discussion

This section presents simulations conducted for extensive case studies on a modified IEEE 12-bus RDN, as illustrated in Figure 4.2. RESs are situated at bus 9 in the network, comprising a solar photovoltaic plant with a total capacity of 100 kWp and a wind farm with a rated capacity of 100 kW. REVs can operate in both Grid-to-Vehicle (G2V) and Vehicle-to-Grid (V2G) modes. Figure 4.3 depicts the arrival and departure of REVs to and from RCSs located at buses two (residential area) and seven (commercial area) in the network, with a capacity for 40 and 30 EVs simultaneously, respectively.

As depicted in Figure 4.3, at 7 AM, there are 32 REVs available at the RCS on bus two, decreasing to 5 by 11 AM as most owners leave for work. Conversely, the RCS on bus seven starts with 0 REVs at 7 AM, reaching full capacity by 11

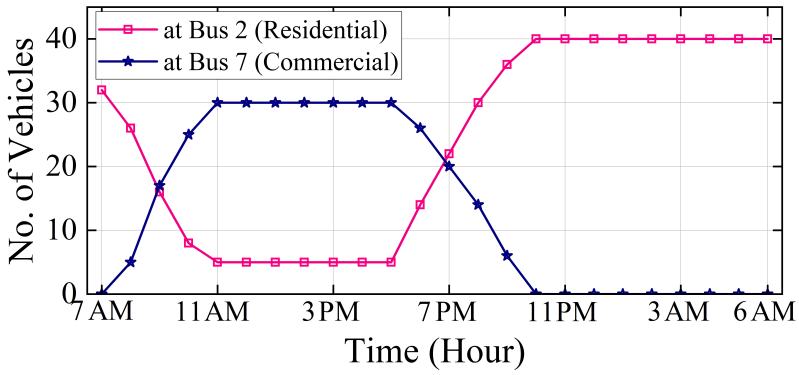

FIGURE 4.3: Pattern of REVs arrival and departure at RCSs located at buses 2 (residential area) and 7 (commercial area).

AM. In the evening, REVs begin departing from the RCS on bus seven starting at 5 PM, reaching 0 total by 10 PM, while arrivals increase at the RCS on bus two from 5 PM, reaching maximum capacity by 10 PM. CCS integrates into the grid at bus 12, with CEVs available for charging during the night, from 7 PM to 7 AM. It is assumed that the bus participating in the DR program is the same as where the CCS is located (*i.e.*, bus 12) to mitigate the effect of increased load demand due to the CCS.

The proposed problem is implemented in an AMPL environment using a KNITRO solver [215], executed on an 11th Gen Intel(R) Core(TM) i5-1135G7 @ 2.40 GHz CPU processor with 8 GB RAM. Figure 4.4 illustrates the hourly rated load demand (in kW) along with the upper and lower uncertainty limits. The load demand exhibits a morning peak around 11 AM and an evening peak from 7 PM to 8 PM, primarily driven by residential consumption. During the night, the load demand decreases, with a minimum between 1 AM and 5 AM. It is assumed that no load will be curtailed during the DA scheduling process.

DNO acquires electricity prices from the utility grid. However, in situations of uncertainty, the DNO only possesses knowledge of the upper and lower limits within which the hourly price fluctuates. Figure 4.4 also displays the electricity prices (in \$/kWh) [216] along with their upper and lower uncertainty limits. The hourly electricity prices significantly increase from 9 AM to 11 AM due to heightened load demand. There's a slight decrease around noon, followed by another peak at 1 PM. Subsequently, prices begin to decline from 2 PM, except for a surge at 8 PM attributed to high demand during that time interval.

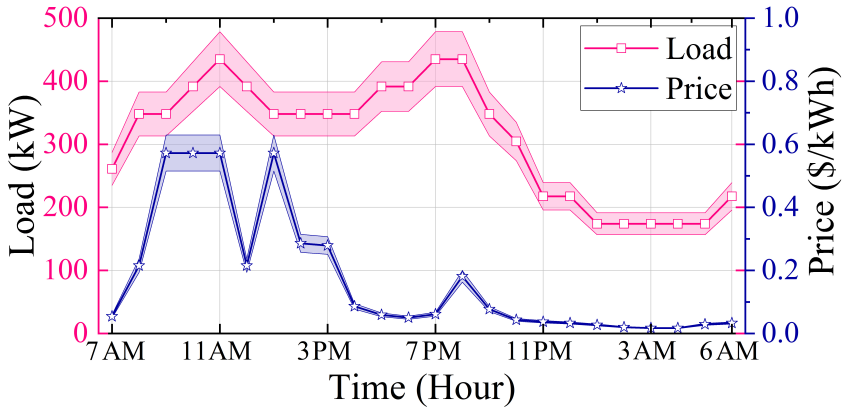

FIGURE 4.4: Hourly load demand and price characteristics.

4.6.1 Case Studies

Analysis has been conducted on five distinct case studies.

Case-1: Base Case

A base case has been established for comparison and analysis, wherein no RESs and charging stations are integrated into the system. The total real power losses in the system amount to 266.96kW, incurring a loss payment of 60.50$. In scenarios involving electricity price uncertainty, the loss payments would range from 60.50$ (at $\Gamma = 0$) to 66.55$ (at $\Gamma = 24$), representing varying degrees of conservativeness. When uncertainties in both electricity price and load demand are factored in, the real power loss increases by 21.95% (at $\Gamma = 24$), consequently inflating the total loss payment by a maximum of 34.21%.

Case-2: RESs Placed in System

In this scenario, no charging stations are installed, but the integration of RESs facilitates a bidirectional energy flow in the system. The inclusion of RESs contributes to a reduction in the total daily real power losses within the network, decreasing from 266.96kW to 178.67kW, and consequently lowering the incurred payments from 60.50$ to 37.07$. Figure 4.5 displays the total hourly power supplied by RESs and compares the hourly power demand from the grid between Cases 1 and 2. Notably, RESs reach a maximum generation of 155.2kW

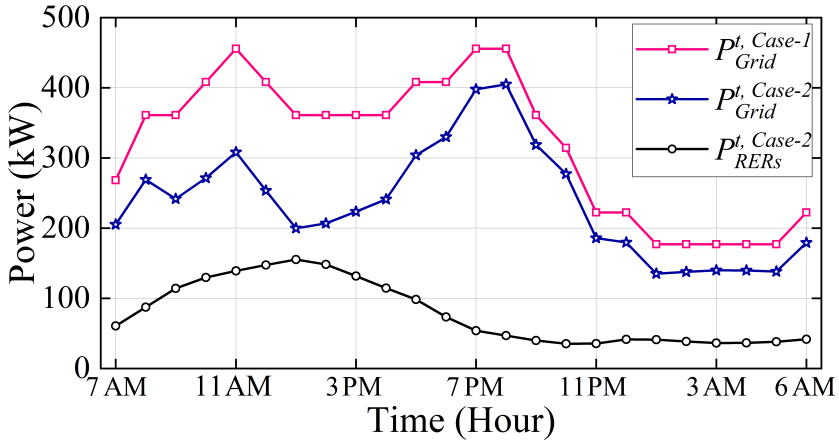

FIGURE 4.5: Hourly power generation from RESs and hourly power demand from the grid in Cases 1 and 2.

at 1 PM, significantly reducing the power demand from the grid. With RESs integrated into the network, the hourly load demands from the grid decrease in Case 2 compared to Case 1.

Case 3: RCSs Placed in System

DA Scheduling of RCSs in SAS Framework: RCSs are scheduled optimally to minimize real power loss payments. The charging/discharging capacities of EV chargers at buses two and seven are set at 3.3kW and 6.6kW, respectively. Other technical specifications for REVs and RCSs are adopted from [217]. In Figure 4.6, the dispatch states of RCSs at buses 2 and 7 are depicted in red and blue bar graphs, respectively. It is evident from Figure 4.6 that both RCSs discharge their available energy from 8 AM to 3 PM when electricity prices are high. Subsequently, the RCS at bus two continues discharging energy until 9 PM, while the RCS at bus seven stores energy from 4 PM to 9 PM to reach the initial SoC. A discharge schedule is initiated for the RCS at bus seven at 8 PM, driven by slightly higher electricity prices in adjacent intervals. The RCS at bus two is scheduled for charging from 11 PM to 6 AM when electricity prices are at their lowest, resulting in a reduction in total loss payment, *i.e.*, 33.79$, despite an increase in overall load demand throughout the day.

The line graph depicted in Figure 4.6 illustrates the hourly DA schedules for RCSs situated at buses 2 and 7, with a focus on minimizing losses as the objective

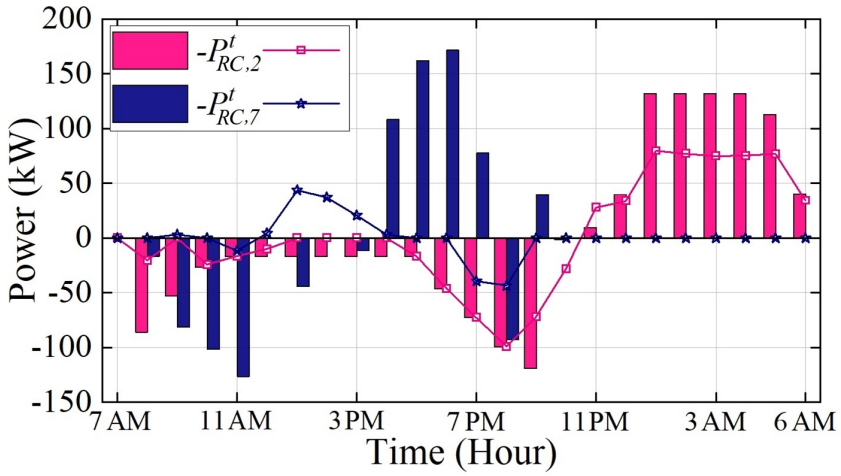

FIGURE 4.6: Hourly DA schedules for RCSs located at buses 2 and 7, aiming to minimize loss payments (represented by bars) and minimize losses themselves (represented by lines), are provided in Case 3.

function. In contrast to the strategy for minimizing real power loss payments, RCSs at buses 2 and 7 are scheduled to discharge during periods of high load demand, specifically at 11 AM and from 7 PM to 8 PM. During low-load demand periods, RCSs store energy to reach their initial SoC. For instance, the RCS at bus two is scheduled for charging from 11 PM to 6 AM when demand is lower. Meanwhile, the RCS at bus seven engages in charging between 1 PM and 3 PM, despite the peak electricity price occurring at 1 PM. Consequently, active losses have been notably reduced to 176.42kW. However, the loss payment has increased to 37.05$, compared to 33.79$ when minimizing losses is the objective function.

Table 4.1 presents a comparison of active losses (in kW) and real power loss payments (in $) across Cases 1, 2, and 3. In scenarios where RESs are not utilized alongside the operation of RCSs, the calculated network active power losses amount to 284.02kW, surpassing the base case's active losses (266.96kW), as detailed in Table 4.1. This exacerbates the current network condition. Hence, incorporating RESs offers significant benefits in mitigating the escalating demand attributed to the integration of numerous RCSs into the network.

DA Scheduling of RCSs in MAS Framework: In this scenario, RCSs autonomously optimize their schedules to maximize their advantages and

TABLE 4.1: Comparison of active losses (kW) and loss payments ($) under various cases

Cases	**Active loss (kW)**	**Loss payment ($)**
Case-1: No RESs & RCSs placed	266.96	60.50
Case-2: RESs placed & no RCSs	178.67	37.07
Case-3(a): RCSs placed & no RESs	284.02	51.88
Case-3(a): RESs & RCSs placed	193.58	33.79

TABLE 4.2: Technical characteristics for commercial electric vehicle

CEV Parameter	**Value**
Battery capacity	300 kWh
Charging power	40 kW
Charging efficiency	0.92
Minimum energy state	15%
Maximum energy state	95%
Average power consumption	75 kWh/100 km

transmit their preferences to the DNO for DA scheduling. Subsequently, the DNO incorporates the RCS schedules into the overall DA schedules. The dispatch schedules for RCSs in Cases 3(a) and 3(b) are compared in Figure 4.7. It can be observed in Figure 4.7 that the discharging/charging schedules for the RCS at bus two in Case 3(b) closely resemble those in Case 3(a), except at 7 AM when RCSs discharge their stored energy to maximize benefits. However, the schedules for the RCS at bus seven exhibit slight variations compared to those in Case 3(a); for instance, the RCS begins storing energy at noon as electricity prices decrease, then discharges again at 1 PM when prices peak. As RCS owners communicate their scheduling preferences to the DNO, the total benefits for RCS owners amount to 374.51$, with a corresponding loss payment of 35.52$, which is higher than the 33.79$ observed in Case 3(a).

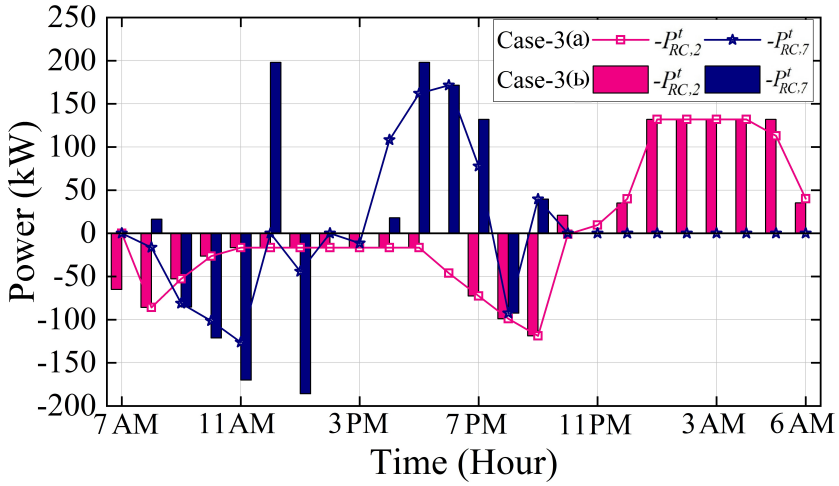

FIGURE 4.7: Comparison between Cases 3(a) and 3(b) regarding the DA hourly schedules for RCSs located at buses 2 and 7.

Case 4: CCSs Placed in System

It is assumed that during the daytime, CEVs deplete almost all of their battery energy ($\overline{\mathrm{E}}_{CEV} - \underline{\mathrm{E}}_{CEV} = 0.95 - 0.15 = 0.80$ kWh) before connecting to the grid. In the current simulation, one CEV is integrated into the CCS available at bus 12. The CCS charging schedule is executed while the DNO endeavors to minimize real power loss payments. The technical specifications for a CEV are outlined in Table 4.2. The DA schedule for the CCS (represented by a bar graph) and the dispatches for RCSs at buses 2 and 7 (depicted via line graphs) are illustrated in Figure 4.8. During nighttime when electricity prices are relatively low, the system experiences losses totaling 202.17kW. However, the associated loss payment amounts to 34.00$, a slight increase compared to scenarios without CCS integration. Conversely, when minimizing losses serves as the objective function, the loss payment incurred by the DNO rises to 37.37$, marking a 9% increase compared to when minimizing loss payments is the focus.

Case 5: DNO Incorporating Demand Response Model

Bus 12 is enlisted for participation in the DR program, where 10% of the rated demand for each time interval is deemed controllable and can be shifted during scheduling. DNO adjusts load demand periods by integrating the DR model into

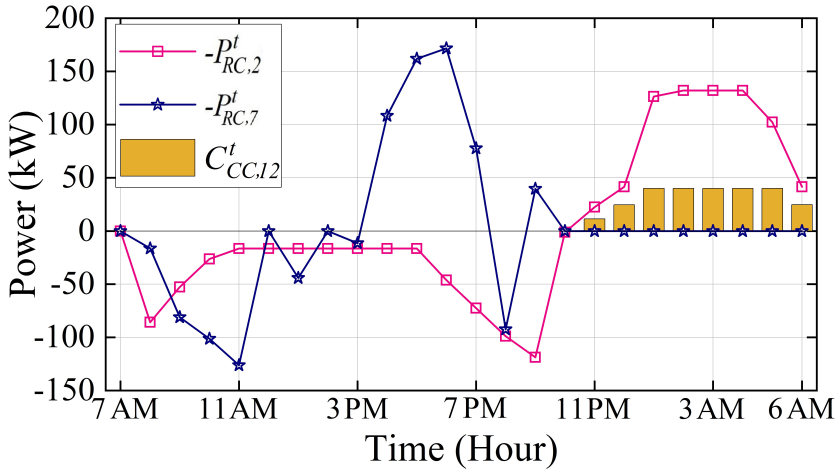

FIGURE 4.8: DA hourly schedules for CCS and RCSs in Case 4.

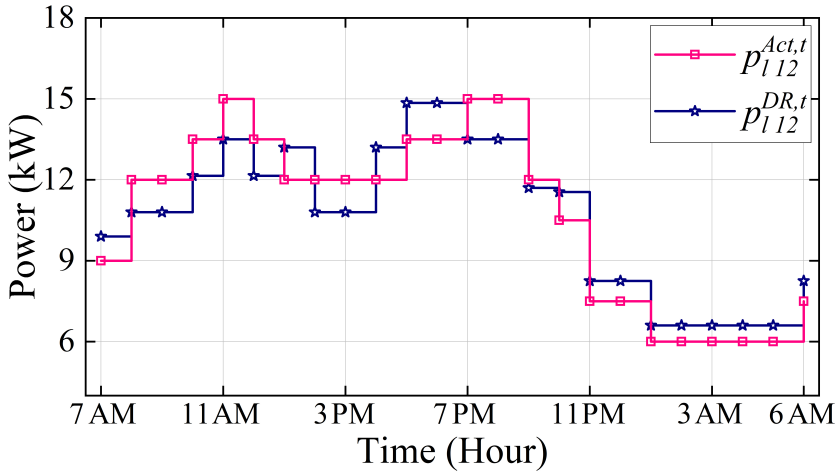

FIGURE 4.9: The controllable load demand undergoes shifts upon the integration of demand response in Case 5.

the DA schedule optimization aimed at minimizing loss payments. Figure 4.9 presents a comparison between the load demand curve before and after the incorporation of the DR model. Despite scheduled CEV charging occurring from 11 PM to 6 AM during periods of low electricity prices, load demand remains unchanged. However, controllable loads from high-price periods (*i.e.*, from 8 AM to 3 PM, excluding noon when prices dip lower than adjacent intervals, and from 7 PM to 9 PM) are shifted to low-price periods. This results in post-DR load demand aligning much closer to the ideal load demand, as depicted in Figure 4.9.

TABLE 4.3: Comparison between loss minimization and loss payment minimization as objective functions

Cases	Loss minimization		Loss payment minimization	
	Active loss (kW)	**Loss payment ($)**	**Active loss (kW)**	**Loss payment ($)**
Case-1	266.96	60.50	266.96	60.50
Case-2	178.67	37.07	178.67	37.07
Case-3(a)	176.42	37.05	193.58	33.79
Case-3(b)	205.34	35.52	205.34	35.52
Case-4	184.77	37.37	202.17	34.00
Case-5	184.24	37.36	202.18	33.66

4.6.2 Comparative Analysis

This study examines the contrast between minimizing operational losses and minimizing real power loss payments through a comparative numerical analysis, as detailed in Table 4.3. It is observed that focusing on loss minimization leads to a notable reduction in active losses. However, when prioritizing loss payment minimization as the objective function, although active losses also decrease significantly, the associated loss payments are comparatively lower. Minimizing the financial burden on the DNO is crucial within the context of the current competitive electricity market paradigm.

This study conducts an impact analysis on uncertainty modeling for worst-case scenarios using robust optimization techniques. The effects of applying robust optimization to minimize loss payments under uncertainty, with a parameter value of $\Gamma = 4$, are evaluated and presented in Table 4.4. It is noted that robust optimization significantly enhances the optimization of DA schedules for RCSs in both single-agent and multi-agent systems, as evidenced by the results of Cases 3(a) and 3(b) in Table 4.4.

Table 4.5 presents a comparison of computational complexity between single-agent system and multi-agent system control strategies by examining the types of variables and constraints in Cases 3(a) and 3(b). In Case 3(a), the DNO formulates the optimal DA schedules for RCSs in a single-layer problem to minimize real

TABLE 4.4: Impact of applying robust optimization (RO) on loss payment minimization under uncertainty with $\Gamma = 4$

Cases	Without RO		With RO	
	Active loss (kW)	**Loss payment ($)**	**Active loss (kW)**	**Loss payment ($)**
Case-1	280.90	72.90	280.90	72.90
Case-2	188.20	45.17	188.20	45.17
Case-3(a)	201.20	41.96	201.59	40.22
Case-3(b)	212.58	43.63	213.59	42.40
Case-4	209.79	42.19	210.19	40.43
Case-5	209.69	41.76	208.75	39.92

power loss payments. However, in Case 3(b), the DA scheduling occurs in two stages. Initially, RCSs determine their schedules to maximize their benefits and communicate their DA schedule preferences to the DNO. Subsequently, the DNO integrates these RCS schedules and devises overall optimized DA schedules in the subsequent stage aimed at minimizing loss payments.

4.7 Summary

This work presents a novel approach aimed at optimizing the DA schedules of EVCSs within the RESs integrated smart distribution system. The optimization objective is focused on minimizing real power loss payments from the perspective of the DNO. Through numerical simulations conducted on a modified IEEE-12 bus RDN, the efficacy of the proposed method is demonstrated. The findings from extensive case studies underscore the superiority of the proposed approach over traditional active loss minimization strategies. Notably, it significantly reduces operational losses within the network while alleviating the financial burden on the DNO during daily operations in competitive market environments. Key highlights of the study include:

1. Implementation of DR model to shape load demand profiles, enabling

TABLE 4.5: Comparison of computational complexities between single-agent and multi-agent systems in Case-3

Variable and constraint type	**SAS**	**MAS**	
		Main Problem	**Sub-Problem**
P_{ij}^{t}	264	264	-
Q_{ij}^{t}	264	264	-
v_{i}^{t}	264	264	-
l_{ij}^{t}	264	264	-
$\left(p_{g,i}^{SPV}\right)^{t}$	12	12	-
$\left(p_{g,i}^{WT}\right)^{t}$	24	24	-
Ω_{i}^{t}	48	-	48
$\mho_{i}^{t}$	48	-	48
$P_{RC,i}^{dch,t}$	37	-	37
$P_{RC,i}^{ch,t}$	37	-	37
$P_{RC,i}^{t}$	38	-	38
$\mathrm{E}_{RC,i}^{t}$	38	-	38
Total no. of variables	1338	1092	246
Bounded variables	508	300	208
unbounded variables	830	792	38
No. of binary variables	96	-	96
total no. of constraints	1180	1056	124
Linear equality constraints	792	792	38
Nonlinear equality constraints	340	264	38
Linear inequality constraints	48	-	48
Computational Time (s)	577.27	0.46	200.56

controllable load shifts from high to low electricity price periods for more efficient DA operations.

2. Utilization of robust optimization techniques to address worst-case uncertainties in electricity price and load demand during DA operations, with a defined level of conservativeness by the DNO.

3. Integration of single-agent and multi-agent system control strategies based on consensus in information flow between RCSs and DNO, facilitating the derivation of DA schedules for RCSs.

4. Overall, the proposed approach offers a practical and effective solution for optimizing DA schedules of EVCSs for smart distribution system, prioritizing real power loss payment minimization, and enhancing operational efficiency in the distribution network.

Chapter 5

Aggregation and Scheduling of DERs in Smart Distribution System

5.1 Preamble

This chapter introduces a comprehensive framework aimed at efficiently administering a substantial array of heterogeneous distributed energy resources (DERs) functioning within smart distribution systems, with the goal of optimizing the operations of local energy communities (LECs) and enhancing grid services. Initially, we establish a methodology for aggregating DERs to assess their combined flexibility, taking into account factors such as their preferences, spatial distribution, and temporal dynamics. Following this, we implement a hierarchical control framework (HCF) to effectively deploy the aggregated flexibility of DERs. The HCF encompasses three primary entities: an electric utility (EU) operator, community aggregators (CAs), and individual DERs. CAs leverage the flexibility derived from the aggregated DERs within their respective LECs to minimize operational expenses while adhering to distribution network constraints. Conversely, the EU operator coordinates dispatch setpoints received from CAs along with disaggregated DERs to regulate node voltages within the distribution system and mitigate power losses, thereby enhancing grid services. Through numerical simulations conducted on a modified IEEE-123 bus radial distribution network, we validate the effectiveness of our approach in proficiently managing DERs for cost-effective operations and enhancing grid services.

The remainder of the chapter is organized as follows: In Section 5.2, the

nomenclature for the variables, and parameters employed in the problem formulation within this chapter. Section 5.3 provides an overview of the proposed aggregation and control framework, as well as the branch power flow model utilized for distribution network modeling. Section 5.4 delves into the modeling of electric vehicle (EVs) aggregation at charging stations (CS) and the representation of deferrable loads for the demand response mechanism. In Section 5.5, the formulation of the HCF-based optimal operation strategy for local energy communities and the electric utility operator is presented. Section 5.6 presents the numerical results, followed by the summary to encapsulate our findings and contributions in Section 5.7.

5.2 Nomenclature

Variables

$P_{ij,t}^{flow}, Q_{ij,t}^{flow}$	Active, reactive branch power flow between buses i and j at time t
$l_{ij,t}^{flow}$	Current flow (squared) between buses i and j at time t
$v_{i,t}^{node}$	Node voltage (squared) at bus i at time t
$E_{i,t}^{CS}$	Residual energy of CS at bus i at time t
$P_{i,t}^{ch,CS}$	Charging power of CS at bus i at time t
$P_{i,t}^{dch,CS}$	Discharging power of CS at bus i at time t
$\zeta_{i,j,t}^{DL}$	State of DL j at bus i at time t
ζ_{i,j,t_0}^{DL}	State of DL j at bus i in current time slot t_0
$P_{i,j,t}^{DL}$	Power consumed by DL j at bus i at time t
$\xi_{i,j,k,t}^{task}$	State of task k for DL j at bus i at time t
$P_{i,g,t}^{RE}, Q_{i,g,t}^{RE}$	Active, reactive power supplied by RESs g at bus i at time t

Parameters

$p_{i,t}^{FL}, q_{i,t}^{FL}$	Inflexible (fixed) active, reactive load demand at bus i at time t
r_{ij}, x_{ij}	Resistance, reactance of a line connecting buses i and j
$N_{i,t}^{a}, N_{i,t}^{d}$	No. of EVs arrived, departed at bus i at time t
$E_{i,n}^{a,EV}$	Residual energy of arrived EV n at bus i
$E_{i,n}^{d,EV}$	Desired energy at departure of EV n at bus i
$\eta_{ch,i}^{CS}, \eta_{dch,i}^{CS}$	Efficiencies of the charging, discharging power of CS at bus i
$\overline{E}_{i,t}^{CS}, \underline{E}_{i,t}^{CS}$	Upper, lower bound of the residual energy of CS at bus i at time t
$\overline{P}_{i,t}^{ch,CS}$	Maximum charging power of CS at bus i at time t
$\overline{P}_{i,t}^{dch,CS}$	Maximum discharging power of CS at bus i at time t
$\overline{P}_{i,n}^{ch,EV}$	Maximum charging power of EV n at bus i
$\overline{P}_{i,n}^{dch,EV}$	Maximum discharging power of EV n at bus i
$\overline{E}_{i,n,t}^{EV}, \underline{E}_{i,n,t}^{EV}$	Upper, lower bound of the residual energy of EV n at bus i at time t
$\eta_{i,n}^{dch,EV}$	Discharging power efficiency of EV n at bus i
$\eta_{i,n}^{ch,EV}$	Charging power efficiency of EV n at bus i
$t_{a,n}^{EV}, t_{d,n}^{EV}$	Arrival, departure time of EV n
$\underline{E}_{i,n}^{EV}$	Minimum of residual energy of EV n at bus i
$\overline{E}_{i,n}^{EV}$	Maximum of residual energy of EV n at bus i
$\alpha_{i,j}, \beta_{i,j}$	Starting, ending time (operational) of DL j at bus i
$\hat{\zeta}_{i,j,t}^{DL}$	State of DL j at bus i in previous time slot t
$Z_{i,j}^{DL}$	No. of time slots (operational) required by DL j at bus i

$E_{i,j}^{DL}$	Energy required by DL j at bus i
$P_{i,j,k}^{task}$	Rated power of task k for DL j at bus i
$Z_{i,j,k}^{task}$	No. of time slots (operational) required by DL j at bus i to finish task k
$S_{i,g,t}^{RE}$	Apparent power capacity of RES g at bus i at time t
$\phi_{i,g}$	Angle defining power factor of RES g at bus i
$P_{i,g,t}^{RE,fore}$	Active power forecast for RES g at bus i at time t

5.3 Framework Overview and Network Modelling

This study considers the various LECs within the distribution network, comprising both static loads and a variety of DERs, including electric vehicle charging stations, deferrable loads (DLs), and renewable energy sources (RESs) represented by photovoltaic (PV) installations and wind turbine (WT) arrays, as depicted in Figure 5.1. The proposed work posits that CAs are responsible for the management of DERs dispersed throughout their respective communities. Moreover, the supervision of LECs and disaggregated DERs, including Energy Storage Systems (ESs) integrated with PV installations and WT arrays, is delegated to an EU operator.

For simplicity, a radial distribution network with a single feeder connected to EU modeled by a tree graph $\mathcal{G} := (\mathcal{N}, \mathcal{E})$, where $i \in \mathcal{N} := 1, 2, \ldots, n$ represents a node and $(i, j) \in \mathcal{E} \subseteq \mathcal{N} \times \mathcal{N}$ represents a distribution line connected i^{th} to j^{th} nodes. The relaxed branch flow model presented in [212] is employed for power flows for this network, as expressed in (5.1)-(5.4); where, for each node $i \in \mathcal{N}$ at t^{th} time interval, denote $v_{i,t}^{node} = \left|V_{i,t}^{node}\right|^2$ refers to magnitude squared of node voltage. Let $s_{i,t}^{FL} = p_{i,t}^{FL} + jq_{i,t}^{FL}$ be node i net complex fixed load demand. Similarly, for each line $(i, j) \in \mathcal{E}$ at t^{th} time interval, denote $l_{ij,t}^{flow} := \left|I_{ij,t}^{flow}\right|^2$ refers to magnitude squared of branch current flows from i node to j node. Let $S_{ij,t}^{flow} = P_{ij,t}^{flow} + jQ_{ij,t}^{flow}$ be the *sending-end* branch flow from i node to j node. A solution of (5.1)-(5.4) to a given s^{FL} is denoted by

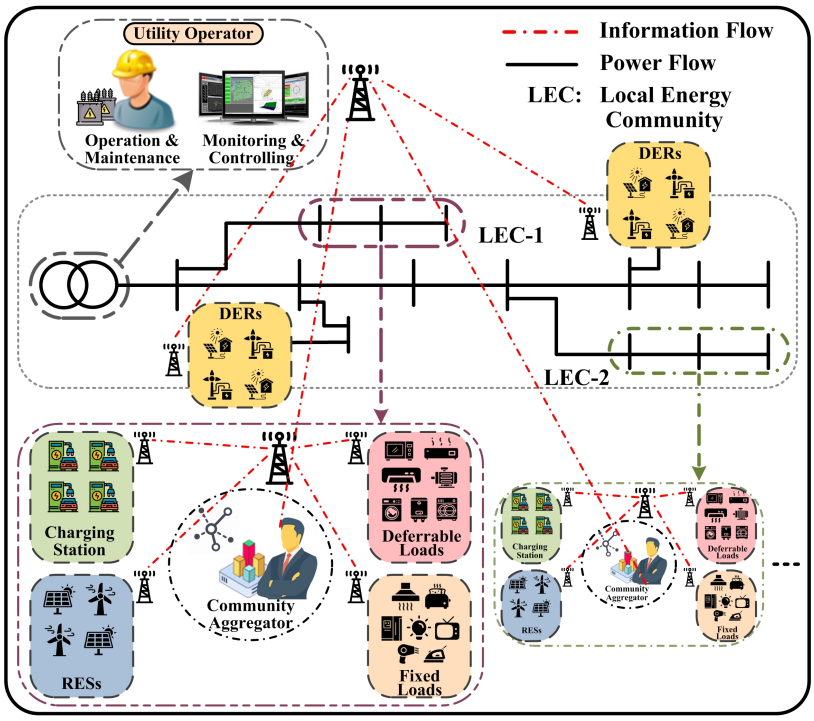

FIGURE 5.1: Schematic of the proposed aggregation and control framework.

$x(s^{FL}) := (S^{flow}, I^{flow}, V^{node}, s_0^{FL})$, is unique for practical radial network where $|V_0| \simeq 1$ and r_{ij}, x_{ij} are small p.u. values.

$$p_{j,t}^{FL} = \sum_{i:i\to j} \left(P_{ij,t}^{flow} - r_{ij} l_{ij,t}^{flow} \right) - \sum_{k:j\to k} P_{jk,t}^{flow} \tag{5.1}$$

$$q_{j,t}^{FL} = \sum_{i:i\to j} \left(Q_{ij,t}^{flow} - x_{ij} l_{ij,t}^{flow} \right) - \sum_{k:j\to k} Q_{jk,t}^{flow} \tag{5.2}$$

$$v_{j,t}^{node} = v_{i,t}^{node} - 2\left(r_{ij} P_{ij,t}^{flow} + x_{ij} Q_{ij,t}^{flow} \right) + \left(r_{ij}^2 + x_{ij}^2 \right) l_{ij,t}^{flow} \tag{5.3}$$

$$v_{i,t}^{node} l_{ij,t}^{flow} = \left(P_{ij,t}^{flow} \right)^2 + \left(Q_{ij,t}^{flow} \right)^2 \tag{5.4}$$

Moreover, we consider the LEC as a sub-network comprising DERs interconnected to the distribution feeder line through a single Point of Common Coupling (PCC). At each time increment, a CA has the capability to monitor various parameters at the PCC, including voltage levels and the exchange of active/reactive power with the feeder. The CA aggregates energy requirements

from dispersed DER units across the LEC and assesses available flexibility to facilitate efficient dispatching, aiming for optimal utilization of its DERs to satisfy the energy needs within the LEC. Subsequently, the CA communicates these dispatch setpoints to the EU operator to address additional energy demands, while the EU operator endeavors to enhance overall grid services.

5.4 DERs Aggregation Model for EV Fleets and Residential Flexible Loads

The electrical grid has experienced a significant surge in the integration of EVs and RESs, notably photovoltaic panels. DERs incorporating diverse technologies, including deferrable loads, RESs, and EVs, are dynamically reshaping the energy landscape, directing it towards a more de-carbonized and resilient configuration. Consequently, acknowledging and leveraging the full potential of DERs becomes unquestionably paramount. To effectively integrate a considerable number of DERs into the overall system operation, it is essential to establish an aggregate model capable of encompassing and accommodating their inherent flexibility. This study primarily focuses on two pivotal categories of DERs: EV fleets at CS and deferrable loads. This section delineates the modeling approach employed for aggregating EV fleets at CS and for aggregating DLs to facilitate demand response.

5.4.1 Aggregation Model for EV Fleets at CSs

In real-world scenarios, the CS can acquire crucial information about EVs upon their connection. This data encompasses details such as the time of arrival and departure, initial and desired energy levels, maximum charging rate, and the duration for which charging is scheduled by the user [218]. The continuous influx and departure of EVs lead to a dynamic variation in the EV count at CS over time. As a result, the EV fleet at the CS is amalgamated into a cohesive unit with time-sensitive power and energy constraints. This process effectively outlines the operational parameters of the CS.

1. The power capacity constraints of EV aggregation

$$P_{i,t}^{dch,CS} \leq \overline{P}_{i,t}^{dch,CS} - \left(\overline{P}_{i,t}^{dch,CS} \Big/ \overline{P}_{i,t}^{ch,CS}\right) P_{i,t}^{ch,CS} \tag{5.5}$$

$$0 \leq P_{i,t}^{ch,CS} \leq \overline{P}_{i,t}^{ch,CS} \tag{5.6}$$

$$0 \leq P_{i,t}^{dch,CS} \leq \overline{P}_{i,t}^{dch,CS} \tag{5.7}$$

$$\overline{P}_{i,t}^{ch,CS} = \overline{P}_{i,t}^{ch,CS} + \overline{P}_{i,n\in N}^{ch,EV}\left(N_{i,t}^{a} - N_{i,t}^{d}\right) \tag{5.8}$$

$$\overline{P}_{i,t}^{dch,CS} = \overline{P}_{i,t}^{dch,CS} + \overline{P}_{i,n\in N}^{dch,EV}\left(N_{i,t}^{a} - N_{i,t}^{d}\right) \tag{5.9}$$

Equation (5.5) originates from the **Extn-LP** approach proposed in [219] for battery modeling, aimed at streamlining the feasible search space. Constraints (5.6) and (5.7) define the maximum and minimum bounds on the charging and discharging powers at the CS located at bus i during time slot t, respectively. Additionally, (5.8) and (5.9) establish the upper limits for the charging and discharging powers at the CS at bus i during time slot t, respectively.

2. The energy capacity constraints of EV aggregation

$$E_{i,t}^{EV(a,d)} = \sum_{n=1}^{N_{i,t}^{a}} E_{i,n}^{a,EV} - \sum_{n=1}^{N_{i,t}^{d}} E_{i,n}^{d,EV} \tag{5.10}$$

$$E_{i,t}^{CS} = E_{i,t-1}^{CS} + \left[\eta_{ch,i}^{CS} P_{i,t}^{ch,CS} - \frac{P_{i,t}^{dch,CS}}{\eta_{dch,i}^{CS}}\right]\Delta t + E_{i,t}^{EV(a,d)} \tag{5.11}$$

$$\left(\eta_{ch,i}^{CS} P_{i,t}^{ch,CS}\right)\Delta t \leq \left(\overline{E}_{i,t}^{CS} - E_{i,t-1}^{CS} - E_{i,t}^{EV(a,d)}\right) \tag{5.12}$$

$$\left(P_{i,t}^{dch,CS}\right)\Delta t \leq \left(E_{i,t-1}^{CS} + E_{i,t}^{EV(a,d)} - \underline{E}_{i,t}^{CS}\right)\eta_{dch,i}^{CS} \tag{5.13}$$

$$\underline{E}_{i,t}^{CS} \leq E_{i,t}^{CS} \leq \overline{E}_{i,t}^{CS} \tag{5.14}$$

$$\underline{E}_{i,t}^{CS} = \underline{E}_{i,t-1}^{CS} + \sum_{n=1}^{N_{i,t}^{a}} \underline{E}_{i,n,t}^{EV} - \sum_{n=1}^{N_{i,t}^{d}} E_{i,n}^{d,EV} \tag{5.15}$$

$$\overline{E}_{i,t}^{CS} = \overline{E}_{i,t-1}^{CS} + \sum_{n=1}^{N_{i,t}^{a}} \overline{E}_{i,n,t}^{EV} - \sum_{n=1}^{N_{i,t}^{d}} E_{i,n}^{d,EV} \tag{5.16}$$

$$\underline{E}_{i,n,t}^{EV} = \begin{cases} 0, & t \in T \setminus \left[t_{a,n}^{EV}, t_{d,n}^{EV}\right] \\ \max \left\{ \begin{array}{l} \underline{E}_{i,n}^{EV}, E_{i,n}^{a,EV} - \frac{\overline{P}_{i,n,t}^{dch,EV}}{\eta_{i,n}^{dch,EV}} \left(t - t_{a,n}^{EV}\right), \\ E_{i,n}^{d,EV} - \eta_{i,n}^{ch,EV} \overline{P}_{i,n,t}^{ch,EV} \left(t_{d,n}^{EV} - t\right) \end{array} \right\}, & t_{a,n}^{EV} \le t \le t_{d,n}^{EV} \end{cases} \tag{5.17}$$

$$\overline{E}_{i,n,t}^{EV} = \begin{cases} 0, & t \in T \setminus \left[t_{a,n}^{EV}, t_{d,n}^{EV}\right] \\ \min \left\{ \begin{array}{l} \overline{E}_{i,n}^{EV}, E_{i,n}^{a,EV} + \eta_{i,n}^{ch,EV} \overline{P}_{i,n,t}^{ch,EV} \left(t - t_{a,n}^{EV}\right), \\ E_{i,n}^{d,EV} + \frac{\overline{P}_{i,n,t}^{dch,EV}}{\eta_{i,n}^{dch,EV}} \left(t_{d,n}^{EV} - t\right) \end{array} \right\}, & t_{a,n}^{EV} \le t \le t_{d,n}^{EV} \end{cases} \tag{5.18}$$

In Equation (5.10), $E_{i,t}^{EV(a,d)}$ represents the net energy at the CS located at bus i during time slot t, considering the energy received from arriving EVs and subtracting the desired energy of departing EVs. Equation (5.11) delineates the energy update procedure for the CS at bus i during time slot t. Constraint (5.12) governs the charging capacity rate, while (5.13) imposes restrictions on the discharging capacity rate, as discussed in [219]. Notably, the combination of (5.12) and (5.6) yields a more stringent condition: $P_{i,t}^{ch,CS} \le \min\left\{\overline{P}_{i,t}^{ch,CS}, \left(\overline{E}_{i,t}^{CS} - E_{i,t-1}^{CS} - E_{i,t}^{EV(a,d)}\right)\right\}$, enforcing a tighter upper bound on the charging power capacity. Similarly, the fusion of (5.13) and (5.7) results in a more rigorous constraint: $P_{i,t}^{dch,CS} \le \min\left\{\overline{P}_{i,t}^{dch,CS}, \left(E_{i,t-1}^{CS} + E_{i,t}^{EV(a,d)} - \underline{E}_{i,t}^{CS}\right)\right\}$, establishing a tighter upper limit on the discharging power capacity. Additionally, (5.14) imposes limitations on the energy at the CS at bus i during time slot t. Constraints (5.15) and (5.16) compute the lower and upper boundaries, respectively, for the net energy at the CS at bus i during time slot t. Finally, constraints (5.17) and (5.18) determine the permissible operational range for an EV n at the CS at bus i during time slot t.

Illustrative Example

To provide a clearer demonstration of the proposed aggregation model for EVs at the CS and to compare it with previously reported aggregation models in references [218] and [220], we conducted a case study involving two specific EVs. The parameters and assumptions used are derived from reference [218] and are presented in Table 5.1. We then utilized equations (5.17) and (5.18) to calculate the operational regions for each of these two individual EVs, with the results

TABLE 5.1: Parameters of Electric Vehicles

EV	$t_{a,n}^{EV}$	$t_{d,n}^{EV}$	$E_{i,n}^{a,EV}$	$\overline{P}_{i,t}^{ch,CS}$ / $\overline{P}_{i,t}^{dch,CS}$	$B_{i,n}^{EV}$
1	0	6	4	4	20
2	2	7	12	4	20

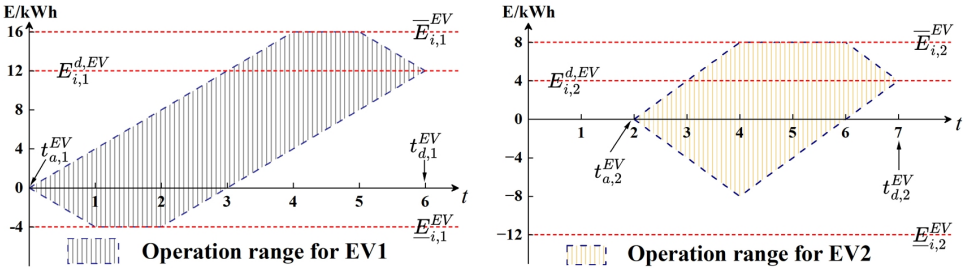

FIGURE 5.2: Operation ranges of the individual EV1 and EV2.

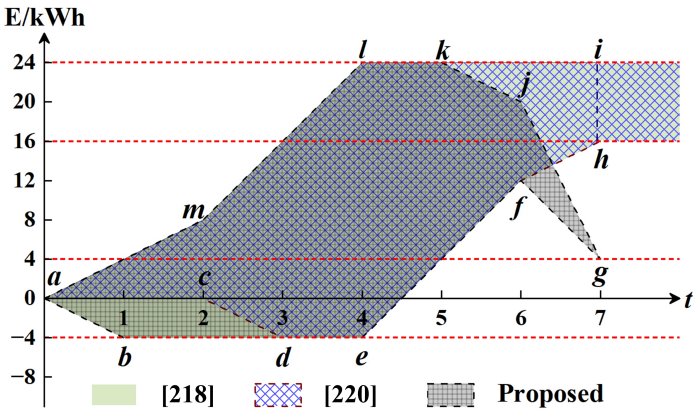

FIGURE 5.3: Operation range for EVs aggregation (EV1 and EV2) models.

shown in Figure 5.2. Furthermore, by employing equations (5.15) and (5.16) from the proposed model, we determined the operational range for the CS, which encompasses both EVs. We also provide a comparative evaluation against the models in references [218] and [220], as depicted in Figure 5.3.

In Figure 5.3, the upper cumulative energy limit of the CS begins to decline in the fifth time slot due to the operational characteristics of the proposed model. This reduction is attributed to the need to satisfy the energy requirements of EV1 before it departed from the CS. Subsequent time slots further highlight this reduction, coinciding with the departures of EV1 in the sixth slot and EV2 in the

seventh, resulting in their energy becoming unavailable for dispatch. Conversely, prior methods illustrated in references [218] and [220] demonstrate a different pattern, wherein the energy limits of EVs continue to accumulate in subsequent time slots even after they depart from the CS.

Furthermore, previous studies, such as those discussed by [218] and [220], assume that EVs may charge up to or above the desired energy specified by their owners, as depicted in Figure 5.3. In this investigation, we pose a critical question: why would an EV owner be inclined to pay for charging beyond their desired energy level? Consequently, the proposed method imposes a constraint on the upper bound to align with the desired energy level at the time of an EV's departure, as illustrated in Figure 5.2.

5.4.2 DLs Aggregation Model for Demand Response

Effectively managing various DLs is crucial for preemptively mitigating sudden surges in power demand within an LEC. To accomplish this, CAs are responsible for gathering data from consumers, which includes spatial and temporal operational characteristics, along with the energy requirements linked to specific household loads. In mathematical terms, the modeling process for aggregating DLs to offer demand response can be outlined as follows.

$$\zeta_{i,j,t}^{DL} = 0, \quad t \in T \backslash \left[\alpha_{i,j}, \beta_{i,j}\right] \tag{5.19}$$

$$\sum_{t=\alpha_{i,j}}^{t_0-1} \hat{\zeta}_{i,j,t}^{DL} + \zeta_{i,j,t_0}^{DL} + \sum_{t=t_0+1}^{\beta_{i,j}} \zeta_{i,j,t}^{DL} = \mathrm{Z}_{i,j}^{DL} \tag{5.20}$$

$$\sum_{t=\alpha_{i,j}}^{t_0-1} \hat{P}_{i,j,t}^{DL} + P_{i,j,t_0}^{DL} + \sum_{t=t_0+1}^{\beta_{i,j}} P_{i,j,t}^{DL} = E_{i,j}^{DL} \tag{5.21}$$

In equation (5.19), a DL j located at bus i must operate within the designated operational time interval $\left[\alpha_{i,j}, \beta_{i,j}\right]$, as defined by the consumer. Constraint (5.20) outlines that a DL j at bus i necessitates a total of $\mathrm{Z}_{i,j}^{DL}$ time slots to fulfill all its tasks, consequently, DL j must commence no later than $\beta_{i,j} - \mathrm{Z}_{i,j}^{DL} + 1$ and conclude no sooner than $\alpha_{i,j} + \mathrm{Z}_{i,j}^{DL}$. Furthermore, a DL j at bus i has a predefined energy demand $E_{i,j}^{DL}$ to complete all tasks, as depicted in equation (5.21).

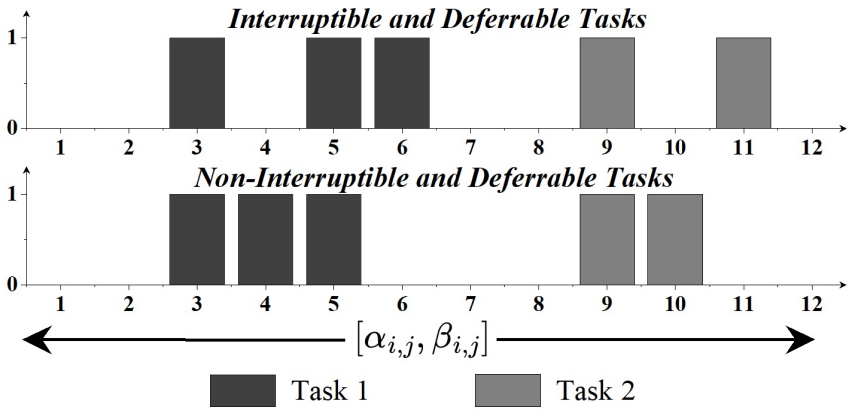

FIGURE 5.4: A graphical example of residential DL with distinct types of tasks.

In the case of a DL j situated at bus i, involving multiple operational tasks indexed as $k = 1, 2, ..., N_{j,k}$, each with different power levels and mutually exclusive, the description is provided in equations (5.22)-(5.23). However, these tasks must follow a sequential order, where the completion of the first task must precede the initiation of the second one, as guaranteed by constraint (5.24).

$$P^{DL}_{i,j,t} = \sum_{k=1}^{N_{j,k}} P^{task}_{i,j,k} \varsigma^{task}_{i,j,k,t} \tag{5.22}$$

$$\zeta^{DL}_{i,j,t} = \sum_{k=1}^{N_{j,k}} \varsigma^{task}_{i,j,k,t} \tag{5.23}$$

$$\sum_{x=1}^{k-1} \sum_{t=\alpha_{i,j,k}}^{t_0-1} \varsigma^{task}_{i,j,x,t} \geq \left(\sum_{x=1}^{k-1} Z^{task}_{i,j,k} \right) \varsigma^{task}_{,i,j,x,t_0} \tag{5.24}$$

This article classifies DL tasks according to their operational features, particularly highlighting the contrast between interruptible and deferrable tasks versus non-interruptible and deferrable tasks. Figure 5.4 provides a visual representation illustrating this differentiation in task types. In the depicted example, the complete time frame for a sequential task spans from 1 to 12; Task 1 requires three-time slots to finish, while Task 2 requires two. Additionally, it's demonstrated that Task 1 concludes before Task 2 begins.

Interruptible and Deferrable Task

For an interruptible and deferrable task, its initiation time may vary within the specified operational window, indicated by $\left[\alpha_{i,j,k}, \beta_{i,j,k}\right]$. Equation (5.25) ensures that the execution of a DL can be postponed, provided that the postponement does not exceed a predefined time limit $\left[\alpha_{i,j,k} + \varphi_{i,j,k}\right]$, where $\varphi_{i,j,k}$ signifies the acceptable delay duration from the perspective of consumers.

$$\sum_{t=\alpha_{i,j,k}}^{t_0-1} \hat{\xi}_{i,j,k,t}^{task} + \xi_{i,j,k,t_0}^{task} + \sum_{t=t_0+1}^{\alpha_{i,j,k}+\varphi_{i,j,k}} \xi_{,i,j,k,t}^{task} \geq 1 \tag{5.25}$$

Non-Interruptible and Deferrable Task

Deferrable refers to the ability to reschedule a task during the course of the day. Conversely, once initiated, finishing it without interruption is crucial to minimize potential decreases in thermal efficiency. Constraints (5.25) and (5.26) are utilized to define the characteristics of non-interruptible and deferrable properties.

$$\sum_{t=t_0+1}^{t_0+Z_{i,j,k}^{task}} \xi_{i,j,k,t}^{task} \geq Z_{i,j,k}^{task} \left(\xi_{i,j,k,t_0+1}^{task} - \xi_{i,j,k,t_0}^{task}\right) \tag{5.26}$$

5.5 Problem Formulation for Optimal Operations in SDS

This study integrates an optimal operation strategy based on a Hierarchical Control Framework to manage the control of DERs flexibility at both the LECs and EU levels. The main goal of the CA is to facilitate the activation of DERs within a LEC, guided by signals from the EU operator and grid constraint considerations, aiming for cost-effective operations. Simultaneously, the EU operator is responsible for coordinating all CAs and providing dispatch setpoints to individual DERs on the feeder while factoring in network constraints to enhance grid services.

5.5.1 Cost Optimal Dispatch Problem Formulation

CA addresses the following problem formulation to optimize its operational cost and ascertain the dispatch setpoints for the DERs available within the LEC.

$$\begin{aligned}\textbf{min} \quad & \sum_{t\in T}\sum_{i\in\mathcal{N}}\left[\lambda^{ToU}_{RL,t}\left(p^{FL}_{i,t}+\sum_{j\in\mathcal{N}^{SL}_i}P^{SL}_{i,j,t}\right)\right. \\ & \left.+\lambda_{RE,t}\left(\sum_{g\in\mathcal{G}_i}P^{RE}_{i,g,t}\right)+\lambda^{ToU}_{CS,t}\left(P^{ch,CS}_{i,t}-P^{dch,CS}_{i,t}\right)\right]\end{aligned} \tag{5.27}$$

$$\text{s.t. } (5.1)-(5.26)\,, v^{node}_i \in \{\underline{V}_i, \overline{V}_i\} \tag{5.28}$$

$$\left(P^{RE}_{i,g,t}\right)^2+\left(Q^{RE}_{i,g,t}\right)^2 \le \left(S^{RE}_{i,g,t}\right)^2 \tag{5.29}$$

$$-\phi_{i,g}P^{RE}_{i,g,t} \le Q^{RE}_{i,g,t} \le \phi_{i,g}P^{RE}_{i,g,t} \tag{5.30}$$

$$0 \le P^{RE}_{i,g,t} \le P^{RE,fore}_{i,g,t} \tag{5.31}$$

The objective (5.27) is aimed at minimizing the overall operational cost. The first term represents payments from the CA to the EU operator for supplying the power needed for fixed and deferrable load demands. Here, $\lambda^{ToU}_{RL,t}$ signifies the standard Time of Use (ToU) electricity rate applicable to power purchased from the EU. The second term in (5.27) indicates payments from the CA to RESs for procuring power at a fixed electricity rate, $\lambda_{RE,t}$. The third term in (5.27) accounts for the cost of electricity for the net power acquired for CSs. Constraints (5.28)-(5.31) ensure the feasibility of power flow in the network and adhere to DERs power bounds.

5.5.2 Problem Formulation for Improving Grid Services

In this work, the objective of the EU operator is to enhance grid services by minimizing voltage regulation and power loss in the distribution network. This is achieved by synchronizing with the specified dispatch setpoints from the CAs and optimizing the dispatch of disaggregated DERs. The mathematical

formulation for the proposed approach is presented as follows.

$$\begin{aligned}\textbf{min} \quad & \sum_{t\in T}\left[\sum_{i\in\mathcal{N}}\left[\gamma_{vd}\left(V_{i,t}^{node}-V_{nom}\right)^2\right]\right. \\ & \left.+\sum_{(i,j)\in\mathcal{E}}\left[\gamma_{loss}\left(r_{ij}l_{ij,t}^{flow}\right)\right]\right]\end{aligned} \tag{5.32}$$

$$\text{s.t. } (5.1)-(5.4) \quad for \quad v_{i,t}^{node}\in\left\{\underline{V}_i,\overline{V}_i\right\}, p_{i,t}^{agg} \tag{5.33}$$

$$p_{i,t}^{agg}=-\sum_{g\in\mathcal{G}_i}P_{i,g,t}^{RE}+P_{i,t}^{ch,CS}+\sum_{j\in\mathcal{N}_i^{SL}}P_{i,j,t}^{SL} \tag{5.34}$$

$$\left(P_{i,g,t}^{RE,DA}\right)^2+\left(Q_{i,g,t}^{RE,DA}\right)^2\leq\left(S_{i,g,t}^{RE,DA}\right)^2 \tag{5.35}$$

$$-\phi_{i,g}P_{i,g,t}^{RE,DA}\leq Q_{i,g,t}^{RE,DA}\leq\phi_{i,g}P_{i,g,t}^{RE,DA} \tag{5.36}$$

$$0\leq P_{i,g,t}^{RE,DA}\leq P_{i,g,t}^{RE,fore} \tag{5.37}$$

$$E_{i,t}^{ES}=E_{i,t-1}^{ES}+\left[\eta_{ch,i}^{ES}P_{i,t}^{ch,ES}-\frac{P_{i,t}^{dch,ES}}{\eta_{dch,i}^{ES}}\right]\Delta t \tag{5.38}$$

$$(5.5)-(5.7),(5.12)-(5.14)\ for\ E_{i,t}^{ES},P_{i,t}^{ch,ES},P_{i,t}^{dch,ES} \tag{5.39}$$

Equation (5.32) comprises two terms: the first term focuses on improving node voltages, while the second term aims to reduce network power losses. The symbol γ in (5.32) denotes the weighting assigned to the indices within the objective function. Constraints described in (5.33)-(5.39) define the permissible operating ranges for DERs and ensure viable network power flow.

5.6 Results and Discussion

The proposed problem is evaluated using a modified IEEE-123 bus radial distribution network (RDN), depicted in Figure 5.5. All simulations are conducted within the A Mathematical Programming Language (AMPL) environment, employing a KNITRO solver [215]. The simulations are executed featuring an 11th Gen Intel(R) Core(TM) i5-1135G7 @ 2.40 GHz CPU processor with 8 GB RAM.

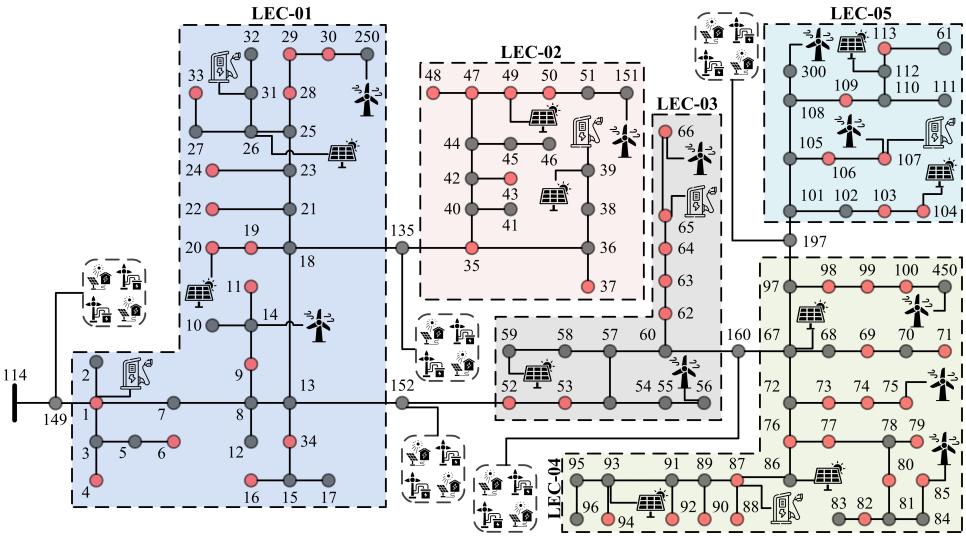

FIGURE 5.5: Modified IEEE 123 bus radial distribution network.

5.6.1 Description of Test System

The modified IEEE-123 bus RDN has been partitioned into five distinct LECs, as depicted in Figure 5.5. Each LEC is furnished with CSs, RESs in the form of PV plants and WT farms, and residential DLs denoted by nodes in red, alongside fixed load demand represented by nodes in black. Configuration details of the CSs and simulation parameters, including EV types and EV charging infrastructure, are obtained from [221]. The power generation profiles of the PV plants and WT farms are derived from historical supply patterns observed during peak summer seasons [222]. Operational data, encompassing energy consumption patterns and scheduling time slots for DLs with multiple tasks, are adapted from [223]. For simplicity, the operational status is presented at hourly intervals. Furthermore, several DERs, including RESs with integrated ESs, have been strategically positioned at bus locations 135, 149, 152, 160, and 197, under the control of the EU operator to enhance grid services.

5.6.2 Community Power Dispatch

To illustrate the power dispatch within LECs managed by CAs, numerical results for LEC-1 are provided. LEC-1 configuration includes PV plant installations at buses 20 and 26, each with an 80 kW capacity, and WT farms at bus 14 (80 kW)

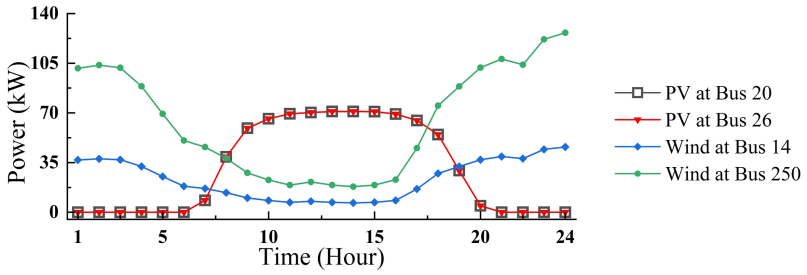

FIGURE 5.6: Hourly power supplied by RESs in LEC-1.

and bus 250 (220 kW). Additionally, CSs are positioned at buses 1 and 31, accommodating 140 and 40 EVs with heterogeneous parameters, respectively, as referred from [221]. Furthermore, there are a total of 252 DLs with a combined power demand of 1918.15 kW distributed across fifteen buses, capable of adjusting their power demands for demand response. The total fixed load demand for LEC-1 is 9435.85 kW, with a consistent hourly demand pattern across all nodes.

Figure 5.6 depicts the hourly power generation from RESs, showcasing a peak power output of 212.03 kW during the 18^{th} hour period. The cumulative power supplied by the RESs over 24 hours amounts to 3596.28 kW. Operational regions and aggregated energy states for the CSs at buses 1 and 31 are displayed in Figure 5.7. The shaded area between the upper and lower power trajectories represents the available aggregate power flexibility for the CSs that effectively meet the charging requirements for EVs. Furthermore, Figure 5.8 presents the hourly maximum charging power, aggregated charging power dispatch for the CSs at buses 1 and 31, and the ToU electricity price derived from [224]. Notably, an observation is made regarding the reduced charging demand of the CSs during the 17^{th} to 22^{nd} time intervals, coinciding with elevated ToU prices, resulting in a significant reduction in operational costs.

In this study, we examine six distinct categories of DLs, with three exhibiting interruptible task characteristics and the remaining three having non-interruptible characteristics. The specific parametric data for each DL can be found in Table 5.2. The net hourly demand of DLs integrated at bus 28 is illustrated in Figure 5.9. Notably, there are a total of 90 DLs located on bus 28, evenly distributed among the six categories detailed in Table 5.2. It is noteworthy that during the 17^{th} to 22^{nd} time intervals, the demand from DLs is

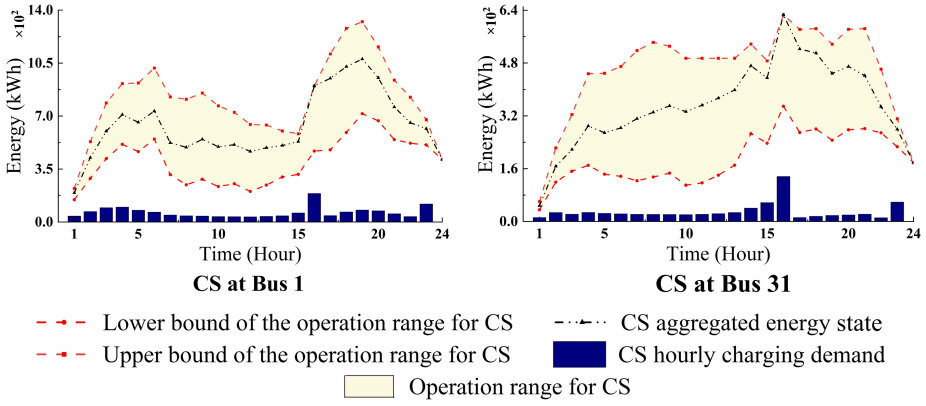

FIGURE 5.7: The operation ranges and the aggregated energy states for CSs at Bus 1 and Bus 31 in LEC-1.

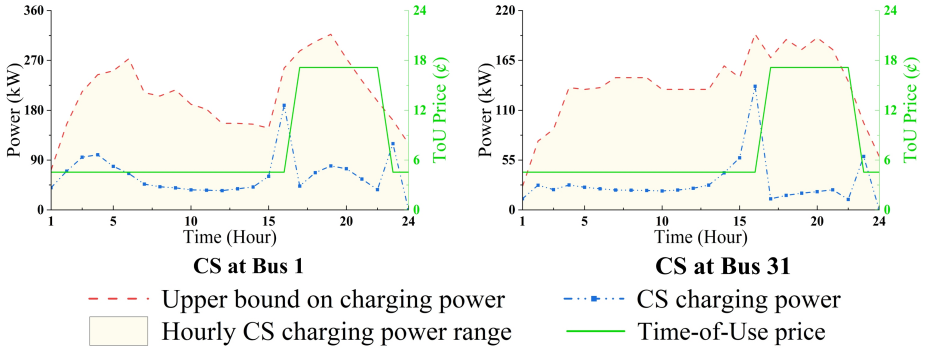

FIGURE 5.8: The aggregated charging power of CSs at Bus 1 and Bus 31 in LEC-1.

observed to be zero, coinciding with high ToU electricity prices. Additionally, Table 5.2 summarizes the total operational costs derived from solving the optimal power dispatch in LECs by all five CAs, along with other significant outcomes like power supplied by the EU operator, RESs generation, and power demanded from CS in an LEC over the 24-hour time horizon.

5.6.3 Dispatch Set-points from EU Operator

This section presents the numerical outcomes related to the dispatch set-points assessed for the disaggregated DERs within the network, with the aim of enhancing grid services. Figure 5.10 illustrates the discharge power and energy state patterns over 24 hours for disaggregated ESs located at buses 149, 135, 152, 160, and 197. Notably, the results indicate that during periods of elevated power

TABLE 5.2: Daily operation data for considered deferrable loads

Term	Interruptible DL			Non-Inturruptible DL		
DL Type	I	II	III	IV	V	VI
Power Level (kW)	5.475	4.875	3.5	0.65/1.26	1.875	2
Required Time	2	2	4	1/2	2	2
Starting Time	8	1	1	4	8	1
Ending Time	20	24	24	16	20	12
Total Energy Usage	10.95	9.75	14	0.65/2.52	3.75	4

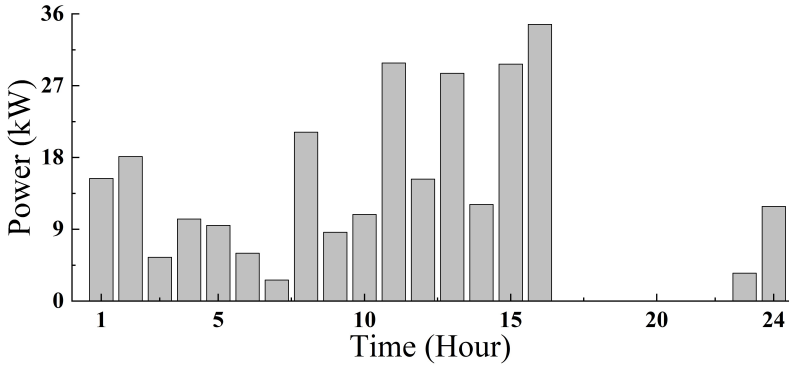

FIGURE 5.9: Net hourly power demand by DL at Bus 28 in LEC-1.

TABLE 5.3: Total Cost of Operation and Power Dispatch in LECs

Term	LEC-01	LEC-02	LEC-03	LEC-04	LEC-05
Operation Cost ($)	1323.16	1105.30	743.29	1397.43	60.82
Power Supplied by EU (kW)	10240.29	8390.97	5436.16	11251.65	-171.65
RES Generation (kW)	3596.28	3924.36	3876.75	6912.71	5885.36
Power Demand from CSs (kW)	2181.05	830.75	857.47	1216.80	811.04

demand from LECs, the ESs discharge, whereas during low-demand intervals, the ESs charge to ensure demand fulfillment locally. For instance, during the 15^{th} hour, when demand is low, all ES units engage in charging, while in the 16^{th}

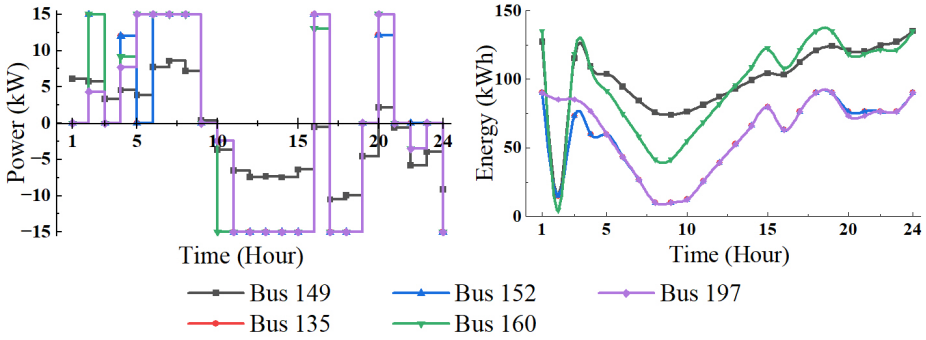

FIGURE 5.10: Discharging power and energy states of disaggregated ESs.

TABLE 5.4: Comparison of Power Losses (kW) and Voltage Deviation (V^2) Under Various Scenarios

	$\gamma_{loss}\times$ power loss (kW)	$\gamma_{vd}\times$ voltage deviation (V^2)
Without DERs (No RESs & ESs)	1003.15	552.10
With RESs (No ESs)	855.49	485.46
With DERs (RESs+ESs)	846.68	483.87

hour, when LECs experience high demand, all ES units except the one at bus 149 switch to maximum discharging mode.

Furthermore, a comparative analysis of power losses and voltage deviations in various scenarios is detailed in Table 5.4. It is worth mentioning that when the EU operator does not dispatch the disaggregated DERs to fulfill LECs' energy demand and when the EU operator utilizes the full potential of DERs, the net power losses are notably improved by 15.60 %. The findings reveal that effective management of disaggregated DERs in coordination with the dispatch set-points received from LECs can significantly enhance grid services, benefitting EU operator.

5.7 Summary

The chapter presents a comprehensive framework designed for the effective management of a substantial fleet of DERs within the smart distribution system, with a specific emphasis on optimizing operations within LECs and enhancing grid services at the EU level. Through rigorous numerical simulations conducted on a modified IEEE-123 bus RDN, the chapter demonstrates the robustness and effectiveness of the proposed methodology. The results highlight the framework's capability to efficiently manage a sizable fleet of DERs within the distribution system, achieving favorable outcomes in terms of economic cost, system security, and computational efficiency. The significant contributions of the work are summarized below.

1. An aggregation model targeted at assessing the combined feasible operational range for a significant EV fleet stationed at a CS. The approach notably improves accuracy and computational efficiency, thereby enhancing the effective management of large-scale EV deployments.

2. Aggregation modelling of DLs characterized by distinct operational tasks, aimed at streamlining demand response initiatives. The proposed approach evaluates the impact of a substantial number of DLs on the distribution system, taking into account their integration within the network.

3. A HCF designed to streamline the collaboration among the EU operator, CAs, and individual DERs, thereby optimizing DER deployment for cost-effective operations within LECs and enhancing grid services. This approach meticulously considers network constraints to ensure effective management.

Chapter 6

Conclusions and Future Scopes

This chapter encapsulates the notable outcomes derived from the research, offering overarching conclusions and discussions on the main findings, alongside recommendations for potential future research extensions.

6.1 Conclusions

In the foreseeable future, utilities are expected to embrace a greater array of smart grid technologies, facilitating the development of a distribution system that is efficient, cost-effective, dependable, and robust. With the growing adoption of renewable energy sources (RESs) like photovoltaic (PV) modules, the need for innovative technologies to manage the uncertainties they introduce will become imperative. Battery energy storage systems (ESs) and electric vehicles (EVs) are poised to become pivotal in the energy management of future distribution systems. Additionally, integrating smart buildings and homes will empower flexible loads to actively engage in demand response initiatives. The primary goal of this thesis was to delve into optimizing the planning and functioning of distributed energy resources (DERs) within smart distribution systems, considering both technical and economic improvements. A summary of the primary content and conclusions derived from the thesis are as follows.

The second chapter was devoted to introducing an approach that empowers network operators to concurrently consider multiple criteria for optimal capacitor siting in the smart distribution system, which was absent in prevailing optimal capacitor placement techniques. The proposed SE-IM approach offers flexibility in selecting multiple criteria and allows for combining index scores

from various methods based on their importance to determine the optimal node for capacitor bank placement. Later, the particle swarm optimization method was utilized to evaluate the optimal size of the capacitor bank, considering whether it is switched or fixed type. The aim of comprehensive techno-economic improvement was achieved by considering problem formulation that minimizes the annual energy loss cost while subjected to various operational constraints. The efficacy of this approach was assessed through implementation on various radial distribution networks (RDN), including an IEEE-12 bus, 34 standard bus, and a 108-bus practical RDN of an Indian utility, demonstrating its superiority over prevailing methods. Furthermore, the analysis of optimal capacitor bank placement in the presence of distributed generation (DG) and load uncertainty underscored the approach's ability to enhance network quantities while adhering to security and reliability constraints.

Chapter three enfolds a novel method for evaluating weights assigned to objectives based on the relative importance in a weighted multi-objective problem concerning optimal DG placement in the smart distribution system. For this, the proposed approach utilizes the formula of Shannon's Entropy to determine the degree of importance of an objective, while considering a range of technical and economic impact objective functions to formulate the weighted multi-objective problem to achieve a practical and economically viable solution. This work further extends the methodology where incorporating the priority information given by the distribution network planner in an inevitable situation. The proposed approach's effectiveness was assessed through its application to a 38-node test system, analyzing various scenarios based on alterations in network physical properties. A comparative analysis demonstrates that the proposed method outperforms existing approaches. Additionally, distribution network buses are classified as voltage-dependent loads to assess the impact of different load models on DG placement problems. Noteworthy benefits of the method include its straightforward execution and its compatibility with similar multi-objective optimization problems.

In Chapter four, a novel approach was presented, focusing on the optimization of day-ahead schedules for Electric Vehicle Charging Stations (EVCSs) within a smart distribution system. The primary goal was to minimize real power loss payments from the perspective of the distribution network

operator (DNO), ensuring system operational security amid the integration of RESs and EVs. Additionally, a demand response mechanism was employed to reduce operational costs by shifting controllable load demands from high-price to low-price periods without curtailing the overall daily load demand. The chapter explored a robust optimization technique to address worst-case scenarios arising from price and load uncertainty, incorporating a predefined level of conservativeness. Furthermore, a cost-effective analysis was conducted, comparing the single-agent and multi-agent frameworks based on consensus between EVCS and DNO for the execution of the proposed problem formulation. The efficiency of the presented method was demonstrated through numerical simulations conducted on a modified IEEE-12 bus RDN. Extensive case studies validate that the proposed approach surpasses the active loss minimization strategy, significantly diminishing operational losses within the network and alleviating the financial burden on the DNO during daily operations in a competitive environment.

In Chapter five, a comprehensive framework was introduced, specifically designed for the effective management of a significant fleet of DERs within the smart distribution system. The focus of this framework is on optimizing operations within Local Energy Communities and enhancing grid services at the electric utility (EU) level. This involved the development of an innovative aggregation model for evaluating the operational range of EV fleets and an approach for demand response initiatives with diverse deferrable loads, taking into consideration factors like preferences, spatial distribution, and temporal dynamics. Subsequently, a hierarchical control framework was implemented to optimize DER deployment, accounting for network constraints and facilitating coordination among EU operators, community aggregators, and individual DERs for techno-economic benefits. The robustness and effectiveness of the proposed methodology were demonstrated through rigorous numerical simulations on a modified IEEE-123 bus RDN, showcasing the framework's proficiency in managing DERs efficiently and achieving favorable outcomes in economic cost, system security, and computational efficiency.

6.2 Contributions

The key contributions arising from the research outlined in this thesis include:

1. A new approach for optimal capacitor placement in smart distribution systems was introduced to achieve comprehensive techno-economic enhancements. The SE-IM method, the novel model proposed for this purpose, enables the consideration of numerous indices in the selection of the optimal node within the distribution network. Subsequently, the model utilizes particle swarm optimization techniques for the optimal sizing of capacitors.

2. An innovative method is suggested to remove subjectivity from the selection of weights associated with objectives in the weighted multi-objective optimal DG placement problem. The proposed approach employs Shannon's Entropy formula to ascertain the relative importance of an objective function within a given multi-objective problem formulation, allowing for the impartial evaluation of weights.

3. A thorough and cost-effective analysis has been conducted for EVs within the smart distribution system. To achieve this, a proposed method optimizes day-ahead schedules for EVCS within the smart distribution system, aiming to minimize payments related to active power loss. The problem formulation integrates demand response modeling to mitigate the intermittency of RESs and employs robust optimization techniques to address worst-case scenarios resulting from uncertainties in load demand and electricity prices.

4. A proposed framework focuses on the aggregation and scheduling of a significant fleet of Distributed Energy Resources (DERs) within a smart distribution system, aiming to optimize operations within Local Energy Communities and enhance grid services at the utility level. An innovative approach is suggested for aggregating EV fleets and deferrable loads available in the smart distribution system.

6.3 Future Scopes

Based on the research conducted in this thesis, outlined below are key considerations and prospective areas for future exploration and development.

1. There is an opportunity to delve into the application of machine learning algorithms. By incorporating these algorithms, the objective is to bolster decision-support capabilities within the proposed approaches, with a focus on predicting and adapting to dynamic changes. Machine learning algorithms can be harnessed to analyze historical data, recognize patterns, and anticipate variations in factors such as energy demand, market prices, and system behavior. This predictive capability can significantly contribute to optimizing decision-making processes, enabling more proactive and adaptive strategies for the management and operation of the smart distribution system.

2. It is crucial to delve into methods that augment the resilience and cybersecurity of the proposed framework, particularly in light of the escalating digitalization of distribution networks. As smart distribution systems heavily rely on interconnected digital technologies and communication infrastructure, there is an inherent need to address potential vulnerabilities and safeguard against cybersecurity threats. By fortifying the resilience and cybersecurity aspects, the proposed techno-economic analysis framework can better adapt to evolving challenges and contribute to the establishment of trustworthy and secure smart distribution networks in the face of increasing digital complexities.

3. It is essential to investigate the feasibility of real-time implementation of the proposed methods within operational distribution networks. Transitioning from theoretical models to practical applications involves addressing challenges related to data integration, communication protocols, and the scalability of the proposed approaches.

4. The techno-economic analysis can evolve into a more holistic evaluation framework, providing insights not only into economic feasibility but also into the broader societal and environmental implications of implementing

smart distribution systems. This multi-faceted approach contributes to a more comprehensive understanding of the overall impact and viability of the proposed methods in real-world scenarios.

5. A promising avenue for exploration involves the integration of peer-to-peer (P2P) energy trading platforms and blockchain technology. This approach aims to foster a more resilient and transparent energy ecosystem by leveraging decentralized and secure mechanisms.

Bibliography

[1] P. Goncalves Da Silva, D. Ilić, and S. Karnouskos, "The impact of smart grid prosumer grouping on forecasting accuracy and its benefits for local electricity market trading," *IEEE Transactions on Smart Grid*, vol. 5, no. 1, pp. 402–410, 2014.

[2] F. Capitanescu, L. F. Ochoa, H. Margossian, and N. D. Hatziargyriou, "Assessing the potential of network reconfiguration to improve distributed generation hosting capacity in active distribution systems," *IEEE Transactions on Power Systems*, vol. 30, no. 1, pp. 346–356, 2015.

[3] E. F. Bompard and B. Han, "Market-based control in emerging distribution system operation," *IEEE Transactions on Power Delivery*, vol. 28, no. 4, pp. 2373–2382, 2013.

[4] M. Khorasany, Y. Mishra, and G. Ledwich, "Design of auction-based approach for market clearing in peer-to-peer market platform," *The Journal of Engineering*, vol. 2019, no. 18, pp. 4813–4818, 2019.

[5] S. Khator and L. Leung, "Power distribution planning: a review of models and issues," *IEEE Transactions on Power Systems*, vol. 12, no. 3, pp. 1151–1159, 1997.

[6] R. Hidalgo, C. Abbey, and G. Joós, "A review of active distribution networks enabling technologies," in *IEEE PES General Meeting*, 2010, pp. 1–9.

[7] R. Li, W. Wang, Z. Chen, J. Jiang, and W. Zhang, "A review of optimal planning active distribution system: Models, methods, and future researches," *Energies*, vol. 10, no. 11, 2017.

[8] Y. Xu, C. Yan, H. Liu, J. Wang, Z. Yang, and Y. Jiang, "Smart energy systems: A critical review on design and operation optimization," *Sustainable Cities and Society*, vol. 62, p. 102369, 2020.

[9] R. Dashti and M. Rouhandeh, "Power distribution system planning framework (a comprehensive review)," *Energy Strategy Reviews*, vol. 50, p. 101256, 2023.

[10] P. S. Georgilakis and N. D. Hatziargyriou, "A review of power distribution planning in the modern power systems era: Models, methods and future research," *Electric Power Systems Research*, vol. 121, pp. 89–100, 2015.

[11] S. A. A. Kazmi, M. K. Shahzad, A. Z. Khan, and D. R. Shin, "Smart distribution networks: A review of modern distribution concepts from a planning perspective," *Energies*, vol. 10, no. 4, 2017.

[12] A. Huda and R. Živanović, "Large-scale integration of distributed generation into distribution networks: Study objectives, review of models and computational tools," *Renewable and Sustainable Energy Reviews*, vol. 76, pp. 974–988, 2017.

[13] S. Jain, S. Kalambe, G. Agnihotri, and A. Mishra, "Distributed generation deployment: State-of-the-art of distribution system planning in sustainable era," *Renewable and Sustainable Energy Reviews*, vol. 77, pp. 363–385, 2017.

[14] G. L. Aschidamini, G. A. da Cruz, M. Resener, M. J. S. Ramos, L. A. Pereira, B. P. Ferraz, S. Haffner, and P. M. Pardalos, "Expansion planning of power distribution systems considering reliability: A comprehensive review," *Energies*, vol. 15, no. 6, 2022.

[15] H. A. Muqeet, R. Liaqat, M. Jamil, and A. A. Khan, "A state-of-the-art review of smart energy systems and their management in a smart grid environment," *Energies*, vol. 16, no. 1, 2023.

[16] N. K. Meena, A. Swarnkar, N. Gupta, and K. R. Niazi, "Optimal integration of ders in coordination with existing vrs in distribution networks," *IET Generation, Transmission & Distribution*, vol. 12, no. 11, pp. 2520–2529, 2018.

[17] A. Noori, Y. Zhang, N. Nouri, and M. Hajivand, "Multi-objective optimal placement and sizing of distribution static compensator in radial distribution networks with variable residential, commercial and industrial demands considering reliability," *IEEE Access*, vol. 9, pp. 46 911–46 926, 2021.

[18] R. Yan, N.-A. Masood, T. Kumar Saha, F. Bai, and H. Gu, "The anatomy of the 2016 south australia blackout: A catastrophic event in a high renewable network," *IEEE Transactions on Power Systems*, vol. 33, no. 5, pp. 5374–5388, 2018.

[19] O. P. Veloza and F. Santamaria, "Analysis of major blackouts from 2003 to 2015: Classification of incidents and review of main causes," *The Electricity Journal*, vol. 29, no. 7, pp. 42–49, 2016.

[20] B. Kasztenny, J. Schaefer, and E. Clark, "Fundamentals of adaptive protection of large capacitor banks - accurate methods for canceling inherent bank unbalances," in *2007 60th Annual Conference for Protective Relay Engineers*, 2007, pp. 126–157.

[21] D. Bruns, G. Newcomb, S. Miske, C. Taylor, G. Lee, and A. Edris, "Shunt capacitor bank series group shorting (caps) design and application," *IEEE Transactions on Power Delivery*, vol. 16, no. 1, pp. 24–32, 2001.

[22] H. Dura, "Optimum number, location, and size of shunt capacitors in radial distribution feeders a dynamic programming approach," *IEEE Transactions on Power Apparatus and Systems*, vol. PAS-87, no. 9, pp. 1769–1774, 1968.

[23] M. Baran and F. Wu, "Optimal capacitor placement on radial distribution systems," *IEEE Transactions on Power Delivery*, vol. 4, no. 1, pp. 725–734, 1989.

[24] S. Mekhamer, S. Soliman, M. Moustafa, and M. El-Hawary, "Load flow solution of radial distribution feeders: a new contribution," *International Journal of Electrical Power & Energy Systems*, vol. 24, no. 9, pp. 701–707, 2002.

[25] R. S. Rao, S. Narasimham, and M. Ramalingaraju, "Optimal capacitor placement in a radial distribution system using plant growth simulation algorithm," *International Journal of Electrical Power & Energy Systems*, vol. 33, no. 5, pp. 1133–1139, 2011.

[26] N. M. Neagle and D. R. Samson, "Loss reduction from capacitors installed on primary feeders [includes discussion]," *Transactions of the American Institute of Electrical Engineers. Part III: Power Apparatus and Systems*, vol. 75, no. 3, pp. 950–959, 1956.

[27] R. F. Cook, "Analysis of capacitor application as affected by load cycle," *Transactions of the American Institute of Electrical Engineers. Part III: Power Apparatus and Systems*, vol. 78, no. 3, pp. 950–956, 1959.

[28] J. V. Schmill, "Optimum size and location of shunt capacitors on distribution feeders," *IEEE Transactions on Power Apparatus and Systems*, vol. 84, no. 9, pp. 825–832, 1965.

[29] M. Aman, G. Jasmon, A. Bakar, H. Mokhlis, and M. Karimi, "Optimum shunt capacitor placement in distribution system—a review and comparative study," *Renewable and Sustainable Energy Reviews*, vol. 30, pp. 429–439, 2014.

[30] A. Arief, Antamil, and M. B. Nappu, "An analytical method for optimal capacitors placement from the inversed reduced jacobian matrix," *Energy Procedia*, vol. 100, pp. 307–310, 2016.

[31] K. Mahmoud and M. Lehtonen, "Direct approach for optimal allocation of multiple capacitors in distribution systems using novel analytical closed-form expressions," *Electrical Engineering*, vol. 103, p. 245–256, 2021.

[32] A. Abdelaziz, E. Ali, and S. Abd Elazim, "Flower pollination algorithm and loss sensitivity factors for optimal sizing and placement of capacitors in radial distribution systems," *International Journal of Electrical Power & Energy Systems*, vol. 78, pp. 207–214, 2016.

[33] A. Bayat and A. Bagheri, "Optimal active and reactive power allocation in distribution networks using a novel heuristic approach," *Applied Energy*, vol. 233-234, pp. 71–85, 2019.

[34] K. Muthukumar and S. Jayalalitha, "Optimal placement and sizing of distributed generators and shunt capacitors for power loss minimization in radial distribution networks using hybrid heuristic search optimization

technique," *International Journal of Electrical Power & Energy Systems*, vol. 78, pp. 299–319, 2016.

[35] S. Segura, R. Romero, and M. J. Rider, "Efficient heuristic algorithm used for optimal capacitor placement in distribution systems," *International Journal of Electrical Power & Energy Systems*, vol. 32, no. 1, pp. 71–78, 2010.

[36] E. A. Almabsout, R. A. El-Sehiemy, O. N. U. An, and O. Bayat, "A hybrid local search-genetic algorithm for simultaneous placement of dg units and shunt capacitors in radial distribution systems," *IEEE Access*, vol. 8, pp. 54 465–54 481, 2020.

[37] H. Ramadan, A. Bendary, and S. Nagy, "Particle swarm optimization algorithm for capacitor allocation problem in distribution systems with wind turbine generators," *International Journal of Electrical Power & Energy Systems*, vol. 84, pp. 143–152, 2017.

[38] S. R. Gampa and D. Das, "Optimum placement of shunt capacitors in a radial distribution system for substation power factor improvement using fuzzy ga method," *International Journal of Electrical Power & Energy Systems*, vol. 77, pp. 314–326, 2016.

[39] A. A. Abou El-Ela, R. A. El-Sehiemy, A.-M. Kinawy, and M. T. Mouwafi, "Optimal capacitor placement in distribution systems for power loss reduction and voltage profile improvement," *IET Generation, Transmission & Distribution*, vol. 10, no. 5, pp. 1209–1221, 2016.

[40] M. Aryanezhad, "Management and coordination of ltc, svr, shunt capacitor and energy storage with high pv penetration in power distribution system for voltage regulation and power loss minimization," *International Journal of Electrical Power & Energy Systems*, vol. 100, pp. 178–192, 2018.

[41] M. Resener, S. Haffner, L. A. Pereira, P. M. Pardalos, and M. J. Ramos, "A comprehensive milp model for the expansion planning of power distribution systems – part i: Problem formulation," *Electric Power Systems Research*, vol. 170, pp. 378–384, 2019.

[42] S. Paul and W. Jewell, "Optimal capacitor placement and sizes for power loss reduction using combined power loss index-loss sensitivity factor and genetic algorithm," in *2012 IEEE Power and Energy Society General Meeting*, 2012, pp. 1–8.

[43] M. Chakravorty and D. Das, "Voltage stability analysis of radial distribution networks," *International Journal of Electrical Power & Energy Systems*, vol. 23, no. 2, pp. 129–135, 2001.

[44] S. Das, D. Das, and A. Patra, "Operation of distribution network with optimal placement and sizing of dispatchable dgs and shunt capacitors," *Renewable and Sustainable Energy Reviews*, vol. 113, p. 109219, 2019.

[45] R. O. Bawazir and N. S. Cetin, "Comprehensive overview of optimizing pv-dg allocation in power system and solar energy resource potential assessments," *Energy Reports*, vol. 6, pp. 173–208, 2020.

[46] S. Civanlar and J. Grainger, "Volt/var control on distribution systems with lateral branches using shunt capacitors and voltage regulators part iii: The numerical results," *IEEE Transactions on Power Apparatus and Systems*, vol. PAS-104, no. 11, pp. 3291–3297, 1985.

[47] N. M. Duong Quoc Hung and R. Bansal, "A combined practical approach for distribution system loss reduction," *International Journal of Ambient Energy*, vol. 36, no. 3, pp. 123–131, 2015.

[48] P. Chiradeja and R. Ramakumar, "An approach to quantify the technical benefits of distributed generation," *IEEE Transactions on Energy Conversion*, vol. 19, no. 4, pp. 764–773, 2004.

[49] W. El-Khattam and M. Salama, "Distributed generation technologies, definitions and benefits," *Electric Power Systems Research*, vol. 71, no. 2, pp. 119–128, 2004.

[50] G. Pepermans, J. Driesen, D. Haeseldonckx, R. Belmans, and W. D'haeseleer, "Distributed generation: definition, benefits and issues," *Energy Policy*, vol. 33, no. 6, pp. 787–798, 2005.

[51] V. Quezada, J. Abbad, and T. Roman, "Assessment of energy distribution losses for increasing penetration of distributed generation," *IEEE Transactions on Power Systems*, vol. 21, no. 2, pp. 533–540, 2006.

[52] M. Ettehadi, H. Ghasemi, and S. Vaez-Zadeh, "Voltage stability-based dg placement in distribution networks," *IEEE Transactions on Power Delivery*, vol. 28, no. 1, pp. 171–178, 2013.

[53] M. Alonso and H. Amaris, "Voltage stability in distribution networks with dg," in *2009 IEEE Bucharest PowerTech*, 2009, pp. 1–6.

[54] G. Celli, E. Ghiani, S. Mocci, and F. Pilo, "A multiobjective evolutionary algorithm for the sizing and siting of distributed generation," *IEEE Transactions on Power Systems*, vol. 20, no. 2, pp. 750–757, 2005.

[55] M. V. M. Gandomkar and M. Ehsan, "A genetic–based tabu search algorithm for optimal dg allocation in distribution networks," *Electric Power Components and Systems*, vol. 33, no. 12, pp. 1351–1362, 2005.

[56] O. I. Elgerd and H. H. Happ, "Electric energy systems theory: An introduction," *IEEE Transactions on Systems, Man, and Cybernetics*, vol. SMC-2, no. 2, pp. 296–297, 1972.

[57] D. Q. Hung, N. Mithulananthan, and R. Bansal, "Analytical strategies for renewable distributed generation integration considering energy loss minimization," *Applied Energy*, vol. 105, pp. 75–85, 2013.

[58] D. Q. Hung, N. Mithulananthan, and K. Y. Lee, "Optimal placement of dispatchable and nondispatchable renewable dg units in distribution networks for minimizing energy loss," *International Journal of Electrical Power & Energy Systems*, vol. 55, pp. 179–186, 2014.

[59] D. Q. Hung, N. Mithulananthan, and R. C. Bansal, "Analytical expressions for dg allocation in primary distribution networks," *IEEE Transactions on Energy Conversion*, vol. 25, no. 3, pp. 814–820, 2010.

[60] A. Nasri, M. E. Hamedani Golshan, and S. Mortaza Saghaian Nejad, "Optimal planning of dispatchable and non-dispatchable distributed

generation units for minimizing distribution system's energy loss using particle swarm optimization," *International Transactions on Electrical Energy Systems*, vol. 24, no. 4, pp. 504–519, 2014.

[61] S. Sultana and P. K. Roy, "Oppositional krill herd algorithm for optimal location of distributed generator in radial distribution system," *International Journal of Electrical Power & Energy Systems*, vol. 73, pp. 182–191, 2015.

[62] N. K. Roy, H. R. Pota, and A. Anwar, "A new approach for wind and solar type dg placement in power distribution networks to enhance systems stability," in *2012 IEEE International Power Engineering and Optimization Conference Melaka, Malaysia*, 2012, pp. 296–301.

[63] C. Canizares, A. De Souza, and V. Quintana, "Comparison of performance indices for detection of proximity to voltage collapse," *IEEE Transactions on Power Systems*, vol. 11, no. 3, pp. 1441–1450, 1996.

[64] G. Jasmon, L. Callistus, and C. Lee, "Prediction of voltage collapse in power systems using a reduced system model," in *International Conference on Control 1991. Control '91*, 1991, pp. 32–36 vol.1.

[65] M. Moghavvemi and M. Faruque, "Power system security and voltage collapse: a line outage based indicator for prediction," *International Journal of Electrical Power & Energy Systems*, vol. 21, no. 6, pp. 455–461, 1999.

[66] I. Musirin and T. Abdul Rahman, "Novel fast voltage stability index (fvsi) for voltage stability analysis in power transmission system," in *Student Conference on Research and Development*, 2002, pp. 265–268.

[67] N. G. Hemdan and M. Kurrat, "Distributed generation location and capacity effect on voltage stability of distribution networks," in *2008 Annual IEEE Student Paper Conference*, 2008, pp. 1–5.

[68] H. Hizarci and B. E. Turkay, "Impact of distributed generation on radial distribution network with various load models," in *2017 52nd International Universities Power Engineering Conference (UPEC)*, 2017, pp. 1–5.

[69] S. A. Chithra Devi, K. Yamuna, and M. Sornalatha, "Multi-objective optimization of optimal placement and sizing of multiple dg placements in radial distribution system using stud krill herd algorithm," *Neural Computing and Applications*, vol. 33, no. 20, pp. 13 619–13 634, 2021.

[70] K. B. B. and S. Maheswarapu, "A solution to multi-objective optimal accommodation of distributed generation problem of power distribution networks: An analytical approach," *International Transactions on Electrical Energy Systems*, vol. 29, no. 10, p. e12093, 2019.

[71] P. Gangwar, S. N. Singh, and S. Chakrabarti, "Multi-objective planning model for multi-phase distribution system under uncertainty considering reconfiguration," *IET Renewable Power Generation*, vol. 13, no. 12, pp. 2070–2083, 2019.

[72] S. S. Tanwar and D. Khatod, "Techno-economic and environmental approach for optimal placement and sizing of renewable dgs in distribution system," *Energy*, vol. 127, pp. 52–67, 2017.

[73] C. Venkaiah and R. V. Jain, "Multi-objective jaya algorithm based optimal location and sizing of distributed generation in a radial distribution system," in *2017 IEEE PES Asia-Pacific Power and Energy Engineering Conference (APPEEC)*, 2017, pp. 1–6.

[74] M. R. Varsha Suresh Galgali and G. A. Vaidya, "Multi-objective optimal placement and sizing of dgs by hybrid fuzzy topsis and taguchi desirability function analysis approach," *Electric Power Components and Systems*, vol. 48, no. 19-20, pp. 2144–2155, 2020.

[75] A. Selim, S. Kamel, A. S. Alghamdi, and F. Jurado, "Optimal placement of dgs in distribution system using an improved harris hawks optimizer based on single- and multi-objective approaches," *IEEE Access*, vol. 8, pp. 52 815–52 829, 2020.

[76] W. Sheng, K.-Y. Liu, Y. Liu, X. Meng, and Y. Li, "Optimal placement and sizing of distributed generation via an improved nondominated sorting genetic algorithm ii," *IEEE Transactions on Power Delivery*, vol. 30, no. 2, pp. 569–578, 2015.

[77] S. R. Behera and B. K. Panigrahi, "A multi objective approach for placement of multiple dgs in the radial distribution system," *International Journal of Machine Learning and Cybernetics*, vol. 10, no. 8, pp. 2027–2041, 2019.

[78] M. Mosbah, S. Arif, and R. D. Mohammedi, "Multi-objective optimization for optimal multi dg placement and sizes in distribution network based on nsga-ii and fuzzy logic combination," in *2017 5th International Conference on Electrical Engineering - Boumerdes (ICEE-B)*, 2017, pp. 1–6.

[79] G. Muñoz-Delgado, J. Contreras, and J. M. Arroyo, "Multistage generation and network expansion planning in distribution systems considering uncertainty and reliability," *IEEE Transactions on Power Systems*, vol. 31, no. 5, pp. 3715–3728, 2016.

[80] C. Yuan, M. S. Illindala, and A. S. Khalsa, "Co-optimization scheme for distributed energy resource planning in community microgrids," *IEEE Transactions on Sustainable Energy*, vol. 8, no. 4, pp. 1351–1360, 2017.

[81] S. Mohamed, M. F. Shaaban, M. Ismail, E. Serpedin, and K. A. Qaraqe, "An efficient planning algorithm for hybrid remote microgrids," *IEEE Transactions on Sustainable Energy*, vol. 10, no. 1, pp. 257–267, 2019.

[82] E. Samani and F. Aminifar, "Tri-level robust investment planning of ders in distribution networks with ac constraints," *IEEE Transactions on Power Systems*, vol. 34, no. 5, pp. 3749–3757, 2019.

[83] J. Zhao, Z. Xu, J. Wang, C. Wang, and J. Li, "Robust distributed generation investment accommodating electric vehicle charging in a distribution network," *IEEE Transactions on Power Systems*, vol. 33, no. 5, pp. 4654–4666, 2018.

[84] N. N. Mansor and V. Levi, "Integrated planning of distribution networks considering utility planning concepts," *IEEE Transactions on Power Systems*, vol. 32, no. 6, pp. 4656–4672, 2017.

[85] A. Ouammi, H. Dagdougui, and R. Sacile, "Optimal planning with technology selection for wind power plants in power distribution networks," *IEEE Systems Journal*, vol. 13, no. 3, pp. 3059–3069, 2019.

[86] M. Asensio, P. Meneses de Quevedo, G. Muñoz-Delgado, and J. Contreras, "Joint distribution network and renewable energy expansion planning considering demand response and energy storage—part i: Stochastic programming model," *IEEE Transactions on Smart Grid*, vol. 9, no. 2, pp. 655–666, 2018.

[87] N. N. Mansor and V. Levi, "Operational planning of distribution networks based on utility planning concepts," *IEEE Transactions on Power Systems*, vol. 34, no. 3, pp. 2114–2127, 2019.

[88] S. S. Fatemi and H. Samet, "Allocation of renewables, switches, and relays considering relays actual operation time," *IEEE Systems Journal*, vol. 14, no. 1, pp. 950–959, 2020.

[89] J. J. Cuenca and B. P. Hayes, "Non-bias allocation of export capacity for distribution network planning with high distributed energy resource integration," *IEEE Transactions on Power Systems*, vol. 37, no. 4, pp. 3026–3035, 2022.

[90] A. Amer, A. Azab, M. A. Azzouz, and A. S. A. Awad, "A stochastic program for siting and sizing fast charging stations and small wind turbines in urban areas," *IEEE Transactions on Sustainable Energy*, vol. 12, no. 2, pp. 1217–1228, 2021.

[91] O. Erdinc, A. Taşcıkaraoğlu, N. G. Paterakis, Dursun, M. C. Sinim, and J. P. S. Catalão, "Comprehensive optimization model for sizing and siting of dg units, ev charging stations, and energy storage systems," *IEEE Transactions on Smart Grid*, vol. 9, no. 4, pp. 3871–3882, 2018.

[92] A. Ali, M. U. Keerio, and J. A. Laghari, "Optimal site and size of distributed generation allocation in radial distribution network using multi-objective optimization," *Journal of Modern Power Systems and Clean Energy*, vol. 9, no. 2, pp. 404–415, 2021.

[93] K. Mahmoud, N. Yorino, and A. Ahmed, "Optimal distributed generation allocation in distribution systems for loss minimization," *IEEE Transactions on Power Systems*, vol. 31, no. 2, pp. 960–969, 2016.

[94] C. Zhang, J. Li, Y.-J. A. Zhang, and Z. Xu, "Data-driven sizing planning of renewable distributed generation in distribution networks with optimality guarantee," *IEEE Transactions on Sustainable Energy*, vol. 11, no. 3, pp. 2003–2014, 2020.

[95] B. Singh, V. Mukherjee, and P. Tiwari, "A survey on impact assessment of dg and facts controllers in power systems," *Renewable and Sustainable Energy Reviews*, vol. 42, pp. 846–882, 2015.

[96] V. Murthy and A. Kumar, "Comparison of optimal dg allocation methods in radial distribution systems based on sensitivity approaches," *International Journal of Electrical Power & Energy Systems*, vol. 53, pp. 450–467, 2013.

[97] S. Gopiya Naik, D. Khatod, and M. Sharma, "Optimal allocation of combined dg and capacitor for real power loss minimization in distribution networks," *International Journal of Electrical Power & Energy Systems*, vol. 53, pp. 967–973, 2013.

[98] M. Kefayat, A. Lashkar Ara, and S. Nabavi Niaki, "A hybrid of ant colony optimization and artificial bee colony algorithm for probabilistic optimal placement and sizing of distributed energy resources," *Energy Conversion and Management*, vol. 92, pp. 149–161, 2015.

[99] S. Kaur, G. Kumbhar, and J. Sharma, "A minlp technique for optimal placement of multiple dg units in distribution systems," *International Journal of Electrical Power & Energy Systems*, vol. 63, pp. 609–617, 2014.

[100] N. Khalesi, N. Rezaei, and M.-R. Haghifam, "Dg allocation with application of dynamic programming for loss reduction and reliability improvement," *International Journal of Electrical Power & Energy Systems*, vol. 33, no. 2, pp. 288–295, 2011.

[101] N. Mohandas, R. Balamurugan, and L. Lakshminarasimman, "Optimal location and sizing of real power dg units to improve the voltage stability in the distribution system using abc algorithm united with chaos," *International Journal of Electrical Power & Energy Systems*, vol. 66, pp. 41–52, 2015.

[102] X. Zhang, G. G. Karady, K. R. Piratla, and S. T. Ariaratnam, "Network capacity assessment of combined heat and power-based distributed generation in urban energy infrastructures," *IEEE Transactions on Smart Grid*, vol. 4, no. 4, pp. 2131–2138, 2013.

[103] N. G. Hemdan and M. Kurrat, "Efficient integration of distributed generation for meeting the increased load demand," *International Journal of Electrical Power & Energy Systems*, vol. 33, no. 9, pp. 1572–1583, 2011.

[104] R. Viral and D. Khatod, "Optimal planning of distributed generation systems in distribution system: A review," *Renewable and Sustainable Energy Reviews*, vol. 16, no. 7, pp. 5146–5165, 2012.

[105] T. Jin, Y. Tian, C. W. Zhang, and D. W. Coit, "Multicriteria planning for distributed wind generation under strategic maintenance," *IEEE Transactions on Power Delivery*, vol. 28, no. 1, pp. 357–367, 2013.

[106] F. Rotaru, G. Chicco, G. Grigoras, and G. Cartina, "Two-stage distributed generation optimal sizing with clustering-based node selection," *International Journal of Electrical Power & Energy Systems*, vol. 40, no. 1, pp. 120–129, 2012.

[107] S. Kotamarty, S. Khushalani, and N. Schulz, "Impact of distributed generation on distribution contingency analysis," *Electric Power Systems Research*, vol. 78, no. 9, pp. 1537–1545, 2008.

[108] C. Yammani, S. Maheswarapu, and S. K. Matam, "Optimal placement and sizing of der's with load models using bat algorithm," in *2013 International Conference on Circuits, Power and Computing Technologies (ICCPCT)*, 2013, pp. 394–399.

[109] M. M. Othman, W. El-Khattam, Y. G. Hegazy, and A. Y. Abdelaziz, "Optimal placement and sizing of distributed generators in unbalanced distribution systems using supervised big bang-big crunch method," *IEEE Transactions on Power Systems*, vol. 30, no. 2, pp. 911–919, 2015.

[110] A. J. Gil Mena and J. A. Martín García, "An efficient approach for the siting and sizing problem of distributed generation," *International Journal of Electrical Power & Energy Systems*, vol. 69, pp. 167–172, 2015.

[111] A. El-Fergany, "Optimal allocation of multi-type distributed generators using backtracking search optimization algorithm," *International Journal of Electrical Power & Energy Systems*, vol. 64, pp. 1197–1205, 2015.

[112] J. A. Martín García and A. J. Gil Mena, "Optimal distributed generation location and size using a modified teaching–learning based optimization algorithm," *International Journal of Electrical Power & Energy Systems*, vol. 50, pp. 65–75, 2013.

[113] P. Prakash and D. K. Khatod, "Optimal sizing and siting techniques for distributed generation in distribution systems: A review," *Renewable and Sustainable Energy Reviews*, vol. 57, pp. 111–130, 2016.

[114] A. Dubey and S. Santoso, "On estimation and sensitivity analysis of distribution circuit's photovoltaic hosting capacity," *IEEE Transactions on Power Systems*, vol. 32, no. 4, pp. 2779–2789, 2017.

[115] A. Dubey, S. Santoso, and A. Maitra, "Understanding photovoltaic hosting capacity of distribution circuits," in *2015 IEEE Power & Energy Society General Meeting*, 2015, pp. 1–5.

[116] Y. P. Agalgaonkar, B. C. Pal, and R. A. Jabr, "Distribution voltage control considering the impact of pv generation on tap changers and autonomous regulators," *IEEE Transactions on Power Systems*, vol. 29, no. 1, pp. 182–192, 2014.

[117] A. Dubey, A. Bose, M. Liu, and L. N. Ochoa, "Paving the way for advanced distribution management systems applications: Making the most of models and data," *IEEE Power and Energy Magazine*, vol. 18, no. 1, pp. 63–75, 2020.

[118] N. Bañol Arias, S. Hashemi, P. B. Andersen, C. Træholt, and R. Romero, "Distribution system services provided by electric vehicles: Recent status, challenges, and future prospects," *IEEE Transactions on Intelligent Transportation Systems*, vol. 20, no. 12, pp. 4277–4296, 2019.

[119] H. Xing, M. Fu, Z. Lin, and Y. Mou, "Decentralized optimal scheduling for charging and discharging of plug-in electric vehicles in smart grids," *IEEE Transactions on Power Systems*, vol. 31, no. 5, pp. 4118–4127, 2016.

[120] N. Erdogan, F. Erden, and M. Kisacikoglu, "A fast and efficient coordinated vehicle-to-grid discharging control scheme for peak shaving in power distribution system," *Journal of Modern Power Systems and Clean Energy*, vol. 6, no. 3, pp. 555–566, 2018.

[121] N. I. Nimalsiri, C. P. Mediwaththe, E. L. Ratnam, M. Shaw, D. B. Smith, and S. K. Halgamuge, "A survey of algorithms for distributed charging control of electric vehicles in smart grid," *IEEE Transactions on Intelligent Transportation Systems*, vol. 21, no. 11, pp. 4497–4515, 2020.

[122] F. Knobloch, S. V. Hanssen, A. Lam, H. Pollitt, P. Salas, U. Chewpreecha, M. A. J. Huijbregts, and J.-F. Mercure, "Net emission reductions from electric cars and heat pumps in 59 world regions over time," *Nature Sustainability*, vol. 3, no. 6, pp. 434–447, 2020.

[123] R. Zhang and S. Fujimori, "The role of transport electrification in global climate change mitigation scenarios," *Environmental Research Letters*, vol. 15, no. 3, p. 034019, 2020.

[124] R. Zhang, J. Zhang, Y. Long, W. Wu, J. Liu, and Y. Jiang, "Long-term implications of electric vehicle penetration in urban decarbonization scenarios: An integrated land use–transport–energy model," *Sustainable Cities and Society*, vol. 68, p. 102800, 2021.

[125] G. Saldaña, J. I. San Martin, I. Zamora, F. J. Asensio, and O. Oñederra, "Electric vehicle into the grid: Charging methodologies aimed at providing ancillary services considering battery degradation," *Energies*, vol. 12, no. 12, 2019.

[126] N. K. Krishnamurthy, J. N. Sabhahit, V. K. Jadoun, D. N. Gaonkar, A. Shrivastava, V. S. Rao, and G. Kudva, "Optimal placement and sizing of electric vehicle charging infrastructure in a grid-tied dc microgrid using modified tlbo method," *Energies*, vol. 16, no. 4, 2023.

[127] S. Ray, K. Kasturi, S. Patnaik, and M. R. Nayak, "Review of electric vehicles integration impacts in distribution networks: Placement, charging/discharging strategies, objectives and optimisation models," *Journal of Energy Storage*, vol. 72, p. 108672, 2023.

[128] A. Janjic, L. Velimirovic, M. Stankovic, and A. Petrusic, "Commercial electric vehicle fleet scheduling for secondary frequency control," *Electric Power Systems Research*, vol. 147, pp. 31–41, 2017.

[129] Y. Wang, T. John, and B. Xiong, "A two-level coordinated voltage control scheme of electric vehicle chargers in low-voltage distribution networks," *Electric Power Systems Research*, vol. 168, pp. 218–227, 2019.

[130] J. Wang, G. R. Bharati, S. Paudyal, O. Ceylan, B. P. Bhattarai, and K. S. Myers, "Coordinated electric vehicle charging with reactive power support to distribution grids," *IEEE Transactions on Industrial Informatics*, vol. 15, no. 1, pp. 54–63, 2019.

[131] T. U. Solanke, V. K. Ramachandaramurthy, J. Y. Yong, J. Pasupuleti, P. Kasinathan, and A. Rajagopalan, "A review of strategic charging–discharging control of grid-connected electric vehicles," *Journal of Energy Storage*, vol. 28, p. 101193, 2020.

[132] D. S. Callaway and I. A. Hiskens, "Achieving controllability of electric loads," *Proceedings of the IEEE*, vol. 99, no. 1, pp. 184–199, 2011.

[133] K. Heussen, S. You, B. Biegel, L. H. Hansen, and K. B. Andersen, "Indirect control for demand side management - a conceptual introduction," in *2012 3rd IEEE PES Innovative Smart Grid Technologies Europe (ISGT Europe)*, 2012, pp. 1–8.

[134] T. P. Lyon, M. Michelin, A. Jongejan, and T. Leahy, "Is "smart charging" policy for electric vehicles worthwhile?" *Energy Policy*, vol. 41, pp. 259–268, 2012.

[135] P. Richardson, D. Flynn, and A. Keane, "Local versus centralized charging strategies for electric vehicles in low voltage distribution systems," *IEEE Transactions on Smart Grid*, vol. 3, no. 2, pp. 1020–1028, 2012.

[136] E. L. Karfopoulos and N. D. Hatziargyriou, "A multi-agent system for controlled charging of a large population of electric vehicles," *IEEE Transactions on Power Systems*, vol. 28, no. 2, pp. 1196–1204, 2013.

[137] O. Sundstrom and C. Binding, "Flexible charging optimization for electric vehicles considering distribution grid constraints," *IEEE Transactions on Smart Grid*, vol. 3, no. 1, pp. 26–37, 2012.

[138] D. Wu and A. Lisser, "A deep learning approach for solving linear programming problems," *Neurocomputing*, vol. 520, pp. 15–24, 2023.

[139] K. Clement-Nyns, E. Haesen, and J. Driesen, "The impact of charging plug-in hybrid electric vehicles on a residential distribution grid," *IEEE Transactions on Power Systems*, vol. 25, no. 1, pp. 371–380, 2010.

[140] N. Rotering and M. Ilic, "Optimal charge control of plug-in hybrid electric vehicles in deregulated electricity markets," *IEEE Transactions on Power Systems*, vol. 26, no. 3, pp. 1021–1029, 2011.

[141] J. Wang, C. Liu, D. Ton, Y. Zhou, J. Kim, and A. Vyas, "Impact of plug-in hybrid electric vehicles on power systems with demand response and wind power," *Energy Policy*, vol. 39, no. 7, pp. 4016–4021, 2011.

[142] T. Sousa, Z. Vale, J. P. Carvalho, T. Pinto, and H. Morais, "A hybrid simulated annealing approach to handle energy resource management considering an intensive use of electric vehicles," *Energy*, vol. 67, pp. 81–96, 2014.

[143] A. Y. Saber and G. K. Venayagamoorthy, "Resource scheduling under uncertainty in a smart grid with renewables and plug-in vehicles," *IEEE Systems Journal*, vol. 6, no. 1, pp. 103–109, 2012.

[144] M. Ansari, A. T. Al-Awami, E. Sortomme, and M. A. Abido, "Coordinated bidding of ancillary services for vehicle-to-grid using fuzzy optimization," *IEEE Transactions on Smart Grid*, vol. 6, no. 1, pp. 261–270, 2015.

[145] T. Lew, R. Bonalli, and M. Pavone, "Sample average approximation for stochastic programming with equality constraints," 2023.

[146] A. H. Hajimiragha, C. A. Canizares, M. W. Fowler, S. Moazeni, and A. Elkamel, "A robust optimization approach for planning the transition to plug-in hybrid electric vehicles," *IEEE Transactions on Power Systems*, vol. 26, no. 4, pp. 2264–2274, 2011.

[147] H. Rahimian and S. Mehrotra, "Frameworks and Results in Distributionally Robust Optimization," *Open Journal of Mathematical Optimization*, vol. 3, 2022. [Online]. Available: https://ojmo.centre-mersenne.org/articles/10.5802/ojmo.15/

[148] H. Yu, S. Niu, Y. Shang, Z. Shao, Y. Jia, and L. Jian, "Electric vehicles integration and vehicle-to-grid operation in active distribution grids: A comprehensive review on power architectures, grid connection standards and typical applications," *Renewable and Sustainable Energy Reviews*, vol. 168, p. 112812, 2022.

[149] F. Gonzalez Venegas, M. Petit, and Y. Perez, "Active integration of electric vehicles into distribution grids: Barriers and frameworks for flexibility services," *Renewable and Sustainable Energy Reviews*, vol. 145, p. 111060, 2021.

[150] J. Hu, H. Morais, T. Sousa, and M. Lind, "Electric vehicle fleet management in smart grids: A review of services, optimization and control aspects," *Renewable and Sustainable Energy Reviews*, vol. 56, pp. 1207–1226, 2016.

[151] Q. Zhang, J. Yan, H. O. Gao, and F. You, "A systematic review on power systems planning and operations management with grid integration of transportation electrification at scale," *Advances in Applied Energy*, vol. 11, p. 100147, 2023.

[152] M. Lydia, S. S. Kumar, A. I. Selvakumar, and G. E. Prem Kumar, "A comprehensive review on wind turbine power curve modeling techniques," *Renewable and Sustainable Energy Reviews*, vol. 30, pp. 452–460, 2014.

[153] B. W. Krishna R. Reddi, Weilin Li and Y. Moon, "System dynamics modelling of hybrid renewable energy systems and combined heating and power generator," *International Journal of Sustainable Engineering*, vol. 6, no. 1, pp. 31–47, 2013.

[154] F. R. Y. Shengrong Bu and P. X. Liu, "Distributed unit commitment scheduling in the future smart grid with intermittent renewable energy resources and stochastic power demands," *International Journal of Green Energy*, vol. 0, no. ja, 2014. [Online]. Available: https://doi.org/10.1080/15435075.2014.893874

[155] C. J. Mozina, "Wind-power generation," *IEEE Industry Applications Magazine*, vol. 17, no. 3, pp. 37–43, 2011.

[156] E. Mancini, M. Longo, W. Yaici, and D. Zaninelli, "Assessment of the impact of electric vehicles on the design and effectiveness of electric distribution grid with distributed generation," *Applied Sciences*, vol. 10, no. 15, 2020. [Online]. Available: https://www.mdpi.com/2076-3417/10/15/5125

[157] N. Gupta, "Gauss-quadrature-based probabilistic load flow method with voltage-dependent loads including wtgs, pv, and ev charging uncertainties," *IEEE Transactions on Industry Applications*, vol. 54, no. 6, pp. 6485–6497, 2018.

[158] A. Cortés, J. Mazón, and J. Merino, "Strategy of management of storage systems integrated with photovoltaic systems for mitigating the impact on lv distribution network," *International Journal of Electrical Power & Energy Systems*, vol. 103, pp. 470–482, 2018.

[159] S. Rafique and G. Town, "Aggregated impacts of electric vehicles on electricity distribution in new south wales, australia," *Australian Journal of Electrical and Electronics Engineering*, vol. 14, no. 3-4, pp. 71–87, 2017.

[160] Y. Kongjeen and K. Bhumkittipich, "Impact of plug-in electric vehicles integrated into power distribution system based on voltage-dependent power flow analysis," *Energies*, vol. 11, no. 6, 2018.

[161] G. Longhi, C. Borges, and G. Gruosso, "A model to estimate the impact of electrical vehicles displacement on medium voltage network," in *IECON 2018 - 44th Annual Conference of the IEEE Industrial Electronics Society*, 2018, pp. 5131–5136.

[162] J. H. Angelim and C. de Mattos Affonso, "Probabilistic assessment of voltage quality on solar-powered electric vehicle charging station," *Electric Power Systems Research*, vol. 189, p. 106655, 2020.

[163] J. Meyer, S. Müller, P. Schegner, S. Z. Djokic, A. J. Collin, and X. Xu, "Comparison of methods for modelling electric vehicle chargers for harmonic studies," in *2016 Power Systems Computation Conference (PSCC)*, 2016, pp. 1–7.

[164] L. González, E. Siavichay, and J. Espinoza, "Impact of ev fast charging stations on the power distribution network of a latin american intermediate city," *Renewable and Sustainable Energy Reviews*, vol. 107, pp. 309–318, 2019.

[165] A. Arif, Z. Wang, J. Wang, B. Mather, H. Bashualdo, and D. Zhao, "Load modeling—a review," *IEEE Transactions on Smart Grid*, vol. 9, no. 6, pp. 5986–5999, 2018.

[166] B. Brinkmann and M. Negnevitsky, "A probabilistic approach to observability of distribution networks," *IEEE Transactions on Power Systems*, vol. 32, no. 2, pp. 1169–1178, 2017.

[167] M. A. Lynch, S. Nolan, M. T. Devine, and M. O'Malley, "The impacts of demand response participation in capacity markets," *Applied Energy*, vol. 250, pp. 444–451, 2019.

[168] J. Caballero-Peña, C. Cadena-Zarate, A. Parrado-Duque, and G. Osma-Pinto, "Distributed energy resources on distribution networks: A systematic review of modelling, simulation, metrics, and impacts," *International Journal of Electrical Power & Energy Systems*, vol. 138, p. 107900, 2022.

[169] C. Marnay, F. Robio, and A. Siddiqui, "Shape of the microgrid," in *2001 IEEE Power Engineering Society Winter Meeting. Conference Proceedings (Cat. No.01CH37194)*, vol. 1, 2001, pp. 150–153 vol.1.

[170] P. Piagi and R. Lasseter, "Autonomous control of microgrids," in *2006 IEEE Power Engineering Society General Meeting*, 2006, pp. 8 pp.–.

[171] J. D. Kueck, R. Staunton, S. D. Labinov, and B. Kirby, "Microgrid energy management system," ORNL/TM-2002/242. Oak Ridge,TN: Oak Ridge National Laboratory, Tech. Rep., 2003.

[172] O. C. Bailey, C. Creighton, R. M. Firestone, C. Marnay, and M. Stadler, "Distributed energy resources in practice: A case study analysis and validation of lbnl's customer adoption model," Berkeley, CA: Lawrence Berkeley National Laboratory, Tech. Rep., 2003.

[173] R. Lasseter and P. Paigi, "Microgrid: a conceptual solution," in *2004 IEEE 35th Annual Power Electronics Specialists Conference (IEEE Cat. No.04CH37551)*, vol. 6, 2004, pp. 4285–4290 Vol.6.

[174] Z. Jiang, "Agent-based control framework for distributed energy resources microgrids," in *2006 IEEE/WIC/ACM International Conference on Intelligent Agent Technology*, 2006, pp. 646–652.

[175] Vallem, Mitra, and Patra, "Distributed generation placement for optimal microgrid architecture," in *2005/2006 IEEE/PES Transmission and Distribution Conference and Exhibition*, 2006, pp. 1191–1195.

[176] M. Jimenez and N. Hatziargyriou, "Research activities in europe on integration of distributed energy resources in the electricity networks of the future," in *2006 IEEE Power Engineering Society General Meeting*, 2006, pp. 4 pp.–.

[177] K. Strunz, "Developing benchmark models for studying the integration of distributed energy resources," in *2006 IEEE Power Engineering Society General Meeting*, 2006, pp. 2 pp.–.

[178] Z. Jiang and R. A. Dougal, "Hierarchical microgrid paradigm for integration of distributed energy resources," in *2008 IEEE Power and Energy Society General Meeting - Conversion and Delivery of Electrical Energy in the 21st Century*, 2008, pp. 1–8.

[179] Z. Jiang and X. Yu, "Hybrid dc- and ac-linked microgrids: Towards integration of distributed energy resources," in *2008 IEEE Energy 2030 Conference*, 2008, pp. 1–8.

[180] H. Lund, A. N. Andersen, P. A. Østergaard, B. V. Mathiesen, and D. Connolly, "From electricity smart grids to smart energy systems – a market operation based approach and understanding," *Energy*, vol. 42, no. 1, pp. 96–102, 2012.

[181] P. Siano, "Demand response and smart grids—a survey," *Renewable and Sustainable Energy Reviews*, vol. 30, pp. 461–478, 2014.

[182] A. Saif, V. Ravikumar Pandi, H. Zeineldin, and S. Kennedy, "Optimal allocation of distributed energy resources through simulation-based optimization," *Electric Power Systems Research*, vol. 104, pp. 1–8, 2013.

[183] A. Rezaee Jordehi, "Particle swarm optimisation for dynamic optimisation problems: a review," *Neural Computing and Applications*, vol. 25, no. 7, pp. 1507–1516, 2014.

[184] M. R. Aghamohammadi and H. Abdolahinia, "A new approach for optimal sizing of battery energy storage system for primary frequency control of islanded microgrid," *International Journal of Electrical Power & Energy Systems*, vol. 54, pp. 325–333, 2014.

[185] W. Gu, Z. Wu, R. Bo, W. Liu, G. Zhou, W. Chen, and Z. Wu, "Modeling, planning and optimal energy management of combined cooling, heating and power microgrid: A review," *International Journal of Electrical Power & Energy Systems*, vol. 54, pp. 26–37, 2014.

[186] Z. Li, Q. Guo, H. Sun, and J. Wang, "Coordinated economic dispatch of coupled transmission and distribution systems using heterogeneous decomposition," *IEEE Transactions on Power Systems*, vol. 31, no. 6, pp. 4817–4830, 2016.

[187] C. Lin, W. Wu, X. Chen, and W. Zheng, "Decentralized dynamic economic dispatch for integrated transmission and active distribution networks using multi-parametric programming," *IEEE Transactions on Smart Grid*, vol. 9, no. 5, pp. 4983–4993, 2018.

[188] C. Lin, W. Wu, B. Zhang, B. Wang, W. Zheng, and Z. Li, "Decentralized reactive power optimization method for transmission and distribution networks accommodating large-scale dg integration," *IEEE Transactions on Sustainable Energy*, vol. 8, no. 1, pp. 363–373, 2017.

[189] E. Dall'Anese, S. S. Guggilam, A. Simonetto, Y. C. Chen, and S. V. Dhople, "Optimal regulation of virtual power plants," *IEEE Transactions on Power Systems*, vol. 33, no. 2, pp. 1868–1881, 2018.

[190] E. Polymeneas and S. Meliopoulos, "Aggregate modeling of distribution systems for multi-period opf," in *2016 Power Systems Computation Conference (PSCC)*, 2016, pp. 1–8.

[191] F. L. Müller, J. Szabó, O. Sundström, and J. Lygeros, "Aggregation and disaggregation of energetic flexibility from distributed energy resources," *IEEE Transactions on Smart Grid*, vol. 10, no. 2, pp. 1205–1214, 2019.

[192] L. Zhao, W. Zhang, H. Hao, and K. Kalsi, "A geometric approach to aggregate flexibility modeling of thermostatically controlled loads," *IEEE Transactions on Power Systems*, vol. 32, no. 6, pp. 4721–4731, 2017.

[193] L. Zhao, H. Hao, and W. Zhang, "Extracting flexibility of heterogeneous deferrable loads via polytopic projection approximation," in *2016 IEEE 55th Conference on Decision and Control (CDC)*, 2016, pp. 6651–6656.

[194] E. Vrettos, F. Oldewurtel, and G. Andersson, "Robust energy-constrained frequency reserves from aggregations of commercial buildings," *IEEE Transactions on Power Systems*, vol. 31, no. 6, pp. 4272–4285, 2016.

[195] W. Mai and C. Y. Chung, "Economic mpc of aggregating commercial buildings for providing flexible power reserve," *IEEE Transactions on Power Systems*, vol. 30, no. 5, pp. 2685–2694, 2015.

[196] S. Han, S. Han, and K. Sezaki, "Development of an optimal vehicle-to-grid aggregator for frequency regulation," *IEEE Transactions on Smart Grid*, vol. 1, no. 1, pp. 65–72, 2010.

[197] W. Shi and V. W. Wong, "Real-time vehicle-to-grid control algorithm under price uncertainty," in *2011 IEEE International Conference on Smart Grid Communications (SmartGridComm)*, 2011, pp. 261–266.

[198] R. Wang, Y. Li, P. Wang, and D. Niyato, "Design of a v2g aggregator to optimize phev charging and frequency regulation control," in *2013 IEEE International Conference on Smart Grid Communications (SmartGridComm)*, 2013, pp. 127–132.

[199] E. L. Karfopoulos, K. A. Panourgias, and N. D. Hatziargyriou, "Distributed coordination of electric vehicles providing v2g regulation services," *IEEE Transactions on Power Systems*, vol. 31, no. 4, pp. 2834–2846, 2016.

[200] G. Wenzel, M. Negrete-Pincetic, D. E. Olivares, J. MacDonald, and D. S. Callaway, "Real-time charging strategies for an electric vehicle aggregator to provide ancillary services," *IEEE Transactions on Smart Grid*, vol. 9, no. 5, pp. 5141–5151, 2018.

[201] J. Hu, G. Yang, H. W. Bindner, and Y. Xue, "Application of network-constrained transactive control to electric vehicle charging for secure grid operation," *IEEE Transactions on Sustainable Energy*, vol. 8, no. 2, pp. 505–515, 2017.

[202] Y. Shi, H. D. Tuan, A. V. Savkin, T. Q. Duong, and H. V. Poor, "Model predictive control for smart grids with multiple electric-vehicle charging stations," *IEEE Transactions on Smart Grid*, vol. 10, no. 2, pp. 2127–2136, 2019.

[203] Y. Zheng, Y. Song, D. J. Hill, and K. Meng, "Online distributed mpc-based optimal scheduling for ev charging stations in distribution systems," *IEEE Transactions on Industrial Informatics*, vol. 15, no. 2, pp. 638–649, 2019.

[204] S. M. G. Mostafa, J. G. Shingh, and H. E. Haque, "An extensive literature review and new proposal on optimal capacitor placement in distribution systems," *Journal of Engineering Advancements*, vol. 1, no. 04, p. 150–169, Dec. 2020.

[205] J.-H. Teng, "A direct approach for distribution system load flow solutions," *IEEE Transactions on Power Delivery*, vol. 18, no. 3, pp. 882–887, 2003.

[206] X. Su, Z. Zhang, Y. Liu, Y. Fu, F. Shahnia, C. Zhang, and Z. Y. Dong, "Sequential and comprehensive besss placement in unbalanced active distribution networks considering the impacts of bess dual attributes on sensitivity," *IEEE Transactions on Power Systems*, vol. 36, no. 4, pp. 3453–3464, 2021.

[207] T. Tewari, A. Mohapatra, and S. Anand, "Coordinated control of oltc and energy storage for voltage regulation in distribution network with high pv

penetration," *IEEE Transactions on Sustainable Energy*, vol. 12, no. 1, pp. 262–272, 2021.

[208] J. Kennedy and R. Eberhart, "Particle swarm optimization," in *Proceedings of ICNN'95 - International Conference on Neural Networks*, vol. 4, 1995, pp. 1942–1948 vol.4.

[209] C. E. Shannon, "A mathematical theory of communication," *The Bell System Technical Journal*, vol. 27, no. 3, pp. 379–423, 1948.

[210] D. Rizy, J. Lawler, J. Patton, and W. Nelson, "Measuring and analyzing the impact of voltage and capacitor control with high speed data acquisition (distribution system)," *IEEE Transactions on Power Delivery*, vol. 4, no. 1, pp. 704–714, 1989.

[211] S. Gupta, V. K. Yadav, and M. Singh, "Optimal allocation of capacitors in radial distribution networks using shannon's entropy," *IEEE Transactions on Power Delivery*, vol. 37, no. 3, pp. 2245–2255, 2022.

[212] M. Farivar and S. H. Low, "Branch flow model: Relaxations and convexification—part i & ii," *IEEE Transactions on Power Systems*, vol. 28, no. 3, pp. 2554–2572, 2013.

[213] H. He, H. Daumé, and J. Eisner, "Learning to search in branch-and-bound algorithms," in *Proceedings of the 27th International Conference on Neural Information Processing Systems - Volume 2*, ser. NIPS'14. MIT Press, 2014, p. 3293–3301.

[214] A. Soroudi, P. Siano, and A. Keane, "Optimal dr and ess scheduling for distribution losses payments minimization under electricity price uncertainty," *IEEE Transactions on Smart Grid*, vol. 7, no. 1, pp. 261–272, 2016.

[215] R. A. Waltz and T. D. Plantenga, *Knitro User's Manual: Version 6.0, Ziena Optimization, Inc.*, March 2009. [Online]. Available: https://www.yumpu.com/en/document/view/37639225/knitro-users-manual-version-60-ziena-optimization-inc.

[216] A. G. Tsikalakis and N. D. Hatziargyriou, "Centralized control for optimizing microgrids operation," *IEEE Transactions on Energy Conversion*, vol. 23, no. 1, pp. 241–248, 2008.

[217] H. Liang, Y. Liu, F. Li, and Y. Shen, "Dynamic economic/emission dispatch including pevs for peak shaving and valley filling," *IEEE Transactions on Industrial Electronics*, vol. 66, no. 4, pp. 2880–2890, 2019.

[218] M. Zhou, Z. Wu, J. Wang, and G. Li, "Forming dispatchable region of electric vehicle aggregation in microgrid bidding," *IEEE Transactions on Industrial Informatics*, vol. 17, no. 7, pp. 4755–4765, 2021.

[219] D. Pozo, "Linear battery models for power systems analysis," *Electric Power Systems Research*, vol. 212, p. 108565, 2022. doi:10.1016/j.epsr.2022.108565.

[220] X. Shi, Y. Xu, G. Chen, and Y. Guo, "An augmented lagrangian-based safe reinforcement learning algorithm for carbon-oriented optimal scheduling of ev aggregators," *IEEE Transactions on Smart Grid*, 2023. doi:10.1109/TSG.2023.3289211.

[221] S. Gao, J. Wu, and B. Xu, "Controllability evaluation of ev charging infrastructure transformed from gas stations in distribution networks with renewables," *Energies*, vol. 12, no. 8, 2019.

[222] "Renewables trend," [Online]. Available: https://www.caiso.com/TodaysOutlook/Pages/supply.html, (Accessed: 2023-06).

[223] Z. Chen, L. Wu, and Y. Fu, "Real-time price-based demand response management for residential appliances via stochastic optimization and robust optimization," *IEEE Transactions on Smart Grid*, vol. 3, no. 4, pp. 1822–1831, 2012.

[224] "City of fort collins utilities residential rates," [Online]. Available: https://www.fcgov.com/utilities/residential/rates/electric, (Accessed: 2023).

Appendix A

Particle Swarm Optimization

Particle Swarm Optimization (PSO) is a stochastic technique to find the optimum solution based on the socio-psychological behavior of birds or fish. The algorithm starts with several random solutions of a particle i as $x_i = \{x_{i1},\ x_{i2},\ x_{i3}, ..., x_{ij}\}$ and updates after each iteration k to get the best solution achieved by i^{th} particle so far as $\rho_i^{best} = \left\{\rho_{i1}^{best},\ \rho_{i2}^{best},\ \rho_{i3}^{best}, ...,\ \rho_{ij}^{best}\right\}$. Concurrently, the best solution so far attained by any particle is also recorded, defined as the global best solution $\left(\psi_{ij}^{best}\right)$. After each iteration, the velocity $\nu_i = \{\nu_{i1},\ \nu_{i2},\ \nu_{i3}, ..., \nu_{ij}\}$ and solution x_{ij} of the i^{th} particle are updated by using following equations:

$$\begin{aligned} \nu_{ij}^{k+1} = \omega \times \nu_{ij}^{k} + \left[c_1 \times \alpha_1 \times \left(\rho_{ij}^{best} - x_{ij}\right)\right] \\ + \left[c_2 \times \alpha_2 \times \left(\psi_{ij}^{best} - x_{ij}\right)\right] \end{aligned} \tag{A.1}$$

$$x_{ij}^{k+1} = x_{ij}^{k} + \nu_{ij}^{k+1} \tag{A.2}$$

where k is the iteration count, c_1 and c_2 are the constants and equal to 2, α_1 and α_2 represents the random variables and ω represents the inertia weight which modifies after every iteration as:

$$\omega = \omega^{\max} - \left[\left(\omega^{\max} - \omega^{\min}\right) \times \frac{k}{\mathrm{K}^{\max}}\right] \tag{A.3}$$

where $\omega^{\max}$ and $\omega^{\min}$ are the maximum and minimum inertia weights and equal to 0.9 and 0.4, respectively. In this article, the total 100 number of iterations $(\mathrm{K}^{\max})$ are carried out for each case to obtain the optimal solution.

Appendix B

Techno-Economic Quantities: Optimal DG Placement Case Results

Table B.1 and Table B.2 present the simulated network quantities following the optimal integration of DG in the 38-node test system.

TABLE B.1: 38-node test network quantities results obtained for cases 3.6.1, 3.6.2, and 3.6.3 considered in Section 3.6

Case	Configuration	P_{Loss} (kW)	Q_{Loss} (kVAr)	V_{min} (p.u.)	AEC ($)
Base Configuration		152.80	101.50	18 / 0.9252	2100053
Case-1	150 kW	135.40	89.30	33 / 0.9316	2070118
	300 kW	121.90	80.20	33 / 0.9339	2042458
	600 kW	102.90	67.70	33 / 0.9384	1991708
Case-2	6^{th} bus	79.20	57.90	18 / 0.9695	1646869
Case-3	0.80 pf	103.0	67.70	33 / 0.9383	2062490
	0.90 pf	101.80	66.80	33 / 0.9383	2033066
	1.0 pf	108.20	71.10	33 / 0.9369	2008025

TABLE B.2: 38-node test network quantities results obtained for case 3.6.4 considered in Section 3.6

Load Type	Configuration	P_{Loss} (kW)	Q_{Loss} (kVAr)	V_{min} (p.u.)	AEC ($)
Constant	Base	202.20	134.8	18 / 0.9133	2251048
Power	300 kW	167.20	110.60	33 / 0.9216	2191100
Industrial	Base	157.60	104.70	18 / 0.9240	2205888
Power	300 kW	124.20	81.60	33 / 0.9340	2146885
Residential	Base	154.20	102.40	18 / 0.9248	2126184
Power	300 kW	123.0	80.90	33 / 0.9337	2068420
Commercial	Base	148.60	98.60	18 / 0.9264	2063673
Power	300 kW	119.10	78.30	33 / 0.9348	2006900
Mix-type	Base	152.80	101.50	18 / 0.9252	2100053
Power	300 kW	121.90	80.20	33 / 0.9339	2042458

Appendix C

Branch and Bound (BnB) Search Technique

A branch-and-bound algorithm involves systematically exploring potential solutions through a state space search. Imagine the set of candidate solutions as a rooted tree, with the entire set at the root. The algorithm traverses branches of this tree, each representing subsets of the solution set. Before enumerating the candidate solutions of a branch, the algorithm evaluates the branch against upper and lower bounds on the optimal solution. If a branch cannot possibly produce a better solution than the best one found so far, it is discarded. **Algorithm 1** represents the BnB search algorithm for obtaining the optimal EV scheduling solution.

Algorithm 1 Branch and Bound algorithm for EV Scheduling

procedure EVSCHEDLING(**EV**, $\mathbf{\Pi_S^*}$, $\mathbf{\Pi_P^\#}$)
  $\mathcal{L} = \left\{\mathcal{F}_0^{EV}\right\}$, set $\mathbb{D}_s^{EV} = \{\ \}$, $\mathbb{D}_p^{EV} = \{\ \}$, $i \leftarrow 0$
  while L $\neq \emptyset$ **do**
    $\mathcal{F}_k^{EV} \leftarrow \pi_s$ pops a node from $\mathcal{L}$
    if $\mathcal{F}_k^{EV}$ is optimal **then**
      $\mathbb{D}_p^{EV} \leftarrow \mathbb{D}_p^{EV} \cup \left\{\left(\varphi\left(\mathcal{F}_k^{EV}\right), \text{expand}\right)\right\}$
    else
      $\mathbb{D}_p^{EV} \leftarrow \mathbb{D}_p^{EV} \cup \left\{\left(\varphi\left(\mathcal{F}_k^{EV}\right), \text{prune}\right)\right\}$
    end if
    if $\mathcal{F}_k^{EV}$ is not fathomed and $\pi_p\left(\mathcal{F}_k^{EV}\right) =$ expand **then**
      $\mathcal{F}_{i+1}^{EV}, \ldots, \mathcal{F}_{i+a}^{EV} \leftarrow$ expand $\mathcal{F}_k^{EV}, \ldots$
      $\mathcal{L} \leftarrow \mathcal{L} \cup \left\{\mathcal{F}_{i+1}^{EV}, \ldots, \mathcal{F}_{i+a}^{EV}\right\}$, $i \leftarrow i + a$
    end if
    if an optimal node $\mathcal{F}_d^{*(A)} \in \mathcal{L}$ **then**
      $\mathbb{D}_s^{EV} \leftarrow \mathbb{D}_s^{EV} \cup \left\{\left(\wp\left(\mathcal{F}_d^{*(EV)}\right) - \wp\left(\mathcal{F}_{i'}^{EV}\right), 1\right) \ldots\right.$
      $\left. \ldots \ : \ \mathcal{F}_{i'}^{EV} \in \mathcal{L} \text{ and } \mathcal{F}_{i'}^{EV} \neq \mathcal{F}_d^{*(EV)}\right\}$
    end if
  end while
  return $\mathbb{D}_s^{EV}, \mathbb{D}_p^{EV}$
end procedure

∗**- node selection, # - node pruning**

List of Publications

Papers in Refereed Journals

[1] Shubham Gupta, Vinod Kumar Yadav, and Madhusudan Singh. Optimal allocation of capacitors in radial distribution networks using shannon's entropy. *IEEE Transactions on Power Delivery*, 37(3):2245–2255, 2022. doi: 10.1109/TPWRD.2021.3107857.

[2] Shubham Gupta, Vinod Kumar Yadav, and Madhusudan Singh. Measuring influence of indices in dn planning. *IEEE Systems Journal*, 17(3):4149–4152, 2023. doi: 10.1109/JSYST.2023.3250226.

[3] Shubham Gupta, Vinod Kumar Yadav, and Madhusudan Singh. Aggregation of distributed energy resources for optimal operation in local energy communities with grid constraints. *IEEE Transactions on Industrial Informatics*, Communicated on 22nd Nov. 2023.

[4] Shubham Gupta, Vinod Kumar Yadav, and Madhusudan Singh. Decision making in multi-objective dg planning for distribution system via shannon's entropy. *Electrical Engineering*, Communicated on 29th Nov. 2023.

[5] Shubham Gupta, Vinod Kumar Yadav, and Madhusudan Singh. Aggregation and scheduling of distributed energy resources in smart distribution system considering multiple uncertainties. *IEEE, Journal of Modern Power System and Clean Energy*, Communicated.

National and International Conference Proceedings

[1] Shubham Gupta, Vinod Kumar Yadav, and Madhusudan Singh. A new novel approach for optimal capacitor placement in radial distribution networks using data envelopment analysis. In *IECON 2021 – 47th Annual Conference of the IEEE Industrial Electronics Society*, pages 1–7, 2021. doi: 10.1109/IECON48115.2021.9589708.

[2] Shubham Gupta, Vinod Kumar Yadav, and Madhusudan Singh. Optimal dg allocation for maximizing operational benefits in unbundled electric distribution system. In *9th IEEE India International Conference on Power Electronics–IICPE2023*, held at DCRUST, Murthal from Nov. 28-Nov. 30, 2023.